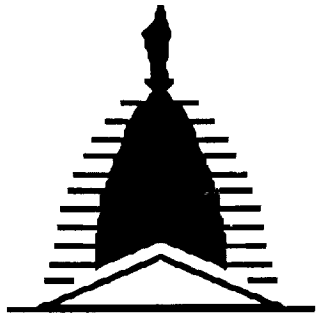

UNIVERSITY of
NOTRE DAME

NASA/USRA UNIVERSITY ADVANCED DESIGN PROGRAM 1988-1989

Final Design Proposal

THE SKY SHARK

An RPV Designed to Investigate
the Pressure Distribution on a Lifting Surface

Department of Aerospace and Mechanical Engineering
University of Notre Dame
Notre Dame, IN 46556

THE SKY SHARK

DESIGN PROPOSAL

DESIGN GROUP MEMBERS

Rob Ziemba, Group Leader / Propulsion
Joe Schudt, Propulsion
Karen Comly, Data Acquisition
Mike Vanthournut, Data Acquisition
Jerome C. Trybus, Structures
Greg Branch, Structures
Maggie Hassan, Aerodynamics
Steve Noll, Aerodynamics
Steve Julian, Stability
Dave Carey, Controls

Aerospace Design AE 441
Department of Aerospace and Mechanical Engineering
University of Notre Dame
May 4, 1989

TABLE OF CONTENTS

A: EXECUTIVE SUMMARY

THE SKY SHARK

In response to the Request for Design Proposal presented in December 1988, Group A has designed an aircraft which will acquire airborne pressure distribution data on a variable lifting surface test specimen. The design objective and requirements are listed below.

Objective:

Design a remotely piloted vehicle which is capable of gathering in flight pressure distribution data on a lifting test specimen, and then test the design by constructing a subscale demonstrator, to prove the flight worthiness of the concept.

Requirements of test specimen:

1. Vary Reynolds number: $4x10^4$ to $1x10^6$
2. Vary angle of attack: -20^o to 40^o
3. Vary sweep angles: -20^o to 30^o
4. Vary chord: 4" to 16"
5. Vary span: 1' to 5'
6. Capable of 2D and 3D effects

The aircraft designed to meet these requirements, the Sky Shark, can be viewed in Figure B-1, in the following section. The aircraft's specifications can be seen in Appendix B-1. In the design of this aircraft, accurate data acquisition and aircraft control (in the context of varying test configurations) were decided to be the most important design considerations. For accurate data acquisition to occur, the test specimen should be situated on the craft such that it experiences the least amount of aerodynamic interference from other parts of the plane. The Sky Shark has the test specimen mounted vertically on top of the fuselage, near the nose. The vertical mounting was chosen as it reduces interference from the wings, it experiences little vibration, and is structurally simple. All these factors help in retrieving better data readings. The section is mounted forward near the center of gravity for two reasons. First, near the nose of the craft, the boundary layer from the fuselage is very thin, and can be ignored. Secondly, by locating the section near the center of gravity, the forces created by the specimen will not induce large moments.

As Figure B-1 shows, the Sky Shark has a forward, mid mounted wing with dihedral. From the stand point of stability, a forward mounted wing allows the c.g. to be positioned at the front of the aircraft, near the test specimen, as desired. The wing is mid-mounted in order to move it down away from the test specimen. The dihedral will provide roll and lateral stability which is needed to counteract the destabilizing effects of the test specimen.

The aircraft will possess rear, fuselage mounted horizontal stabilizers with oversized elevators for longitudinal stability and control. For lateral stability and control, a single vertical tail will be used, with oversized rudders. The control surfaces are oversized in order to correct for any moments created by the test specimen. Roll control will be directed by ailerons on the wings. In order to balance the side forces created by the test specimen, winglets have been positioned on the the wing tips. These winglets are a fairly new concept in control and will be used to balance the side force without creating large yaw moments that would result if the vertical stabilizer was used.

The aircraft will be powered by two ducted fans, mounted to the fuselage behind the wing. The ducting of the propellors will reduce interference effects inherent to propellor driven crafts. This will allow for more accurate data acquisition.

The Sky Shark is capable of meeting most of the mission requirements. For chord lengths of .8 ft to 1.4 ft, the Sky Shark allows testing for the total requested Reynolds number range, $4x10^4$ to $1x10^6$. If it is desired to test smaller chords, only Reynolds numbers up to $5x10^5$ can be reached. The requested angles of attack and sweep can be attained in flight by the aircraft. Due to the vertical mounting of the test specimen, span requirements can now be halved, allowing the Sky Shark to easily meet this request. The aircraft also allows for both 2-D, and 3-D effects. The 2-D effects are achieved by placing an end plate on the test specimen tip.

The Sky Shark will start its mission on the ground, where it will be fueled, and a test specimen attached. The aircraft will be launched by means of a catapult system. Once in the air, it will cruise at altitudes of 100-3000 ft, where data acquisition will occur. The Sky Shark will fly a rectangular pattern, 1200 ft long by 500 ft wide. The pressure data will be taken for a specific test specimen during steady level flight along the length of the rectangular pattern, and stored on board. The craft will allow 20 minutes of

testing, with a maximum mission endurance of 45 minutes. The Sky Shark will land on conventional landing gear, which have been retracted up to this point.

The design of the Sky Shark sees no major obstacles in its concept. However, some potential trouble spots should be pointed out. Although the greatest effort has been expended in making this aircraft as stable as possible, forces and moments from the test specimen may cause problems. This design proposal has assumed that very modern automatic control systems will be incorporated into the aircraft. Such advanced control systems are essential to the success of the Sky Shark. With these systems, the Sky Shark is a highly viable concept for the purpose of in flight data acquisition.

B: CONFIGURATION AND PARAMETERS

THE SKY SHARK

Figure B-1

The Sky Shark

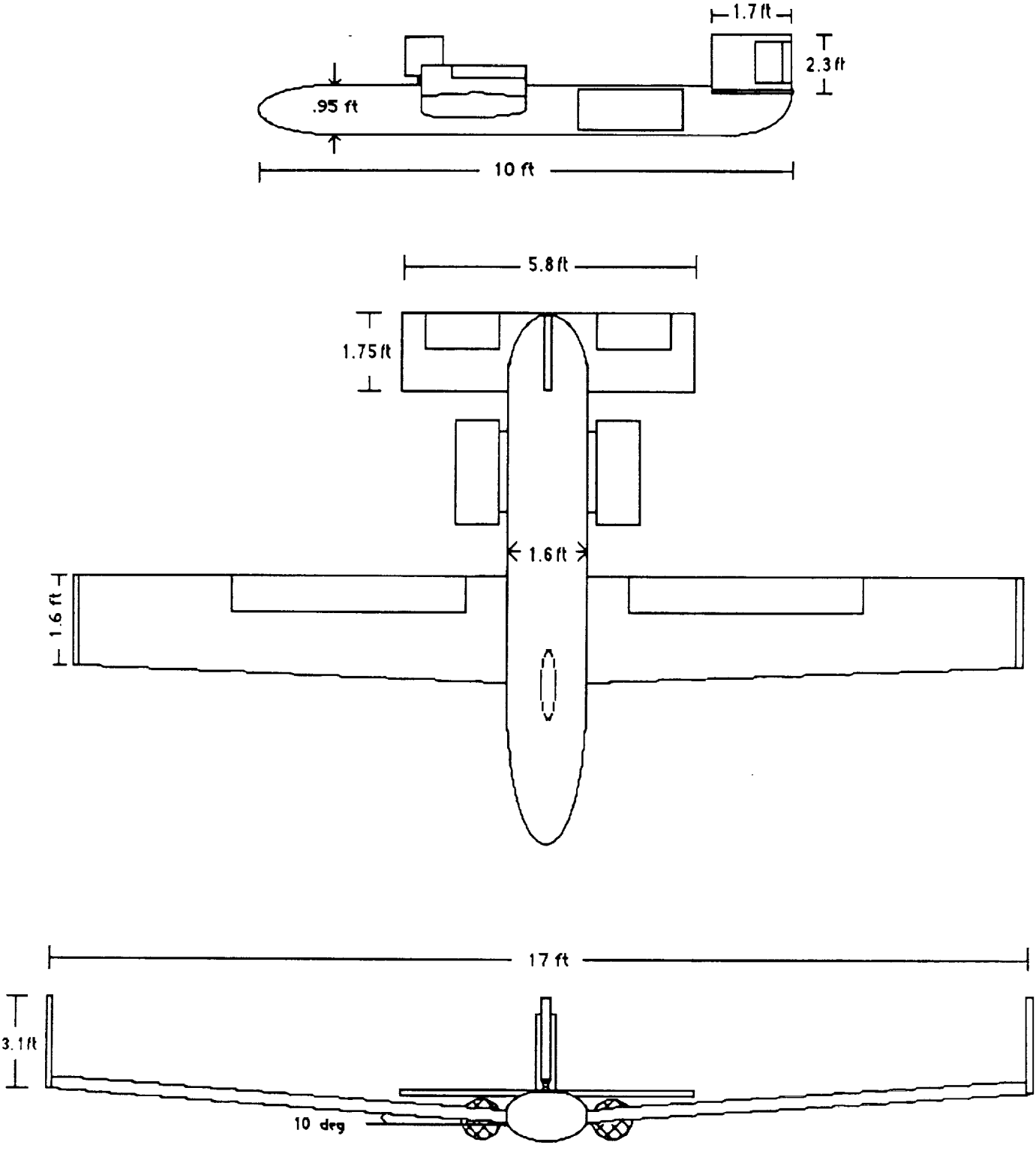

Appendix B-1

Sky Shark Parameters

PARAMETER	AMOUNT
WEIGHT TOTAL	60 LBS
WEIGHT PAYLOAD	15 LBS
Swing	34 FT^2
ASPECT RATIO	9
CHORD	2 FT
SPAN	17.5 FT
Svert. tail	3.9 FT^2
Shor. tail	10.2 FT^2
FUSELAGE LENGTH	10 FT
Cdo	.023
AVAILABLE THRUST	30 LBS
Vmax	190 FT/S
Vmin	40 FT/S
CEILING	17,047 FT
MAX RATE OF CLIMB	35.8 FT/S
RANGE	46.9 Mi
ENDURANCE	40 MIN
TAPER	.8
DIHEDRAL	10^O

C: MISSION PROFILE

THE SKY SHARK

The mission of the Sky Shark is to serve as an airborne aerodynamic data acquisition system for collecting surface pressure distributions and other appropriate near field flow information on two and three dimensional lifting surfaces. In an attempt to meet the requirements needed to perform the mission, the Sky Shark must fly over a range of Reynolds numbers from 400,000 to 1,000,000 or over the equivalent velocity range of approximately 50 ft/s to 190 ft/s. The Sky Shark can cover this velocity range successfully and has an acceleration capability of approximately 5 ft/s^2.

The Sky Shark will be launched from a catapult system and will climb to a desired altitude within the range of 100 to 3000 ft. (See Figure C-1). The aircraft will then travel in a rectangular path, 500 ft. by 1200 ft.. During the flight the Sky Shark's data acquisition system will take approximately twenty minutes of data while flying the 1200 ft. paths. The pressure distribution data will be stored on board the aircraft. Necessary associated data such as angle of attack, angle of roll, angle of yaw, velocity, etc. needed for the pilot to fly the aircraft will be sent to the ground through a telemetry system. The entire flight will last thirty minutes with a maximum length of forty minutes. Test sections of varying spans, 1 to 5 ft., will be used in the different flights. The sweep angle and angle of attack will be varied during flight from -20 to +30 degrees and -20 to +40 degrees respectively.

The Sky Shark will land within an 150 ft. radius landing zone. The aircraft will be capable of clearing a 50 ft obstacle at a glide slope angle of 10 degrees with a touchdown speed of approximately 40 ft/s. The landing will be facilitated by commercially available, spring loaded RPV landing gear. Turn around time from aircraft landing to relaunching will be about 15 minutes.

C: FIGURES

THE SKY SHARK

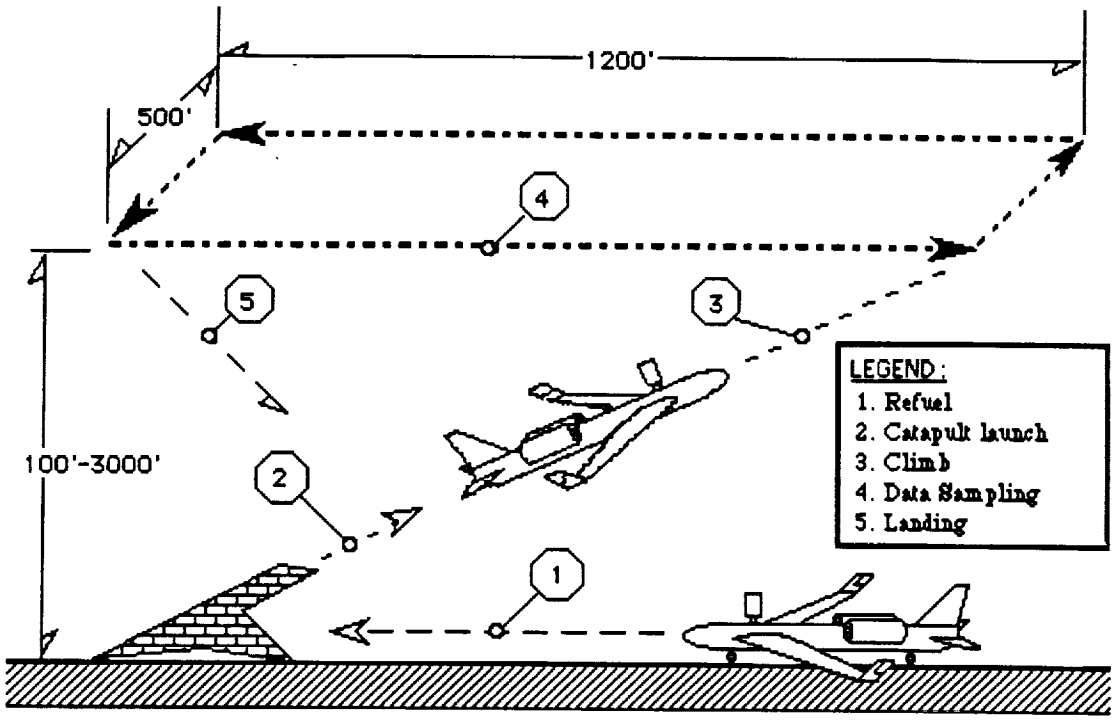

Mission Profile

D: CONCEPT SELECTION STUDIES

THE SKY SHARK

Before reaching the final design concept, several alternative concepts were seriously considered. As previously mentioned, two important design goals were established to be used as guide lines in the concept selection, highly accurate data acquisition and aircraft control (in the context of varying test configurations).

The major factor in the design of the aircraft was the location of the test specimen. According to our first guideline the test specimen needed to be located on the craft in an area which would experience the least amount aerodynamic interference. The first design concept considered, seen in Figure D-1, has the test specimen mounted on a pole in front of the fuselage. This puts the test specimen in a position where it will receive no interference from the rest of the craft. Unfortunately, along with structural dilemnas, this concept provides problems with the second design guideline, that of control. Under test conditions, the test specimen will generate lift and drag forces, and thus destabilizing moments. These moments can be reduced if the test specimen is located near the aircraft's center of gravity. However, with the test specimen located in front of the nose of the aircraft, the moment arm is increased considerably, resulting in very large pitching moments. Due to this problem, this concept was discarded as a possible design.

The next concept considered was an attempt to alleviate the problems experienced from the first concept. This design, veiwed in Figure D-2 has the test specimen mounted horizontally above the fuselage. As the figure shows the specimen is located toward the front of the craft, over the estimated location of the center of gravity. As mentioned earlier, by locating the specimen near the center of gravity, the magnitude of specimen induced moments is decreased due to a shortening of the moment arm. Although this concept helped the control problem it posed several problems pertaining to the accuracy of data acquisition. With the test specimen spanning over the wing, the potential for aerodynamic interference from the wing is present. Vibrational problems, arising from this mounting, may also harm test results. The possibility of structural problems supported the decision to eliminate this concept from further consideration.

Finally, a mounting concept which satisfied both design priorities was suggested. This mounting concept, the vertically mounted test specimen, is utilized in the final design, as seen in Figure B-1. The specimen is located over the center of gravity, as in the second concept; however, the vertical

mounting allows much more accurate testing. Since the specimen is vertical, it is not affected by wing interference. This mounting also reduces the vibrational and structural problems created by a horizontally mounted concept.

With the mounting concept selected, the rest of the plane needed a conceptual design. Two major concepts were considered, a rear wing, canard type configuration, and a typical front wing configuration. The canard configuration can be seen in Figure D-3. This concept, which was at first very popular, was found to be a poor choice for our mission. With a rear wing aircraft, the center of gravity must be located slightly in front of the wing in order to remain stable. This places the center of gravity in the aft section of the aircraft, which poses problems in the location of the test specimen. As previously mentioned, the test specimen must be located near the center of gravity to avoid large moments. If the specimen is moved to the rear of the aircraft it will experience an increased amount of interference. Thus this design concept is not feasible for the testing mission. Instead the forward located wing concept was selected. The final concept can be viewed in Figure B-1.

D: FIGURES

THE SKY SHARK

Figure D-1

Alternate Concept #1

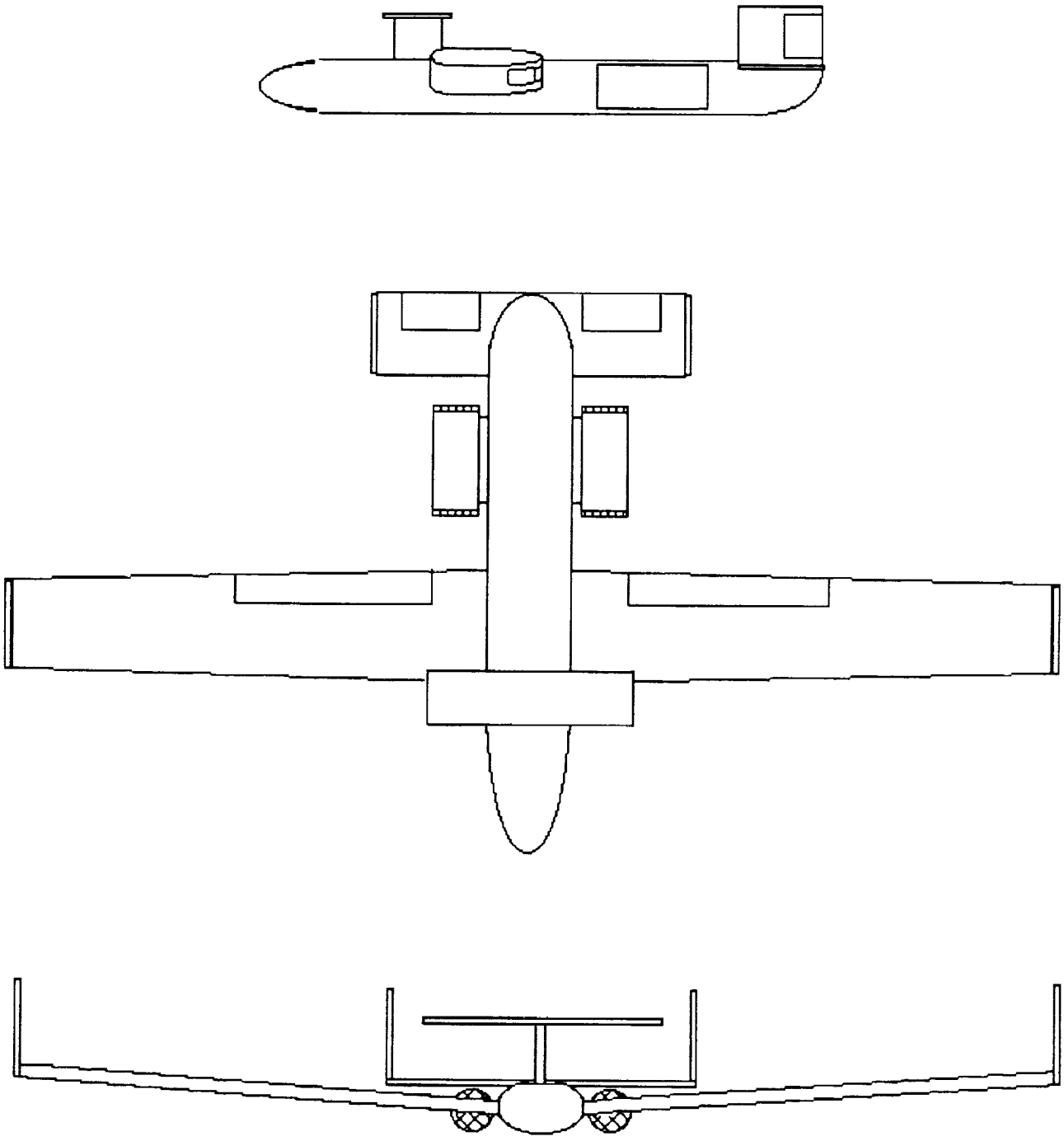

Figure D- 2

Alternate Concept # 2

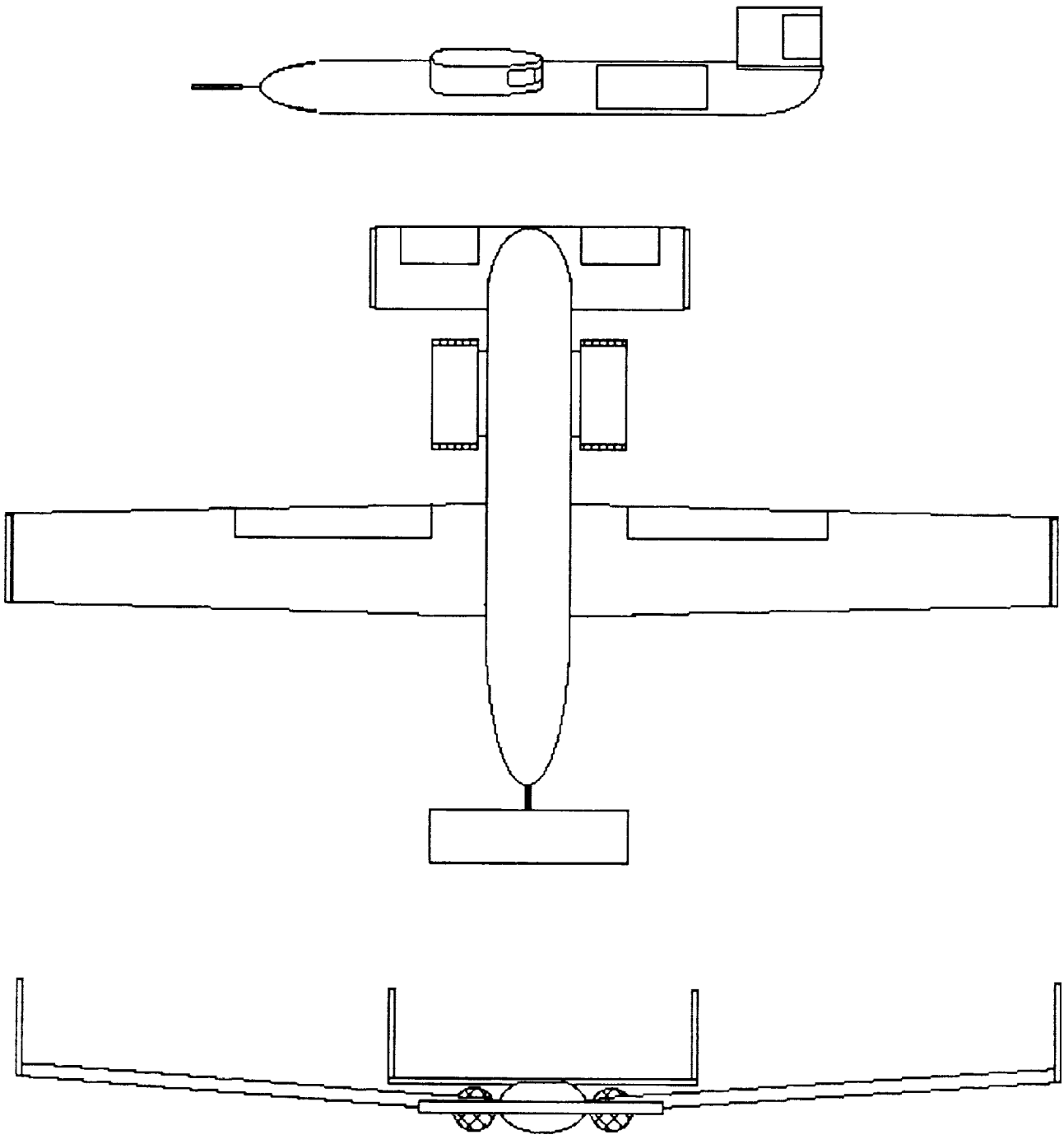

Figure D-3

Alternate Concept #3

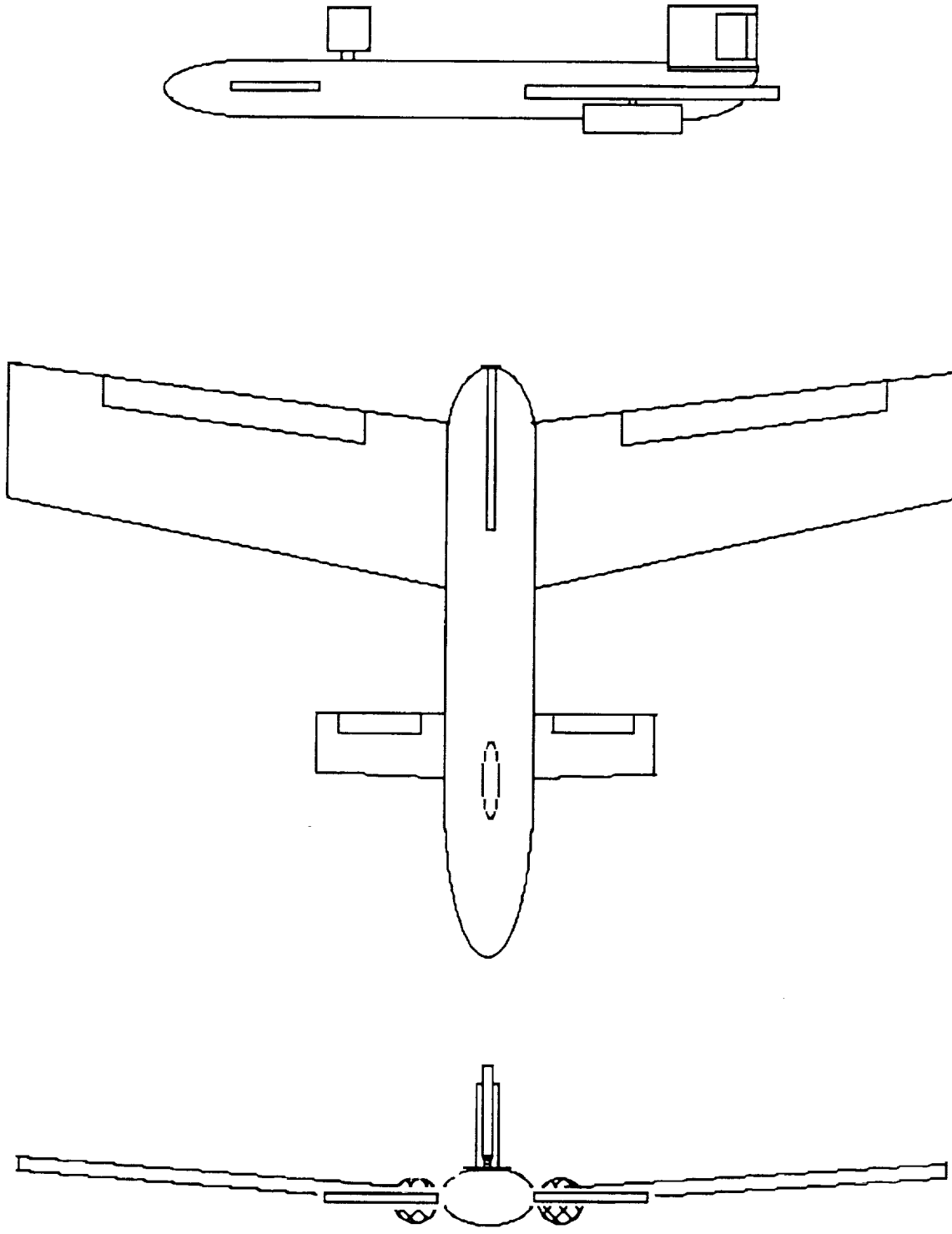

E: AERODYNAMIC DESIGN

THE SKY SHARK

In considering the different areas involved in aerodynamics, itself, it can be seen that there are three major subdivisions:

Airfoil Selection

Wing Configuration

Drag prediction

All three of these subdivisions will be discussed and examined in the following sections.

AIRFOIL SELECTION:

In an attempt to find the most appropriate airfoil for the Sky Shark many different types of airfoils were examined including Eppler, NACA, and Gottingen. It was originally decided to use a Gottingen 410 which is basically a symmetrical airfoil. It has a Clmax of .9 which is increased to 1.35 with a 30 degree flap deflection, and a Cl_α of 3.05/ rad. This decision was reconsidered later on in project due to this airfoil's substantial thickness ratio which causes an increase in drag over the wing. Another factor which lead to the reconsideration of this airfoil is the fact that there was a lack of experimental data found on this particular airfoil.

The airfoil finally decided upon was the NACA 1408. This airfoil is very slightly cambered and a good deal thinner than the Gottingen 410. The thickness of the respective airfoils can be seen on Figures E-1and E-2. It was decided to stay with an airfoil that was as symmetrical as possible because of the many positive attributes of symmetrical airfoils. Symmetrical airfoils perform better at higher velocities than highly cambered airfoils. They also eliminate the need for negative angles of attack and they have higher stall angles. Due to the demands of the mission, which call for flying over a wide range of Reynolds numbers and through a large variety of angles of attack, and because of the attributes of a symmetrical airfoil, the symmetrical or near symmetrical airfoil was decided to be the most appropriate for the Sky Shark.

The slight camber in the NACA 1408's design was found to provide an increase in lifting capabilities without sacrificing any of the above mentioned characteristics. The lift curve of the NACA 1408 can be seen and compared to that of the Gottingen 410 in Figures E3 and E4. The effects of a plain 30 degree flap deflection can also be seen and compared in these figures as well. The 30 degree flap deflection results in an increase in lift capabilities of approximately 44%.

In Chart E-1 (in Appendix) the important section characteristics are listed for both airfoils. It can be seen that the NACA 1408 has a 30% higher Cl_{max} then the Gottingen 410. The stall velocity has a corresponding decrease in value of approximately 16.5%. The lift curve slope of the Gottingen is 3.05 /rad and the lift curve slope of the NACA is 5.87/rad. In studying the chart it can be seen that there are many other benefits to using the NACA 1408 over the Gottingen 410.

WING CONFIGURATION:

The mission of Sky Shark is to be an airborne aerodynamic data acquisition system for collecting surface pressure distributions and other appropriate near field flow information on two and three dimensional lifting surfaces. In an attempt to meet the requirements needed to perform the mission, the Sky Shark must fly over a range of Reynolds number from 480,000 to 1,800,000 or over the equivalent velocity range of approximately 50 ft/s to 190 ft/s. A study was performed to help determine the optimum wing configuration for the successful completion of this mission. The study was performed through the use of two different computer programs which examined the effect that taper and incidence angle have on the lift coefficient and drag coefficient of the wing. The results of this study can be found on Chart E-2 (in Appendix).

Before going on to discuss the results of this study it is important to understand the constraints placed upon this mission. The first constraint placed upon this study is the mission profile itself. As mentioned previously, the Sky Shark must fly over a large range of Reynolds numbers and velocities, with a maximum thrust available of 15 lbs per engine or a total of 30 lbs. This obviously puts limitations on the amount of drag that can be generated. In this case, to successfully cover the velocity range with an acceleration capability of approximately 5 ft/s, the maximum allowable drag is 21 lbs, which translates into approximately 7.25 lbs of drag off the wing since wing drag is approximately 35 % of the total drag. A second limitation on the study is the weight of the remotely piloted vehicle (RPV). The Sky Shark is expected to weigh approximately 60. This places minimums on the amount of lift that must be generated. Another restriction is caused by the stability and control needs of this RPV. To guarantee roll stability, which is a considerable problem due to the vertically mounted test specimen, a 10 degree

dihedral is necessary on the wing. The presence of dihedral on a wing also effects lift and drag characteristics. A final constraint that must be considered is the lifting forces needed to take-off and land the RPV safely. To ensure such safety this vehicle requires a Cl_{max} of at least 1.2. Plain slotted flaps have been incorporated into the wing design to provide an increase in lift of approximately 44%. These flaps were chosen because of their ability to meet the mission requirements and because they are easier to manufacture then other types of flaps.

In this particular study, the effects of taper and incidence angle on the wing were examined. When examining each of these two variables individually, all other characteristics were held constant. The wing characteristics used in this study can be seen on Chart E-2 (in Appendix). The first trait to be examined was the effect taper had on the lift and drag coefficients of the wing. A range of taper ratios from .4 to 1.0 were examined. It was found that as the taper ratio increased (decrease in taper) from .4 to 1.0 the lift coefficient decreased from a maximum of .33742 to a minimum of .32329 and the drag coefficient increased from .02119 to .02976. Although these values followed the trend expected, they were extremely high. This is due to the fact that in the Lin Air Program steady level flight is not assumed. The angle of attack used in this part of the study provided the wing with an extremely large lifting force capability. The program, which is based on the circulation method of computing lift, provided a lifting force of almost 10 times the magnitude required for steady level flight. This extremely high value for the lift coefficient correspondingly caused the induced drag to be very great and beyond the capabilities of the engines.

Although these first values are not a reflection of the forces that the Sky Shark will undergo, they do, however, provide an indication of the trend caused by variations in taper. A graphical representation of these results can be seen in Figures E-5, E-6 and E-7. The first figure demonstrates the relationship between lift coefficient and angle of attack at various taper ratios. This figure shows that the taper ratio has little effect on the lift coefficient. The change in the lift value with taper is on the order of slightly less than 2%, with the higher degree of taper having the slightly higher lift coefficient. This leads to the conclusion that although taper has traditionally been used to redistribute lift over the wing it does not in fact provide any significant increase in the overall lift of the wing. The second figure provides a

comparison of the drag coefficients with changes in taper and the third figure provides the drag polar and its parallel variations with taper. In this case there is a more significant difference with changes in taper. These disparities become more pronounced with an increasing taper ratio. The highest degree of disparity is approximately 10% between taper of .8 and 1.0. So although taper does not significantly increase the lift of a particular wing it was found to cut back on the drag forces.

In order to make this study more practical to the overall Sky Shark mission an incidence angle was chosen for each taper ratio that provided a lift coefficient approximately equal to that which is necessary at steady level flight. This lift coefficient generated drag coefficients which were then used to calculate the drag of the Sky Shark over a velocity range from 50 ft/s to 190 ft/s. The numerical results of this study can be found in Chart E-3 (in Appendix) and a graphical representation of the drag results can be found in Figure E-8. As can be seen from this plot the drag disparities increase with increasing taper ratio and increasing velocity. This follows form with what wasdiscussed previously.

The second part of the trade study entailed examining the effect incidence angle has on the lift and drag coefficients of the wing. The incidence angle was varied through a range 0 degrees to 8 degrees. As was expected, the lift coefficient increased from a minimum value of .08053 at 0 degrees to a maximum value of .73585 at 8 degrees. The drag likewise did what was expected and increased from .01217 to .06166 over the same angle span. The rest of the results are listed on Chart E-2 and can be seen graphically on Figures E-9 and E-10. In trying to determine the optimum incidence angle the same considerations that were taken into account in the first part of this trade study such as maximum allowable drag and minimum lift coefficients had to considered. Another aspect that had to taken into account for this study was tip stall. The airfoil being used, the NACA 1408, stalls at angles of attack of approximately 11-12 degrees. Therefore, mounting the wing at high angles of incidence, not only increases drag significantly but also limits the aircraft's maneuverability by limiting the angles of attack at which it can fly.

In looking at the results of this incidence angle study, it is obvious that with an increase in incidence angle, there is a drastic increase in the drag coefficient and a favorable increase in the lift coefficient . Therefore, a

compromise must be made between these two factors. It can be seen that an incidence angle between 2.5 and 3.0 degrees provides not only one of the highest lift coefficients that has a drag coefficient that falls within the drag limitations but also provides the best trade off between the lift and drag.

In looking at the results of the taper ratio study there are various things to consider. Taper has been shown to be effective way to reduce wing drag. It was also shown, however, that it does not have any significant effect on the lifting force except in the sense of more evenly distributing it over the span of the wing and increasing the wing aerodynamic efficiency . All of these factors seem to lead to the conclusion that the lower the taper ratio, the better. Another aspect has to considered however, and that is the complication caused by large tapering in the sense of manufacturing and cost. For this particular case, the magnitude of the drag on the Sky Shark has not been deemed too much of problem and likewise there is no strong need to redistribute the lifting force over the wing span. Because of this, high degrees of taper are not necessary. A taper ratio between the range of .75 and .8 provides a substantial decrease in drag and a sufficient lift coefficient without being too taxing on the manufacturing and cost side of the project.

Three tools were used to perform this trade study. The first of which was the LinAir program written by Mr Ilan Kroo, copywrite 1987, and available in the Aerospace Computer Lab. This program calculated the lift and drag coefficients from inputted data values. The second and third programs were EXCEL and Cricket Graph which are for use on Macintosh computers. These programs were used primarily for more basic calculations and graphing results.

This study was an effort to determine the optimum wing configuration for the Sky Shark. The variables of taper and incidence angle were examined and their trends studied. It was found that the optimum incidence angle was between 2.5 and 3.0 degrees and the optimum taper was between .75 and .8. These parameters will aid in helping the Sky Shark meet it's mission profile of airborne aerodynamic data collection successfully.

Other aspects that were considered in the design of the wing was the need for aerodynamic twist and wing sweep. Both aerodynamic twist and wing sweep introduce major complications in the manufacturing and building of the wing. It was found that since the taper ratio of the wing was fairly high that there was no danger of stall and therefore no need for

aerodynamic twist. Wing sweep is used prinicipally at sonic and supersonic speeds and is therefore also not needed in this case.

DRAG ON AN ELLIPTIC CYLINDER:

The first step in the design process of an aircraft is to determine the component and overall weights. Then, before any other calculations such as stability and control, propulsion, materials, and performance, a size and shape had to be chosen for our fuselage that would minimize the drag and surface area yet maximize volume. Volume was an overriding consideration due to the amount of equipment that needed to be carried in the fuselage. Different sizes were discussed during the initial design phase such as circular cylinders, rectangular/square, and elliptic cylinders. Rectangular was immediately disposed of due to the fact that it would be a high drag shape. Elliptic and circular cylinders were close, but elliptic was chosen for our needs since many of the components were "short" which did not require a rounded, but rather, elliptical fuselage. Elliptic was also chosen for the fact that it gives "very low drag under all conditions." The final volume decided upon to accommodate our needs was approximately 11 cubic feet. This volume is less than the initially calculated volume since the propulsion system using ducted fans was moved to external pods on the outside rear of the fuselage. This eliminated a tremendous amount of room needed inside the fuselage that would be taken up by the propulsion units.

The total drag was the main concern since the two ducted fans used to power the Sky Shark provide a combined thrust of approximately 30 pounds. Thus, to minimize drag, the surface area needed to be minimized to cut down on skin friction drag. Also, as one would expect, less surface area means less material which, in turn, means less cost and less weight. After the profile of the fuselage was defined as an elliptical cylinder, the fineness ratio (twice the length of the semi-major axis divided by the length of the fuselage) was found to be very influential in determining the drag of the aircraft. As the fineness ratio approaches 1 the fuselage becomes a sphere, and when it approaches infinity, it resembles a flat plate. Actually the most important design variables were found to be the volume and the fineness ratio. Since there was very little of no information in Hoerner's Fluid Dynamic Drag on elliptic cylinders, Professor Dunn suggested that the report on The Martian Airship from the Spring of 88 be looked into. From that report, the drag coefficient was found to be the drag on a flat plate "enhanced with the effect of airship thickness, via the fineness ratio" (Ref 5) defined below:

$$C_{D_{wet}} = C_{D_f} \cdot (1 + 1.5(l/d)^{-1.5} + 7(l/d)^{-3})$$

The wetted surface area and volume were found using the following equations:

$$S_{wet} = 2 \cdot \pi \cdot ((a^2 + b^2)/2)^{.5} \qquad \text{Volume} = \text{Length} \cdot S_{wet}$$

The total drag on the fuselage was found using the following formula from Anderson's Introduction to Flight:

$$\text{Drag} = q \cdot S_{wet} \cdot C_{D_{wet}}$$

where $q = 1/2 \cdot \rho \cdot V^2$. The density was taken for a representative altitude of 1500 feet above sea-level and the velocity taken as 70 ft/s which is the cruise velocity. A computer program was implemented (see Appendix E-1) to perform these calculations and to make the plots.

As seen in Figure E-11, the wetted surface area increased linearly with increasing fineness ratio and volume. The results for several volumes were plotted for comparison. Also, the drag area of the aircraft was inspected versus fineness ratio and at several volumes for comparison. The drag area is defined as:

$$\text{Drag Area} = \text{Swet.}\ CD_V^{2/3}$$

where $C_{D_V}^{2/3} = S_{wet} \cdot C_{D_{wet}} / \text{Volume}^{2/3}$.

$C_{D_V}^{2/3}$ is the volumetric drag coefficient which is based on $\text{Volume}^{2/3}$ rather than surface area. The optimum fineness ratio was found from Figure E-12 to be 4.0 which corresponds to a drag area of approximately 10.0 square feet. However, due to limitations encountered with placing components inside the fuselage and the length the tail needed to be from the center of gravity of the aircraft to control the extra forces caused by the test specimen, it was determined that the length of the fuselage needed to be 10 feet long and .95 feet high. Thus, knowing this and that the eccentricity (e) of our elliptic cylinder was .8, the diameter (width) of the fuselage could be determined. Thus, the diameter of the fuselage was found to be 1.58 feet. These

measurements yield a fineness ratio of 6.33.

Checking Figure E-11 shows that the wetted surface area for a fineness ratio of 6.33 is approximately 40 square feet. The total drag, shown in Figure E-13, corresponding to this surface area and fineness ratio is approximately 9.7 pounds which is low enough so that the two ducted fans can overcome this drag along with the drag of the other aircraft components.

Comparing the geometries for the optimum fineness ratio and the one chosen shows that although the chosen l/d is 36.8% greater than the optimum, the surface area is 7.5% larger. For total drag, that for the optimum case is 22.6% less than for the fineness ratio of 6.33. However, since the two ducted fans are putting out a combined thrust of 30 pounds the decrease in drag does not justify an increase in surface area. The increase in surface area leads to an increase in material which results in increased cost and weight. Thus the final design, has a volume of 11 cubic feet, a fineness ratio of 6.33 (e=.8, a=.79, b=.47, l=10 feet) and a total drag of 9.7 pounds at a velocity of 70 ft/s and an altitude of 1500 feet.

E: APPENDICES

THE SKY SHARK

CHART E1

NACA 1408 AND GO 410

AIRFOIL SECTION CHARACTERISTICS

	WITHOUT FLAP		WITH 30 DEGREE FLAP DEFLECTION	
	NACA	Go	NACA	Go
$Cl_{\alpha=0}$	.100	-.075	.71	-.095
$\alpha_{L=0}$	.0175 rad	.0174 rad	-.105 rad	.0174 rad
Cl_{α}	5.87 / rad	3.05 / rad	5.87 / rad	3.05 / rad
Cl_{max}	1.35	.9	1.94	1.36
α_{stall}	.262 rad	.199 rads	.183 rad	.146 rads
V_{stall}	34.16 ft/s	44.2 ft/s	28.5 ft/s	36.78 ft/s

	A	B	C	D	E	F
1	TAPER	CD	CL	INCIDENCE AN	CLi	CDi
2	0.4	0.02119	0.33472	0	0.08053	0.01217
3	0.425	0.02333	0.33448	0.5	0.12168	0.01434
4	0.45	0.02371	0.33418	1	0.16282	0.01662
5	0.475	0.02394	0.33385	1.5	0.20395	0.01904
6	0.5	0.02406	0.33349	2	0.24506	0.02158
7	0.525	0.02414	0.33309	2.5	0.28615	0.02424
8	0.55	0.02446	0.33267	3	0.32721	0.02703
9	0.575	0.02468	0.33223	3.5	0.36825	0.02994
10	0.6	0.02481	0.33177	4	0.40926	0.03298
11	0.625	0.02503	0.33129	4.5	0.45023	0.03614
12	0.65	0.0252	0.3308	5	0.49117	0.03942
13	0.675	0.02532	0.3303	5.5	0.53207	0.04283
14	0.7	0.02579	0.32979	6	0.57292	0.04635
15	0.725	0.02591	0.32926	6.5	0.61373	0.05
16	0.75	0.02612	0.32874	7	0.65449	0.05377
17	0.775	0.02659	0.3282	7.5	0.6952	0.05766
18	0.8	0.02706	0.32766	8	0.73585	0.06166
19	0.825	0.02728	0.32712			
20	0.85	0.0276	0.32657			
21	0.875	0.02802	0.32603	CONSTANTS		
22	0.9	0.02849	0.32548			
23	0.925	0.02865	0.32493	TAPER =.8		
24	0.95	0.02912	0.32438	ALL OTHERS AS BEFORE		
25	0.975	0.02949	0.32383			
26	1	0.02976	0.32329			
27						
28	CONSTANTS					
29						
30	WING AREA=	34 FT2	ALPHA=	1 DEGREE		
31	SPAN=	17 FT	CD(LIFT)=	0.044		
32	DIHEDRAL=	12 DEGREES	MACH=	0.1		
33	ROOT INCIDENC	E=3 DEGREES	TIP INCIDENCE	3 DEGREES		
34	ASPECT RATIO	8.5	EFFICIENCY=	0.85		

	A	B	C	D	E
1	velocities	Drag 1.0	drag (.8)	Drag (.6)	Drag (.4)
2	60	1.5216768	1.12137984	0.7814016	0.54698112
3	70	2.0711712	1.52632256	1.0635744	0.74450208
4	80	2.7052032	1.99356416	1.3891584	0.97241088
5	90	3.4237728	2.52310464	1.7581536	1.23070752
6	100	4.22688	3.114944	2.17056	1.519392
7	110	5.1145248	3.76908224	2.6263776	1.83846432
8	120	6.0867072	4.48551936	3.1256064	2.18792448
9	130	7.1434272	5.26425536	3.6682464	2.56777248
10	140	8.2846848	6.10529024	4.2542976	2.97800832
11	150	9.51048	7.008624	4.88376	3.418632
12	160	10.8208128	7.97425664	5.5566336	3.88964352
13	170	12.2156832	9.00218816	6.2729184	4.39104288
14	180	13.6950912	10.0924186	7.0326144	4.92283008
15	190	15.2590368	11.2449478	7.8357216	5.48500512
16					
17	CONSTANTS				
18					
19	DENSITY=	2.24X10-3			
20	S=	34 FT2			
21	ANGLE OF ATTACK = .5 DEGREES				

```
      DIMENSION SWET(25,5),L(25),DAREA(25,5),D(25,5)
      DIMENSION DIAM(25),VOLUME(5)
      REAL L,LENGTH
      B=.474
      V=70.
      CDF=.002
      PI=4.*ATAN(1.)
      RHO=2.2743E-3
      Q=.5*RHO*V**2
      LENGTH=0.
      DO 5 K=1,5
        VOLUME(K)=2*K+5
      Z=1.
      DO 10 I=1,25
      LENGTH=Z
      DIAM(I)=2*VOLUME(K)/(PI*B*LENGTH)
      L(I)=LENGTH/DIAM(I)
      SWET(I,K)=2.*PI*(SQRT(((.5*DIAM(I))**2+B**2)/2))*LENGTH
      CDWET=CDF*(1.+1.5*(L(I))**.667+7*(L(I))**.333)
      CDV23=CDWET*SWET(I,K)/(VOLUME(K)**.667)
      D(I,K)=Q*CDWET*SWET(I,K)
      DAREA(I,K)=CDV23*SWET(I,K)
      Z=Z+.5
   10 CONTINUE
    5 CONTINUE

      CALL TPLOT(-011,L,SWET,25,25,5)
      CALL TLABEL('L/D','Swet (square feet)')
      CALL TITLE ('FINENESS RATIO VERSUS WETTED SURFACE AREA')
      READ(1,*) X
      CALL TPLOT(-011,L,DAREA,25,25,5)
      CALL TLABEL('L/D','DRAG AREA')
      CALL TITLE('FINENESS RATIO VERSUS DRAG AREA')
      READ(1,*) X
      CALL TPLOT(-011,L,D,25,25,5)
      CALL TLABEL('L/D','TOTAL DRAG (pounds)')
      CALL TITLE('FINENESS RATIO VERSUS TOTAL DRAG')
      STOP
      END
```

APPENDIX E.1

E: FIGURES

THE SKY SHARK

FIG E1: NACA 1408 Airfoil Section

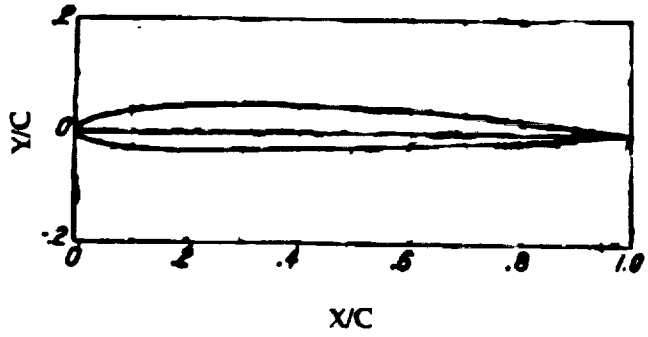

FIG E2: Gottingen 410 Airfoil Section

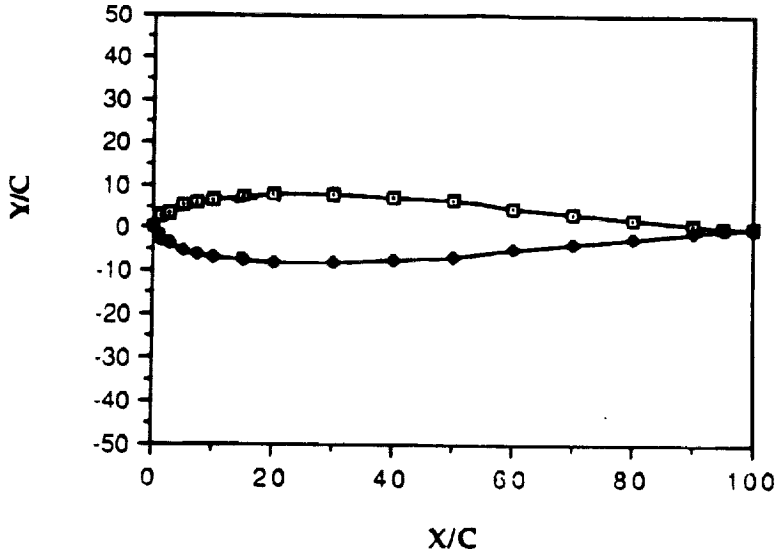

FIG E3: NACA 1408 Lift Curve Slope

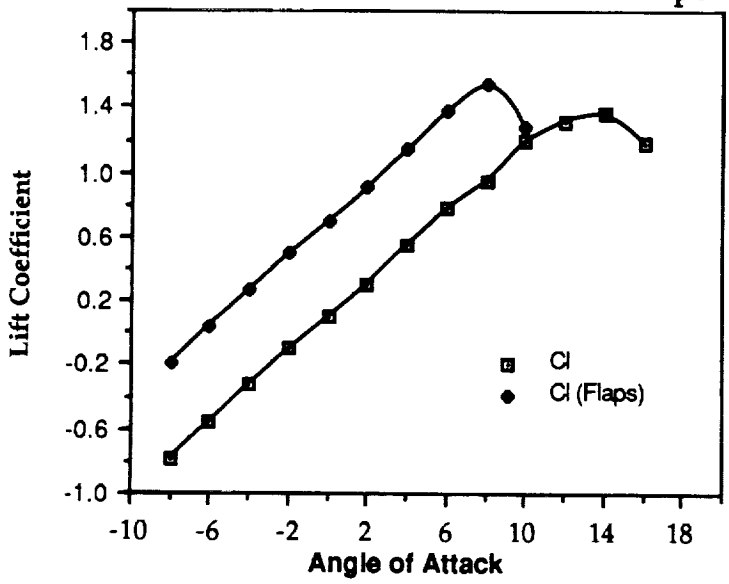

FIG E4: Gottingen Lift Curve Slope

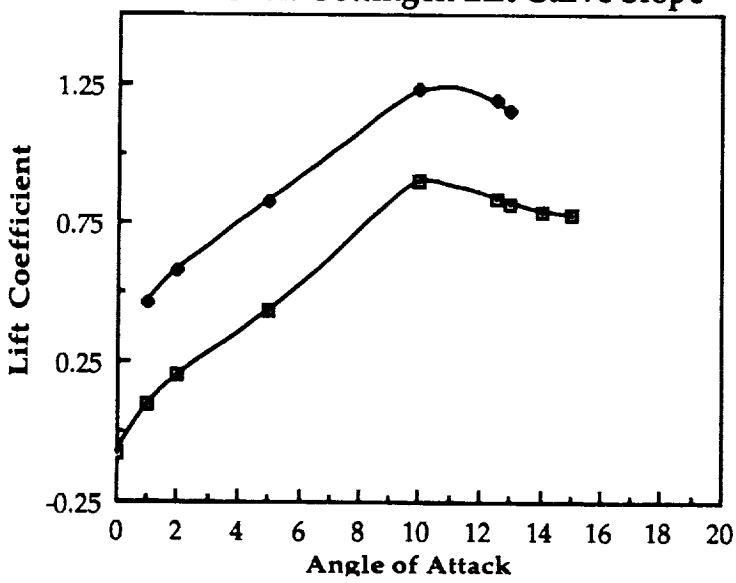

FIG E5: Cl vs Angle of Attack at Various Taper Ratios

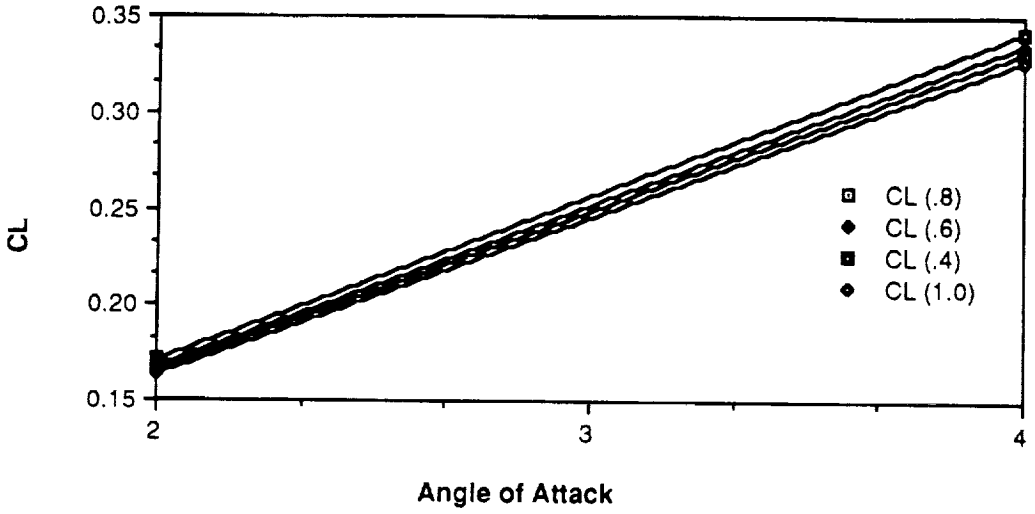

FIG E6: Cd vs Angle of Attack at Various Taper Ratios

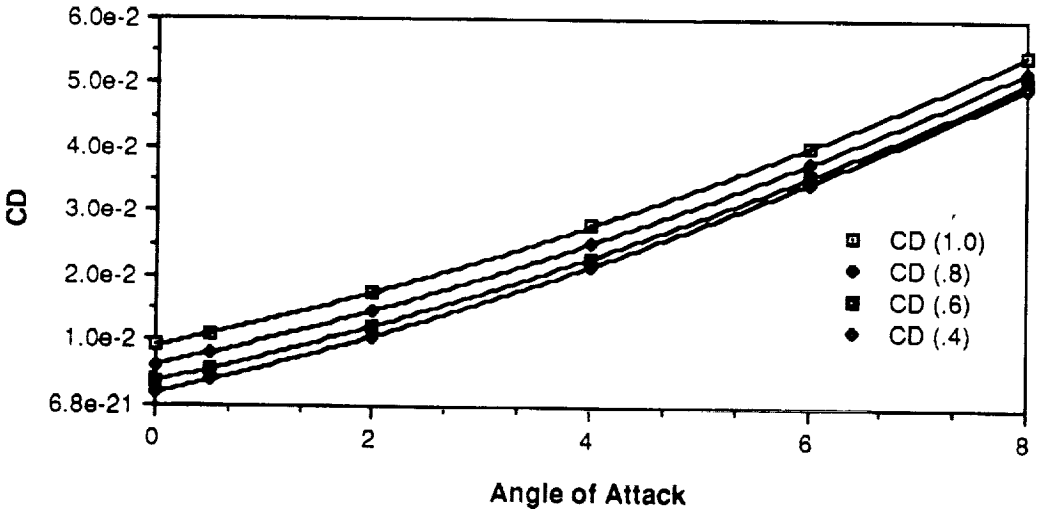

FIG E7: Drag Polar for Various Taper Ratios

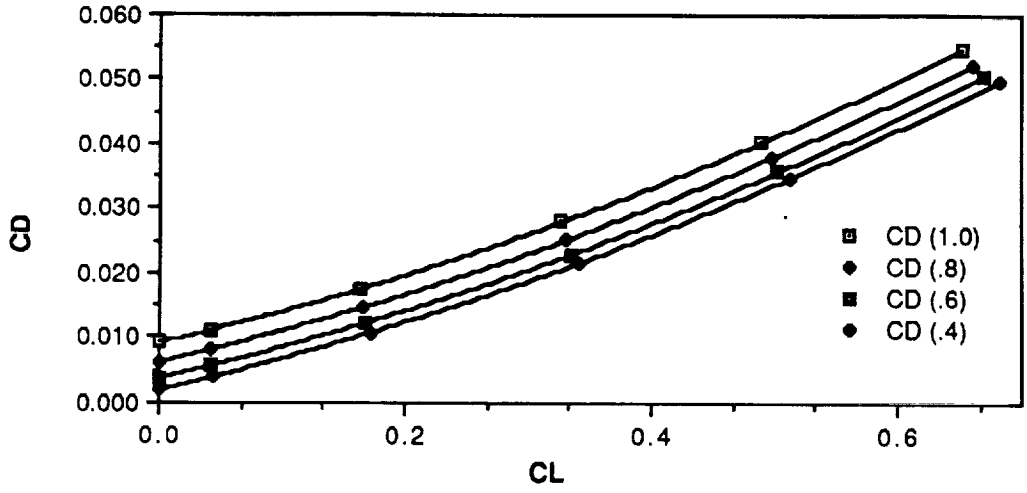

FIG E8: Drag vs Velocity for Various Taper Ratio

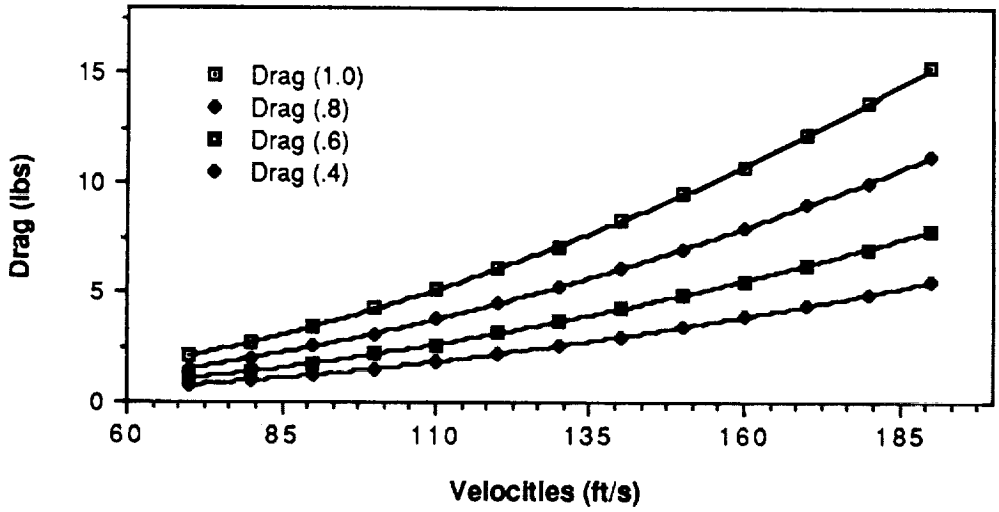

FIG E9: CL as a Function of Incidence Angle

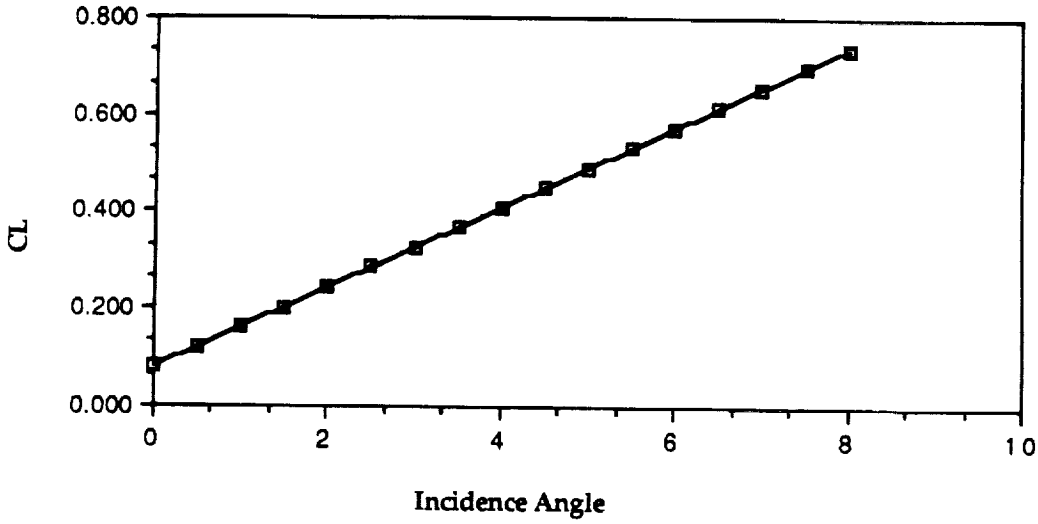

FIG E10: Cd as a Function of Incidence Angle

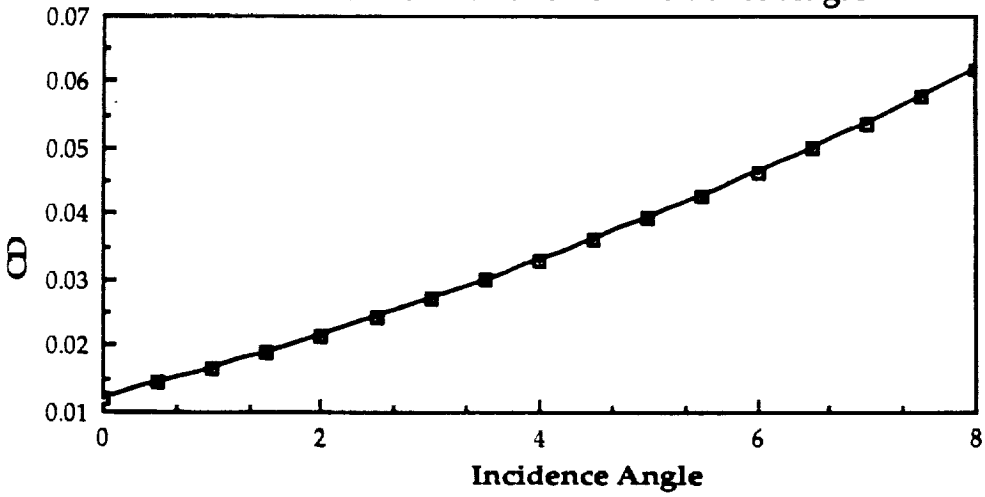

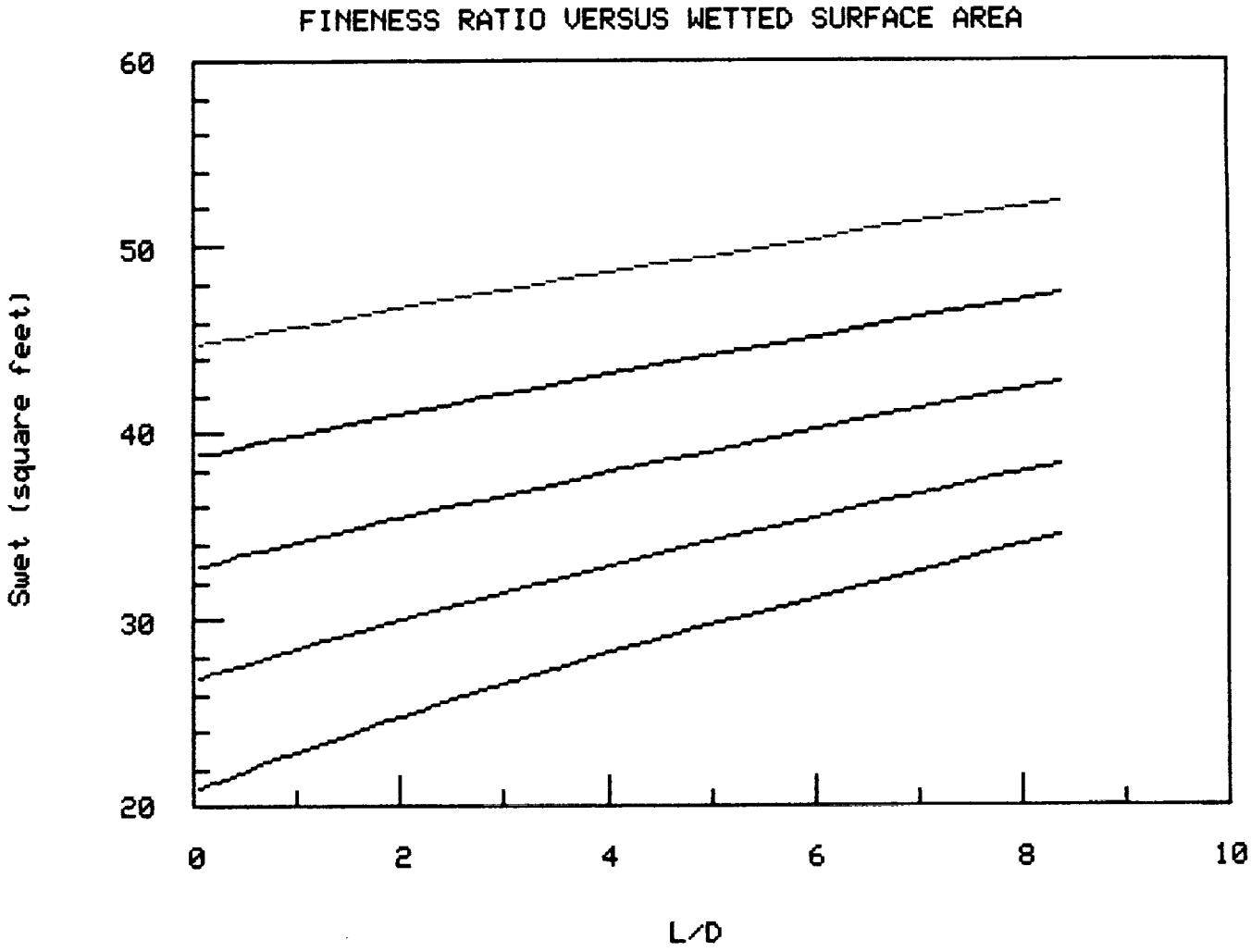

FIGURE E.11

Blue: 15 ft^3
Violet: 13 ft^3
Green: 11 ft^3
Red: 9 ft^3
Black: 7 ft^3

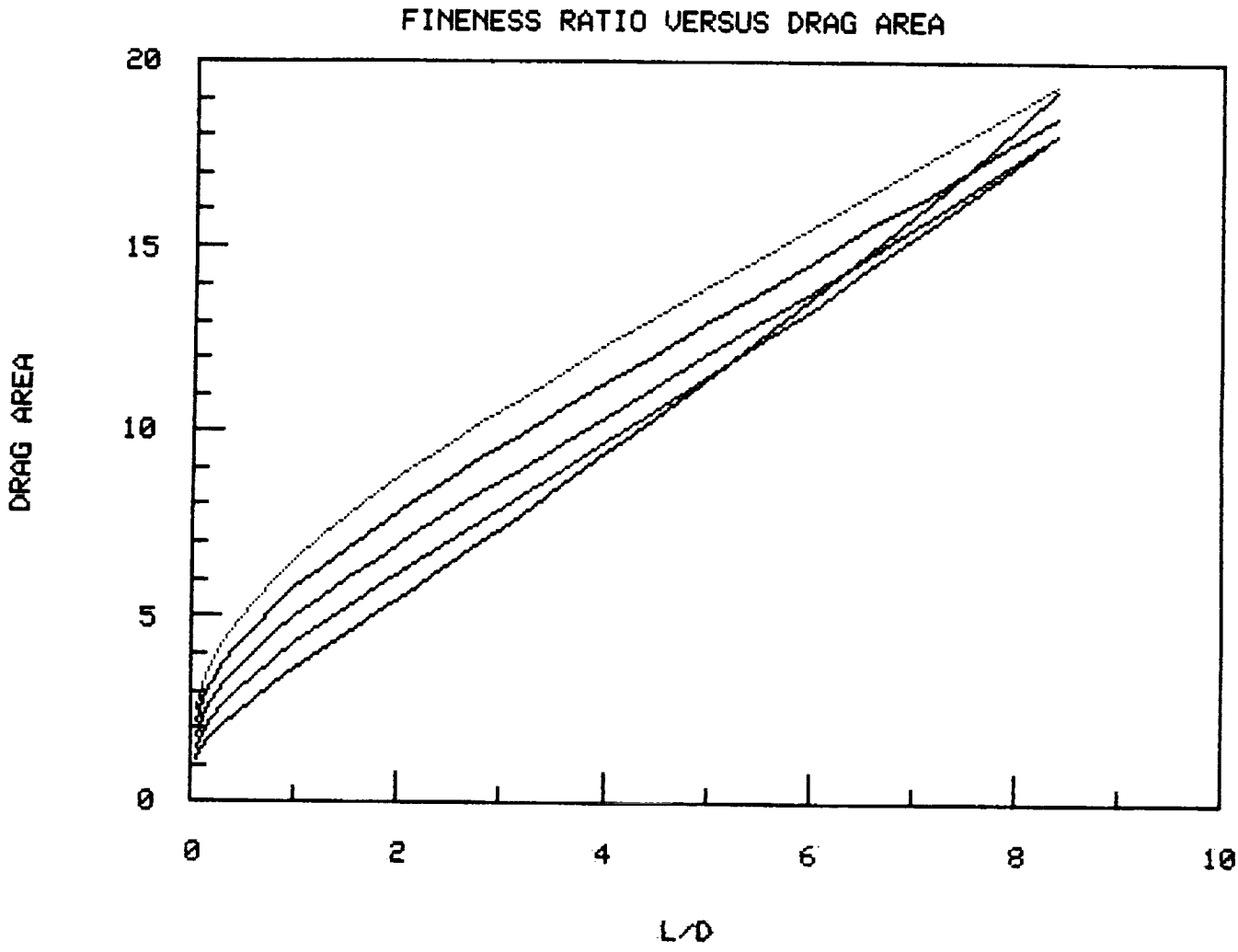

FIGURE E.12

Blue: 15 ft^3
Violet: 13 ft^3
Green: 11 ft^3
Red: 9 ft^3
Black: 7 ft^3

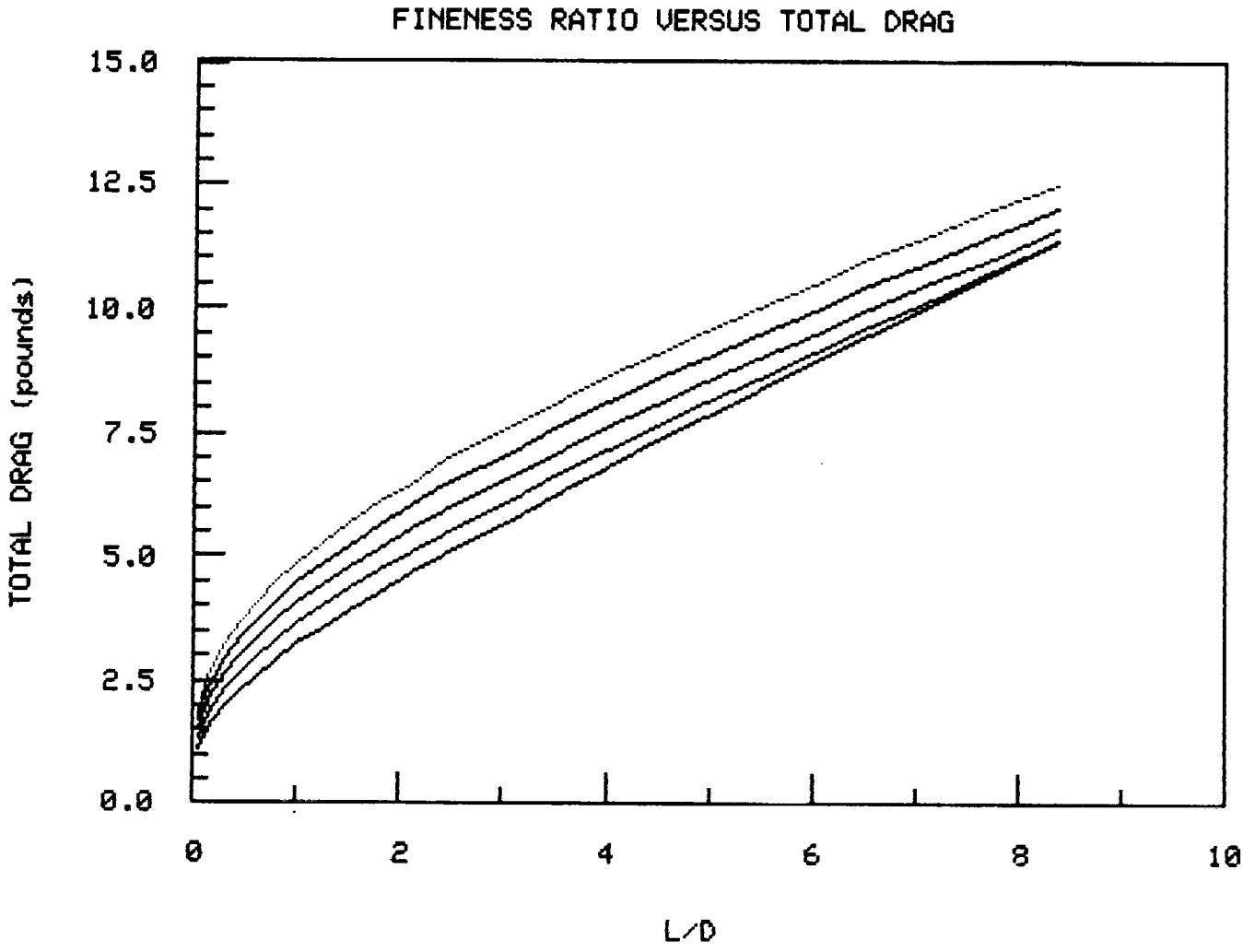

FIGURE E.13

Blue: 15 ft^3
Violet: 13 ft^3
Green: 11 ft^3
Red: 9 ft^3
Black: 7 ft^3

F: PROPULSION SYSTEM

THE SKY SHARK

PROPULSION SELECTION:

The choice of a propulsion system was a crucial step in the design of the Sky Shark. The aircraft will have two ducted fan engines as its means of propulsion. The ducted fan system, as shown in Figure F-1, consists of a ducted cowling, an impeller, a stator, and the engine which drives the impeller. This system was chosen for reasons dealing with accurate data acquisition. One of the primary design goals of the Sky Shark was to allow the aircraft to be extremely accurate in its reading of pressure distributions on the test specimen. One major fear of the design team was the effect the propulsion unit might have on test readings. It was felt that a propellor driven aircraft might cause aerodynamic interference due to propwash. By cowling the propellor, as in the ducted fan system, these potential problems can be alleviated.

In order for the ducted fan to be an effective mean of propulsion, the proper engine must be chosen. Several factors affected the choice of the engine, including thrust, weight, specific fuel consumption (SFC), cost, RPM, and tip speed. In choosing an engine for the Sky Shark and its mission, thrust and weight were the primary design variables. Cost was considered a secondary variable, and was used as the final deciding variable. With an initial estimate of the thrust needed from the power plant, eight engines were picked for closer examination. The eight engines, and some of there specifications can be seen in Appendix F-1. Before the engines were selected a list of preliminary requirements was created, including brake horsepower (BHP), and RPM ranges. The thrust range needed from the powerplant was determined from a power required plot for the Sky Shark. Using the drag breakdown method, a drag polar was derived and used to calculate the power required, where,

$$C_d = .023 + .044\, C_l^2$$

$$D = 1/2\, \rho\, V^2\, S C_d$$

$$P_r = DV$$

The power required was then plotted over a velocity range from 0 ft/s to 200 ft/s. This range was chosen as the desired velocity range for the Sky

Shark due to mission requirements. The purpose of the aircraft is to gather airborne data on a test specimen over a Reynolds number range of $4x10^4$ to $1x10^6$. In order for the higher Reynolds numbers to be reached, a flight speed of 190 ft/s is desired. In order to get an idea of the thrust needed to attain a flight speed of 190 ft/s, power available curves were plotted for thrust ratings of 30 lb, 40 lb, and 50 lb. In order to reach 190 ft/s, 30-35 lbs of thrust is required. Since the Sky Shark has a twin ducted fan system, each engine must be capable of producing approximately 15-18 lbs of thrust. For a ducted fan engine, for every BHP the engine can produce around 5 lbs of thrust. Thus, the engines selected for the study were required to produce approximately 3 BHP.

Engine RPM was also used as a preliminary criteria. From the book R/C Ducted Fans by Frank Fanelli, it was found that ducted fan engines are most efficient when the impellor is run at a tip speed of 300 mph. A formula was found in Fanelli's book which estimated RPM for a particular engine and tip speed, where,

$$\text{tip speed} = 2\pi r \times \text{RPM} \times 60 / 63360$$

In this formula r is equal to the radius of the impeller. For the Sky Shark, a 4" radius impeller will be used. Thus, for an optimum tip speed of 300 mph, the optimum RPM is near 12,000. This can be seen graphically in Figure F-2, where tip speed is plotted verses RPM for an 8" diameter impeller. It is also important to note that at tip speeds over 350 mph, the ducted fan becomes inefficient. For the 8" impeller, this corresponds to a tip speed of 15,000. Thus, when selecting the eight engines for further examination, RPM was also considered.

With the eight engines selected by general requirements , it was time to examine these engines in more detail. To begin, the power available for each engine was plotted against the power required. The results can be seen in Figure F-3. Of the eight engines, five of them met the power requirements needed to attain a maximum velocity of 190 ft/s, the FK 50, the Q35XS, the OPS .65, the ENYA VT-240, and the MAX-108. A maximum velocity of 175 ft/s, 15 ft/s below the desired velocity, was used as the cut off point. Three of the possible engines could not power the Sky Shark over 175 ft/s, the P80, the MAX-65, and the S2000. These engines were eliminated from further

consideration.

The five remaining engines all possessed the power to allow the Sky Shark to accomplish its mission requirements; therefore, the choice of the most desirable engine was performed by examining other engine characteristics. Weight and cost were the primary considerations used. The total weight of each engine was determined and is listed in Appendix F-2. The total engine weight was found to have two contributing factors, the engine weight and the weight of the fuel needed for the 40 minute mission. The fuel weight was found by multiplying the specific fuel consumption, in Appendix F-1 , by the flight endurance time of 40 minutes. Ounces were converted to pounds and put into Appendix F-2.

In order to understand the affect of weight upon the performance of the engine, a thrust to weight ratio (T/W) was calculated for each of the engines. A T/W of 2 or higher was considered desirable, and four of the engines satisfied this criteria, the Max-108, the FK 50, the Max-654, and the P80 Aero. The comparative nature of T/W for the various engines can be seen in Figure F-3. Of these four engines, two had met the thrust requirement previously established, the Max 108 (2.10) and the FK 50 (2.85).

Of these two engines, the Fk 50, with the much higher T/W, appears to be the best engine. However, one other parameter must be considered, cost. While the FK 50 has the higher T/W , it is much more expensive than the Max 108. As Appendix F-1 showed, the FK 50 costs $995, while the Max 108 costs $175, a difference of $820. The Max 108 was chosen to power the Sky Shark due to its low weight, low cost, and its thrust rating. The Max 108's specifications are listed below for convenience, and its power curve is shown in Figure F-4.

BHP: 3
RPM: 16,000
TOTAL WEIGHT: 7.15 LBS
SFC: 2.2 OZ/MIN
COST: $175

PROPELLOR DESIGN:

An acceptable design for the propellor was one for which the diffusion coefficient, a dimensionless quantity indicating the magnitude of the stress loading on a blade, did not excede a value of .6 at the hub or the tip. This value was an approximation made for the maximum loading certain families of blade profiles may withstand. It was also considered desirable to have a low static pressure gradient across the rotor, preventing the stator from undergoing a large loading in order to match the equilibrium condition.

The parameters defined in this analysis were the change in stagnation enthalpy across a blade row (ΔH), dimensionless angular velocity (Ω), blade angle of attack (alpha), relative incidence flow angle to the rotor blades (β_1), dimensionless fan radius (R), solidity (sigma), and radial location (y). ΔH was a quantity which indicated the change in enthalpy across the blade row and determined β_2. A computer program (Appendix F-3) returned both radial (V1 and V2) and axial (W1 and W2) velocity profiles at points far upstream and downstream of the impeller, as well as diffusion coefficients (D) for the blade and the degree of reaction (°R) for the blade at the hub and tip. The definitions of these quantities were presented below.

$$W = \frac{w}{w_o} \qquad V = \frac{v}{w_o} \qquad \Psi = \frac{\psi}{w_o r_{hub}^2} \qquad H = \frac{h_{tip}}{w_o^2} \qquad y = \frac{r}{r_{hub}} \qquad R = \frac{r_{tip}}{r_{hub}}$$

For this design the radius and omega quantities were fixed based on a simple propeller theory analysis and a tip speed calculation. The thrust required was estimated to be approximately 30 lbs for a low drag aircraft configuration traveling at 190 ft/s. The radius and angular velocity were determined based upon a given thrust and tip velocity. The resulting angular velocity and impeller diameter were determined to be 16,000 rpm and 8 in, respectively. Based upon statistical data from model ducted fan units, the hub size was estimated at a 2 in diameter. The freestream and angular velocities gave a value of .482 for Ω and R was set at 4.

Relation of Parameters to System Performance:

The resultant quantities, velocity profile, diffusion coefficients and

degrees of reactivity, were determined through calculation of the stream function at N different radial locations for points both far upstream and far downstream of the blade row. For this analysis a perfect incompressible flow was considered, and this was supported by a mach number of .35 at the tip of the blade. For simplicity, the system was also defined as having no variation in the change of stagnation enthalpy (ΔH) across the length of the blade and the swirl term was neglected, giving a final streamline equation of the form:

$$\Psi = \left(\frac{\beta}{\alpha} + \frac{1}{2}\right) y \frac{U_1(\alpha y)}{U_1(\alpha)} - \left(\frac{\beta}{\alpha} + \frac{R^2}{2}\right) y \frac{W_1(\alpha y)}{R U_1(\alpha)} + \frac{\beta}{\alpha}$$

å

The U1 and W1 terms indicated the following functions:

$$U_1(\alpha y) = J_1(\alpha y) Y_1(\alpha R) - J_1(\alpha R) Y_1(\alpha y)$$

$$W_1(\alpha y) = J_1(\alpha) Y_1(\alpha y) - Y_1(\alpha) J_1(\alpha y)$$

The J_1 and Y_1 terms indicated the appropriate first order Bessel functions. $ß_2$ was then related to $ß_1$ based upon enthalpy change and angular velocity as follows:

$$\beta_2 = \beta_1 + \frac{\Delta H}{\Omega}$$

Axial velocity components were then determined from the derivative of the stream function as shown:

$$W = -\frac{1}{y}\frac{d\Psi}{dy}$$

The radial velocity was a function of the stream function, flow angle and vertical location as shown:

$$V = \left(\frac{1}{y}\right)(-\alpha\Psi + \beta)$$

After the velocity profiles had been calculated, tip and hub velocity magnitudes were determined, enabling the calculation of diffusion coefficient

and degree of reaction terms. These quantities were defined as follows:

$$D = \left(1 - \frac{V_e}{V_i}\right) + \frac{\Delta H}{2\Omega V_i \sigma}$$

$$^{\circ}R_h = 1 + \frac{1}{2\Delta H}\left(V^2_{e\,hub} - V^2_{i\,hub}\right)$$

$$^{\circ}R_t = 1 + \frac{1}{2\Delta H}\left(W^2_{1\,tip} + V^2_{1\,tip} - W^2_{2\,tip} - V^2_{2\,tip}\right)$$

These analysis and techniques are more thoroughly presented and derived in the reference. The computer code generated to solve this system of equations is included in Appendix F-3.

Results:

Initial quantities for blade angle of attack, relative flow incidence angle, solidity, and enthalpy change were estimated. Alpha was initially set at .15. The flow incidence angle was estimated by considering flow coming straight at the blade row turning at 16,000 rpm. and was set at -1.3997. The solidity was initially set to 1., indicating a blade spacing equal to the blade chord length. The enthalpy change was arbitrarily set to a value of .9. Resultant velocity profiles for this case were recorded in Figure F-5. These profiles showed an increase in the radial velocity and a slight change in the axial velocity, as would be expected. Diffusion coeficients for this case were .476 at the hub and .508 at the tip. The degree of reaction was determined to be 1.553 and 1.121 at the hub and tip respectively.

The first parameter varied was the solidity. Data was generated for solidity factors ranging from .3 to 5.0 and the diffusion coeficients were recorded in Figure F-6. It was interesting to note that, also shown in the radial equilibrium equations, the solidity did not affect the axial or radial velocity profiles. As shown in the Figures, D decreases with increasing solidity at the hub and tip. This was a useful insight in that it can be seen that a high blade loading, indicated by a coefficient of diffusion, can be decreased by the addition of more blades.

With all other parameters held constant, variations were made in

blade angle of attack, alpha, from .05 to .4. Velocity profiles for angles of attack of .05 and .15 were calculated in order to determine the effects of angle of attack variation. Figures F-7 and F-8 illustrated the changes in both upstream and downstream axial velocity profiles. As a was increased , the upstream axial velocity profile became more pronounced, slower at the hub and quicker at the tip. With an increase in a, the downstream axial velocity profile showed the opposite tendency, decreasing at the tip while increasing at the hub. Figure F-9 illustrated the change in the upstream radial velocity profile. As a was increased, the magnitude of the radial velocity profile decreased along it's entire length. The downstream radial velocity profile remained unaffected by a change in blade angle of attack. Plots of diffusion coefficient variation with a and degree of reaction variation with a were included as Figures F-10 and F-11. The diffusion coefficient at the tip of the blade showed minor variation, varying from approximately .53 at a=.05 to .46 at a=.40. Where this might have indicated a potential way of decreasing blade loading, the diffusion coefficient at the hub shows an increase with increasing a. At a=.05, the hub diffusion coefficient was approximately .35, while at a=.4 the diffusion ccoefficient had climbed to .70. Degree of reaction values at the hub showed a heavy decrease with increasing angle of attack while values at the tip showed a slight increase.

The flow incidence angle was varied from .3 to 1.3 and its effects on diffusion and degree of reaction were examined. Changes in β_1, flow incidence angle, might be physically implemented through the use of inlet guide vanes to alter flow angle. Diffusion coefficients at both the hub and tip decreased with increasing flow angle, as shown in Figure F-12. The decrease at the hub was substantial, approximately 60%, from a diffusion coefficient of .95 at β_1=.30 to .37 at β_1=1.5. Decreases at the tip where small. Changes in degree of reaction were recorded in Figure F-13. As shown, variation in the tip value was very small while the hub value increased from -.75 to 1.75 across the β_1 range from .3 to 1.5.

Variation in the enthalpy drop across the blade row, was then investigated. The enthalpy drop across a blade row was a function determined by the blade aerodynamics and may be varied or chosen with careful selection of a blade family. A plot of the diffusion coefficient as a function of ΔH was shown in Figure F-14. Variation at the hub was linearly increasing , from a value of .1 at ΔH=.3 to .65 at ΔH=1.1. Variation at the tip

was a slight cup followed by a linear increase, from a value of -.03 at ΔH=.3 to .70 at ΔH=1.1. A plot of the variation in the degree of reaction with ΔH was shown in Figure F-15. The degree of reaction at the hub had very small variation, while the value at the tip showed a substantial decrease with increasing ΔH. The tip values progressed from 2.7 at ΔH=.3 to 1.2 at ΔH=1.1.

The data presented in this trade study would be useful in continuuing the design of the ducted fan. Certain trends became evident with variation of the parameters at the designer disposal. The decrease in blade loading for an increase in solidity, for example. At this point more sophisticated design methods would have to be utilized incorporating blade profiles and developing values for thrust and torque.

F: APPENDICES

THE SKY SHARK

APPENDIX F-1

Engine Specifications

ENGINE	BHP	RPM	WEIGHT (lbs)	SFC (oz/min)	COST ($)
Max 108 FSR (OS)	3.0	16,000	1.65	2.20	175
Enya-VT-240 (Enya)	3.2	10,500	3.80	2.40	654
P80 AERO (Picco)	2.2	14,500	1.25	1.65	149
FK 50 (Karan)	4.4	9,200	5.70	0.80	995
Max-654R-DF (OS)	2.8	22,000	1.23	2.10	225
Q 35XS (Quadra)	3.1	9,000	3.20	2.32	140
OPS .65 Speed (Shamrock)	3.7	20,500	4.40	2.78	300
S2000 RC (Supertigre)	2.8	13,000	2.64	2.10	150

APPENDIX F-2

THRUST AND WEIGHT DATA FOR 1ENGINE IN THE 40 MINUTE MISSION SCENARIO

ENGINE	WEIGHT OF ENGINE (lbs)	WEIGHT OF FUEL (lbs)	TOTAL WEIGHT (lbs)	THRUST (lbs)	T/W
Max 108 FSR (OS)	1.65	5.50	7.15	15	2.10
Enya-VT-240 (Enya)	3.80	6.00	9.80	16	1.63
P80 AERO (Picco)	1.25	4.13	5.38	11	2.05
FK 50 (Karan)	5.70	2.00	7.70	22	2.85
Max-654R-DF (OS)	1.23	5.25	6.48	13.8	2.12
Q 35XS (Quadra)	3.20	5.81	9.00	15.5	1.72
OPS .65 Speed (Shamrock)	4.40	6.94	11.34	18.5	1.63
S2000 RC (Supertigre)	2.64	5.25	7.89	14	1.77

Appendix F-3

```
      PROGRAM RADIAL

C     THIS PROGRAM CALCULATES V1,V2,W1,W2,DS,DR,RH, AND RT
C     VALUES BASED UPON THE RADIAL EQUILIBRIUM FLOW METHOD OF
C     ANALYSIS AS DERIVED IN CHAPT. 9 OF AEROTHERMODYNAMICS OF
C     GAS TURBINE AND ROCKET PROPULSION - OATES, GORDON C. 1988
C     AIAA Inc.
C     BESSEL FUNCTION GENERATORS FROM NUMERICAL RECIPES
C     NOTE: EQ 9.102 IS INCORRECT!!!!

      REAL DELH,OM,ALPHA,BETA1,BETA2,R,RH,RT,SIGRH,Y,YY(50),V1(50),
     .V2(50),W1(50),W2(50),DS,DR,PH1,PH2,JX1,JX2

      OPEN(16,FILE='RADIAL.DAT')
      READ(16,*) DELH,OM,ALPHA,BETA1,R,SIGRH
      CLOSE(16)

      OPEN(15,FILE='RADIAL.OUT')
      BETA2=BETA1+DELH/OM
      N=20

      DO 10 I=1,N
      YY(I)=1.+REAL(I-1)*(R-1.)/REAL(N-1)
      Y=YY(I)

      YX1=ALPHA*Y
      YX2=ALPHA*R
      JX1=ALPHA*Y
      JX2=ALPHA*R

      JX1= BESSJ1(JX1)
      JX2= BESSJ1(JX2)
      YX2= BESSY1(YX2)
      YX1= BESSY1(YX1)

      U1Y=JX1*YX2-JX2*YX1

      JX1=ALPHA
      JX2=ALPHA*Y
      YX1=ALPHA*Y
      YX2=ALPHA

      JX1= BESSJ1(JX1)
      JX2= BESSJ1(JX2)
      YX1= BESSY1(YX1)
      YX2= BESSY1(YX2)

      W1Y=JX1*YX1-JX2*YX2

      JX1=ALPHA*Y
      JX2=ALPHA*R
      YX1=JX2
      YX2=JX1

      JX1= BESSJ0(JX1)
      YX1= BESSY1(YX1)
      JX2= BESSJ1(JX2)
      YX2= BESSY0(YX2)

      U0Y=JX1*YX1-JX2*YX2
```

```
      JX2=ALPHA*Y
      YX1=JX2
      YX2=ALPHA

      JX1= BESSJ1(JX1)
      YX1= BESSYO(YX1)
      JX2= BESSJO(JX2)
      YX2= BESSY1(YX2)

      WOY=JX1*YX1-JX2*YX2

      JX1=ALPHA
      JX2=ALPHA*R
      YX1=JX2
      YX2=ALPHA

      JX1= BESSJ1(JX1)
      JX2= BESSJ1(JX2)
      YX1= BESSY1(YX1)
      YX2= BESSY1(YX2)

      U1A=JX1*YX1-JX2*YX2

      PH1=-(BETA1/ALPHA+.5)*Y*U1Y/U1A-(BETA1/ALPHA+R*R*.5)*
     .Y*W1Y/(R*U1A)+BETA1/ALPHA
      PH2=-(BETA2/ALPHA+.5)*Y*U1Y/U1A-(BETA2/ALPHA+R*R*.5)*
     .Y*W1Y/(R*U1A)+BETA2/ALPHA
      W1(I)=(BETA1+ALPHA*.5)*UOY/U1A+(BETA1/R+ALPHA*R*.5)*
     .WOY/U1A
      W2(I)=(BETA2+ALPHA*.5)*UOY/U1A+(BETA2/R+ALPHA*R*.5)*
     .WOY/U1A

      V1(I)=(-ALPHA*PH1+BETA1)/Y
      V2(I)=(-APLHA*PH2+BETA2)/Y

10    CONTINUE

      DO 20 I=1,N

      WRITE(15,100)(YY(I)-1.)/(R-1.),V1(I),V2(I),W1(I),W2(I)
100   FORMAT(F7.4,2X,E10.4,2X,E10.4,2X,E10.4,2X,E10.4)
20    CONTINUE

      VSI=SQRT(W2(1)*W2(1)+V2(1)*V2(1))
      VSE=SQRT(W1(1)*W1(1)+V1(1)*V1(1))
      VRI=SQRT(W1(N)*W1(N)+(OM*R-V1(N))**2)
      VRE=SQRT(W2(N)*W2(N)+(OM*R-V2(N))**2)

      DH=(1-VSE/VSI)+DELH/(2.*OM*SIGRH*VSI)
      DR=(1-VRE/VRI)+DELH/(2.*OM*SIGRH*VRI)

      WRITE(15,*) DH,DR

      RH=1.+(1./(2.*DELH))*(VSE*VSE-VSI*VSI)
      RT=1.+(1./(2.*DELH))*(W1(N)*W1(N)+V1(N)*V1(N)-W2(N)*W2(N)-V2(N)
     .*V2(N))

      WRITE(15,*) RH,RT

      CLOSE(15)
      STOP
      END

      FUNCTION BESSJO(X)
```

```
      DATA P1,P2,P3,P4,P5/1.D0,-.1098628627D-2,.2734510407D-4,
     *     -.2073370639D-5,.2093887211D-6/, Q1,Q2,Q3,Q4,Q5/-.1562499995D-
     *1,
     *     .1430488765D-3,-.6911147651D-5,.7621095161D-6,-.934945152D-7/
      DATA R1,R2,R3,R4,R5,R6/57568490574.D0,-13362590354.D0,651619640.7D
     *0,
     *     -11214424.18D0,77392.33017D0,-184.9052456D0/,
     *     S1,S2,S3,S4,S5,S6/57568490411.D0,1029532985.D0,
     *     9494680.718D0,59272.64853D0,267.8532712D0,1.D0/
      IF(ABS(X).LT.8.)THEN
        Y=X**2
        BESSJ0=(R1+Y*(R2+Y*(R3+Y*(R4+Y*(R5+Y*R6)))))
     *       /(S1+Y*(S2+Y*(S3+Y*(S4+Y*(S5+Y*S6)))))
      ELSE
        AX=ABS(X)
        Z=8./AX
        Y=Z**2
        XX=AX-.785398164
        BESSJ0=SQRT(.636619772/AX)*(COS(XX)*(P1+Y*(P2+Y*(P3+Y*(P4+Y
     *       *P5))))-Z*SIN(XX)*(Q1+Y*(Q2+Y*(Q3+Y*(Q4+Y*Q5)))))
      ENDIF
      RETURN
      END

      FUNCTION BESSJ1(X)
      REAL*8 Y,P1,P2,P3,P4,P5,Q1,Q2,Q3,Q4,Q5,R1,R2,R3,R4,R5,R6,
     *     S1,S2,S3,S4,S5,S6
      DATA R1,R2,R3,R4,R5,R6/72362614232.D0,-7895059235.D0,242396853.1D0
     *,
     *     -2972611.439D0,15704.48260D0,-30.16036606D0/,
     *     S1,S2,S3,S4,S5,S6/144725228442.D0,2300535178.D0,
     *     18583304.74D0,99447.43394D0,376.9991397D0,1.D0/
      DATA P1,P2,P3,P4,P5/1.D0,.183105D-2,-.3516396496D-4,.2457520174D-5
     *,
     *     -.240337019D-6/, Q1,Q2,Q3,Q4,Q5/.04687499995D0,-.2002690873D-3
     *,
     *     .8449199096D-5,-.88228987D-6,.105787412D-6/
      IF(ABS(X).LT.8.)THEN
        Y=X**2
        BESSJ1=X*(R1+Y*(R2+Y*(R3+Y*(R4+Y*(R5+Y*R6)))))
     *       /(S1+Y*(S2+Y*(S3+Y*(S4+Y*(S5+Y*S6)))))
      ELSE
        AX=ABS(X)
        Z=8./AX
        Y=Z**2
        XX=AX-2.356194491
        BESSJ1=SQRT(.636619772/AX)*(COS(XX)*(P1+Y*(P2+Y*(P3+Y*(P4+Y
     *       *P5))))-Z*SIN(XX)*(Q1+Y*(Q2+Y*(Q3+Y*(Q4+Y*Q5)))))
     *       *SIGN(1.,X)
      ENDIF
      RETURN
      END

      FUNCTION BESSY0(X)
      REAL*8 Y,P1,P2,P3,P4,P5,Q1,Q2,Q3,Q4,Q5,R1,R2,R3,R4,R5,R6,
     *     S1,S2,S3,S4,S5,S6
      DATA P1,P2,P3,P4,P5/1.D0,-.1098628627D-2,.2734510407D-4,
     *     -.2073370639D-5,.2093887211D-6/, Q1,Q2,Q3,Q4,Q5/-.1562499995D-
     *1,
     *     .1430488765D-3,-.6911147651D-5,.7621095161D-6,-.934945152D-7/
      DATA R1,R2,R3,R4,R5,R6/-2957821389.D0,7062834065.D0,-512359803.6D0
     *,
     *     10879881.29D0,-86327.92757D0,228.4622733D0/,
     *     S1,S2,S3,S4,S5,S6/40076544269.D0,745249964.8D0,
```

```
  Y=X**2
  BESSY0=(R1+Y*(R2+Y*(R3+Y*(R4+Y*(R5+Y*R6)))))/(S1+Y*(S2+Y
*       *(S3+Y*(S4+Y*(S5+Y*S6)))))+.636619772*BESSJ0(X)*LOG(X)
 ELSE
   Z=8./X
   Y=Z**2
   XX=X-.785398164
   BESSY0=SQRT(.636619772/X)*(SIN(XX)*(P1+Y*(P2+Y*(P3+Y*(P4+Y*
*       P5))))+Z*COS(XX)*(Q1+Y*(Q2+Y*(Q3+Y*(Q4+Y*Q5)))))
 ENDIF
 RETURN
 END

 FUNCTION BESSY1(X)
 REAL*8 Y,P1,P2,P3,P4,P5,Q1,Q2,Q3,Q4,Q5,R1,R2,R3,R4,R5,R6,
*    S1,S2,S3,S4,S5,S6,S7
 DATA P1,P2,P3,P4,P5/1.D0,.183105D-2,-.3516396496D-4,.2457520174D-5
*,
*    -.240337019D-6/, Q1,Q2,Q3,Q4,Q5/.04687499995D0,-.2002690873D-3
*,
*    .8449199096D-5,-.88228987D-6,.105787412D-6/
 DATA R1,R2,R3,R4,R5,R6/-.4900604943D13,.1275274390D13,-.5153438139
*D11,
*    .7349264551D9,-.4237922726D7,.8511937935D4/,
*    S1,S2,S3,S4,S5,S6,S7/.2499580570D14,.4244419664D12,
*    .3733650367D10,.2245904002D8,.1020426050D6,.3549632885D3,1.D0/
 IF(X.LT.8.)THEN
   Y=X**2
   BESSY1=X*(R1+Y*(R2+Y*(R3+Y*(R4+Y*(R5+Y*R6)))))/(S1+Y*(S2+Y*
*       (S3+Y*(S4+Y*(S5+Y*(S6+Y*S7))))))+.636619772
*       *(BESSJ1(X)*LOG(X)-1./X)
 ELSE
   Z=8./X
   Y=Z**2
   XX=X-2.356194491
   BESSY1=SQRT(.636619772/X)*(SIN(XX)*(P1+Y*(P2+Y*(P3+Y*(P4+Y
*       *P5))))+Z*COS(XX)*(Q1+Y*(Q2+Y*(Q3+Y*(Q4+Y*Q5)))))
 ENDIF
 RETURN
 END
```

F: FIGURES

THE SKY SHARK

Figure F-1

A Ducted Fan Engine

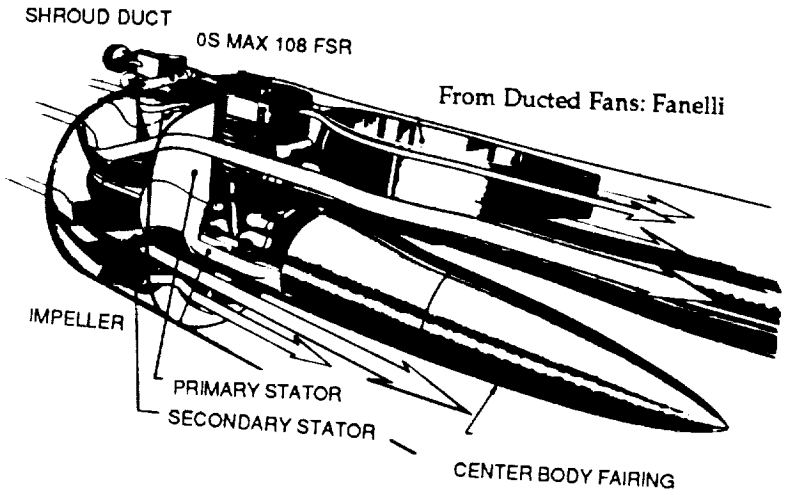

Figure F-2

Tip Speed Vs RPM for an 8" Prop

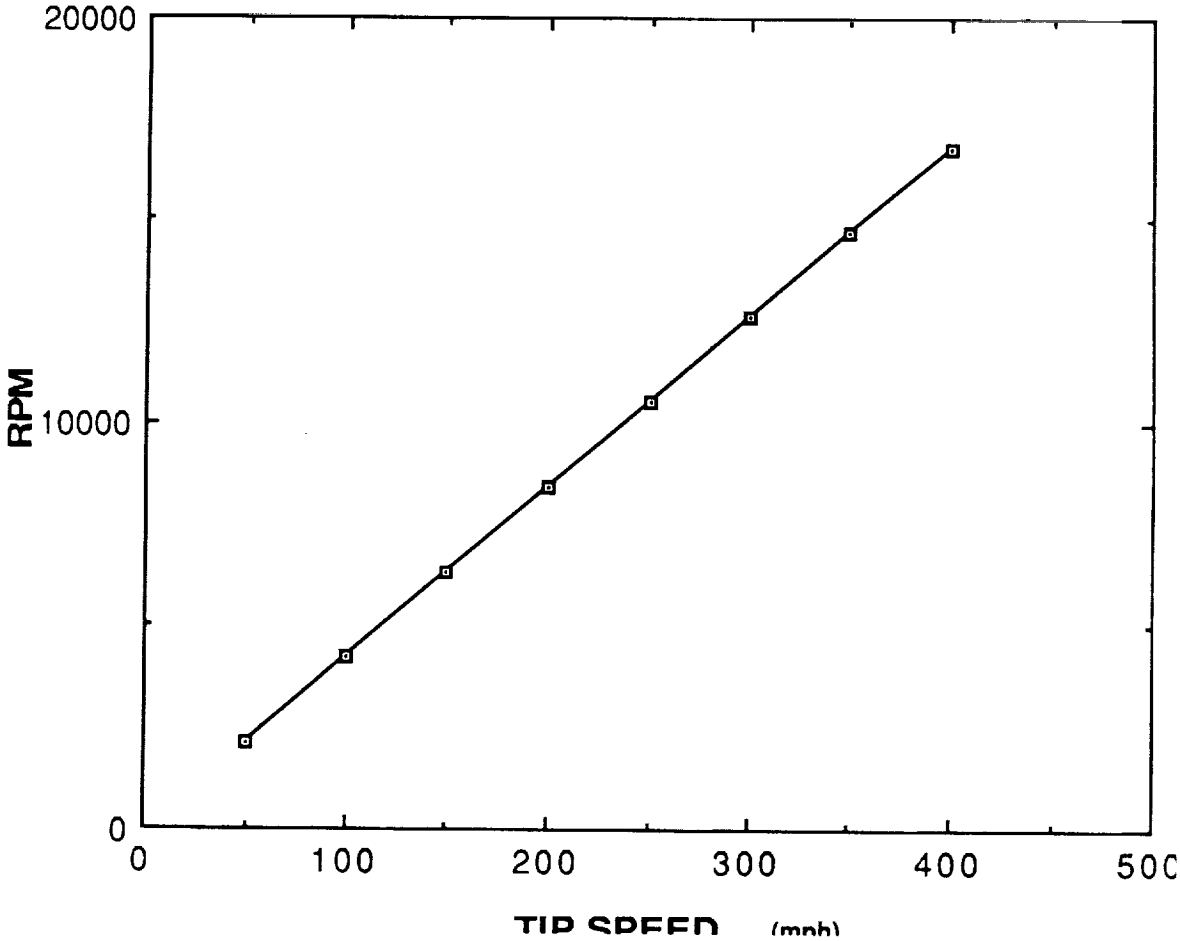

Figure F-3

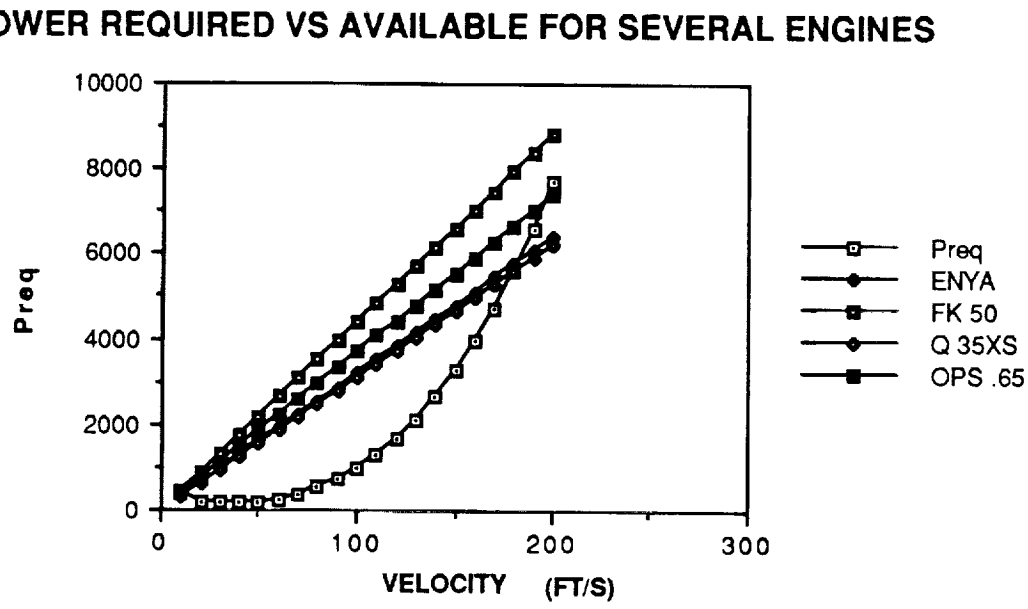
POWER REQUIRED VS AVAILABLE FOR SEVERAL ENGINES
10000
8000
6000
4000
2000
0
Preq
0
100
200
300
VELOCITY (FT/S)
Preq
ENYA
FK 50
Q 35XS
OPS .65

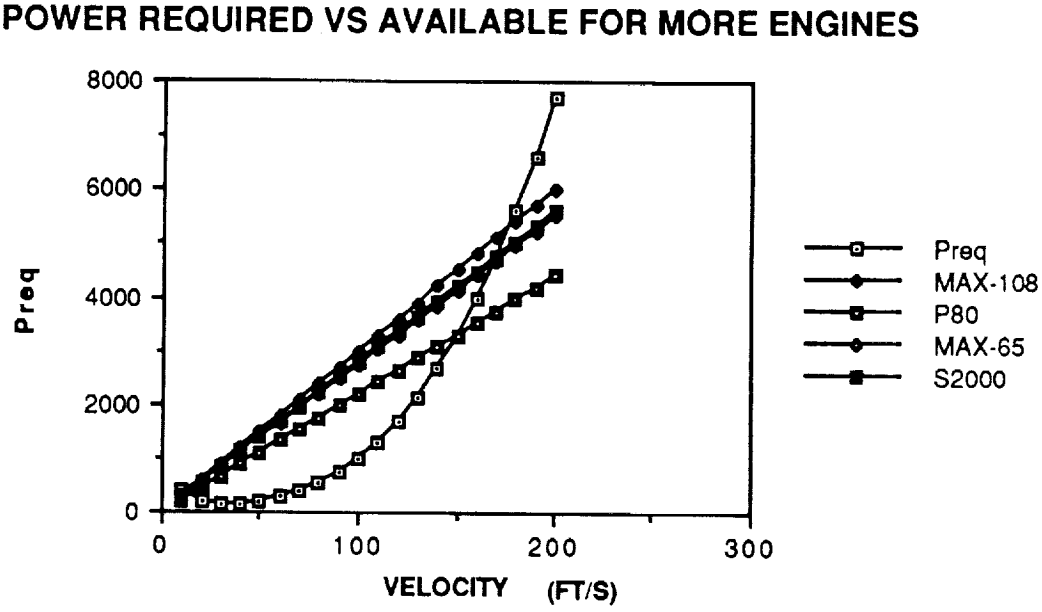
POWER REQUIRED VS AVAILABLE FOR MORE ENGINES
8000
6000
4000
2000
0
Preq
0
100
200
300
VELOCITY (FT/S)
Preq
MAX-108
P80
MAX-65
S2000

Figure F-4

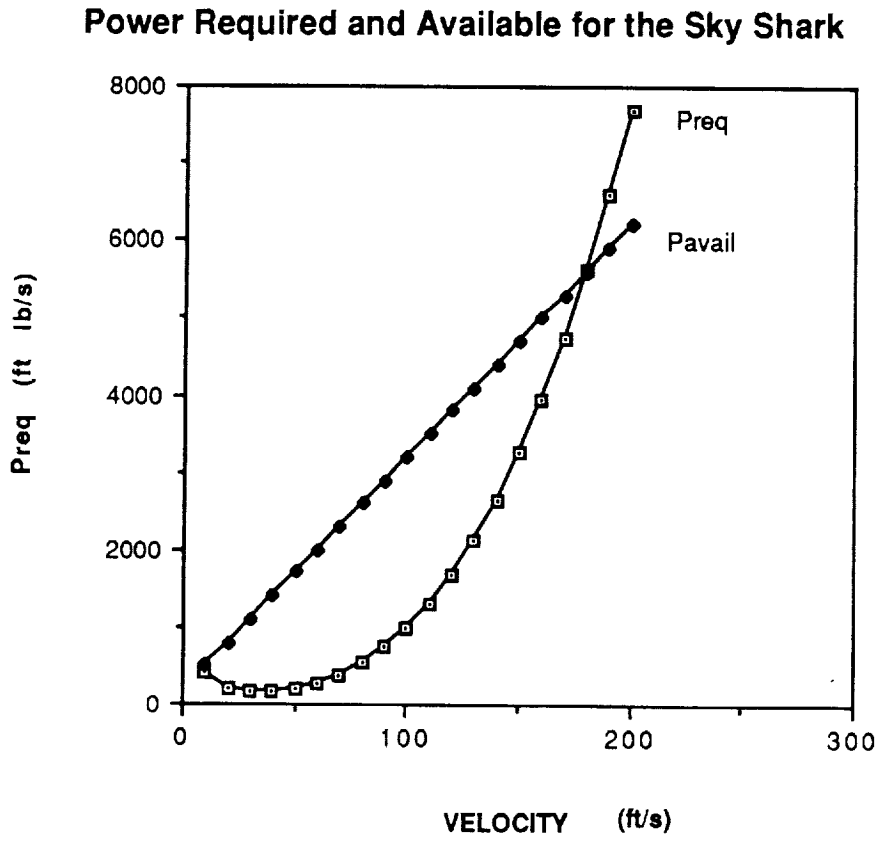
Power Required and Available for the Sky Shark
8000
6000
4000
2000
0
Preq (ft lb/s)
Preq
Pavail
0
100
200
300
VELOCITY (ft/s)

Figure F5 **Radial and Axial Velocity Profiles for Base Case**

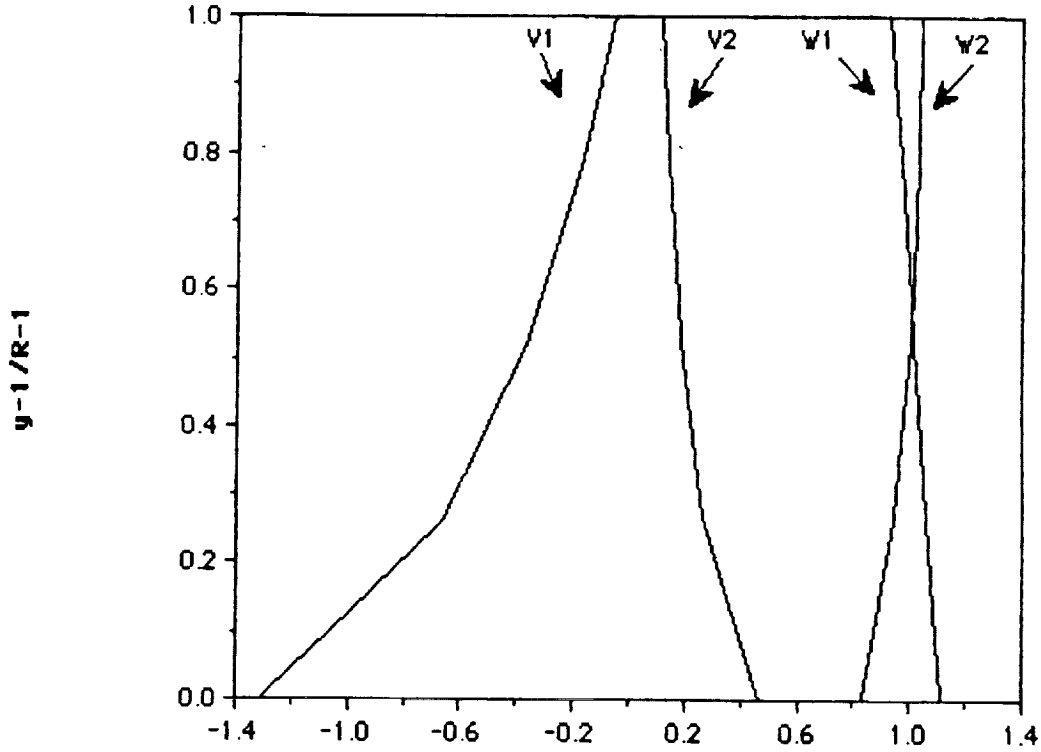

Figure F6 **Diffusion Variance at Hub and Tip Locations as a Function of Solidity**

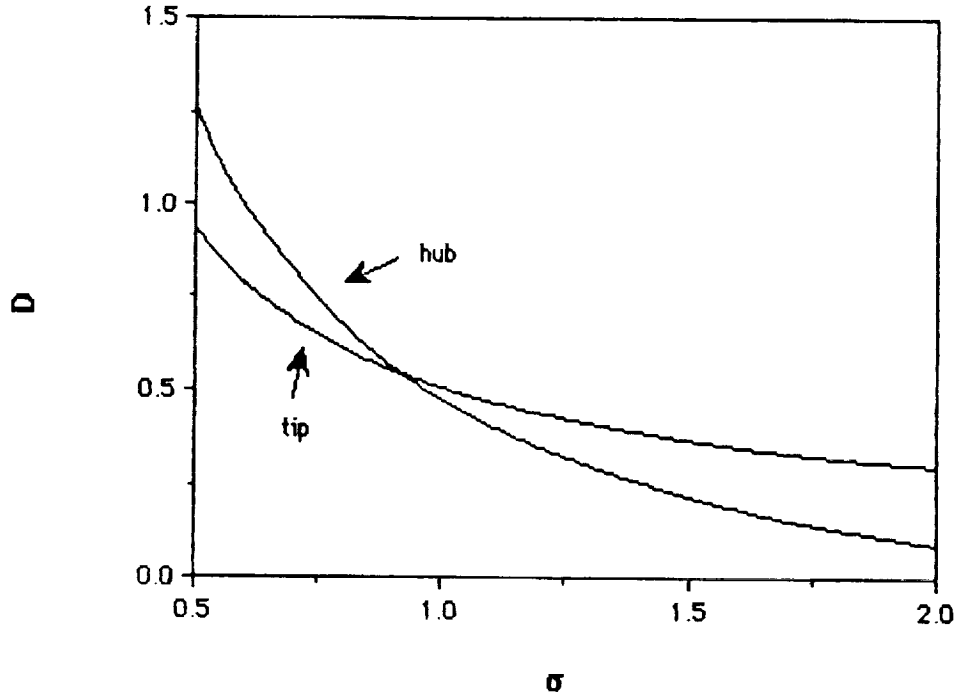

Figure F7 **Upstream Axial Velocity variation with Blade Angle of Attack**

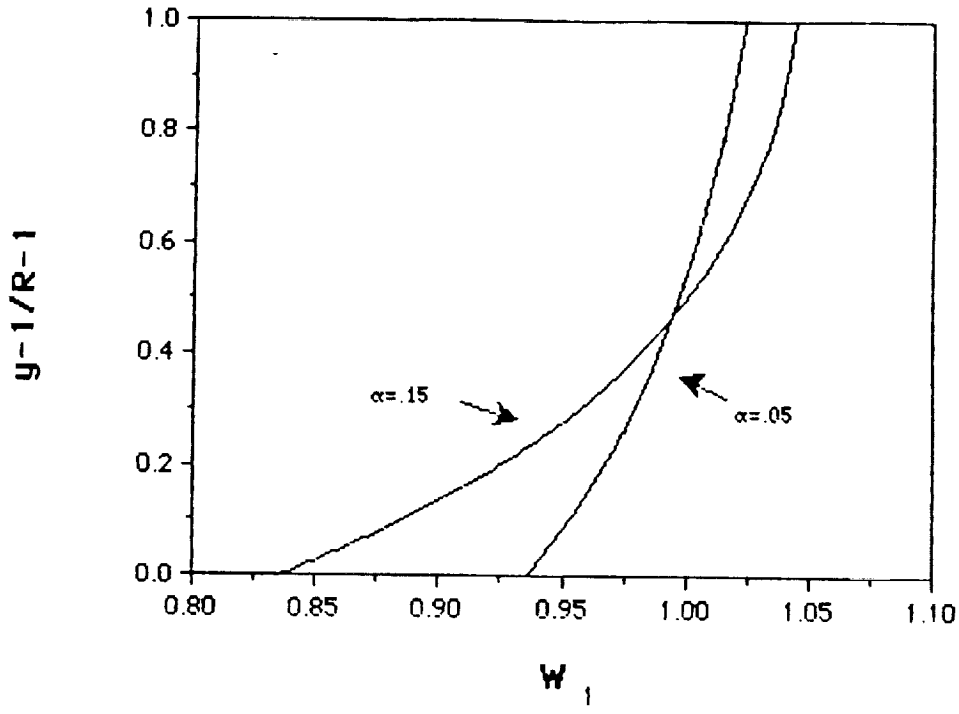

Figure F8 **Downstream Axial Velocity variation with Blade Angle of Attack**

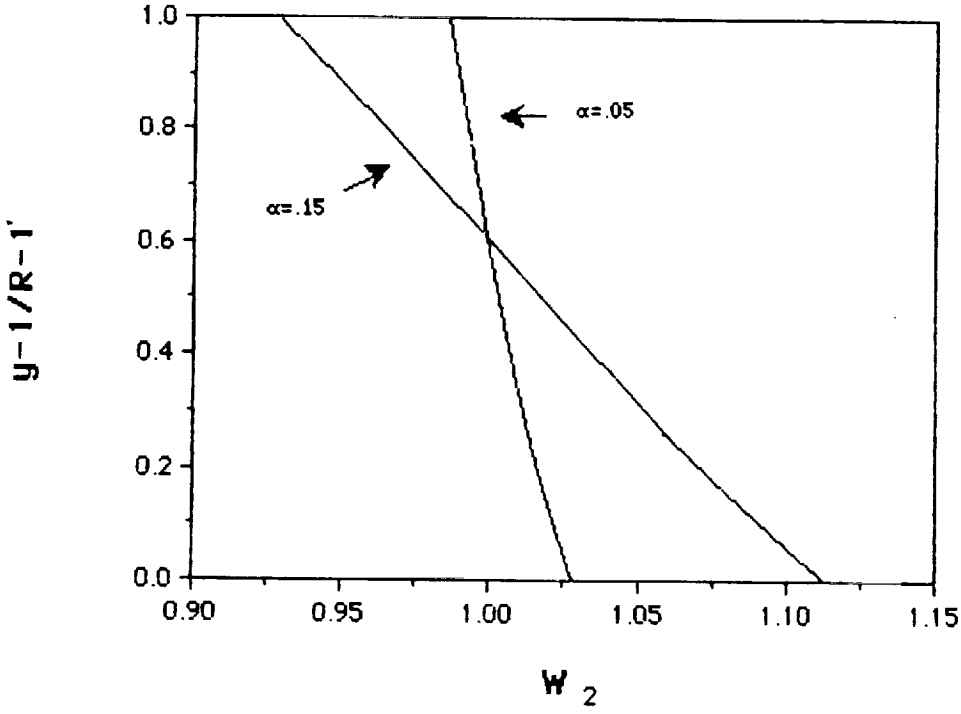

Figure F9

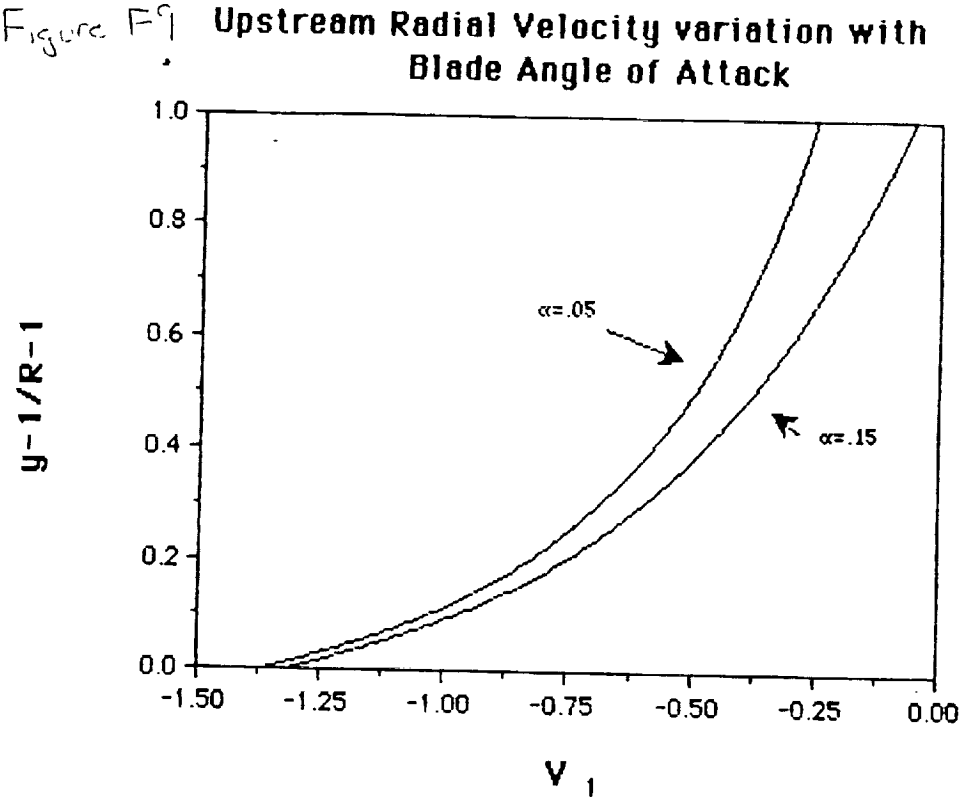
Upstream Radial Velocity variation with Blade Angle of Attack
1.0
0.8
0.6
0.4
0.2
0.0
y-1/R-1
α=.05
α=.15
-1.50
-1.25
-1.00
-0.75
-0.50
-0.25
0.00
V 1

Figure F 10 Diffusion Coefficient variation with Blade Angle of Attack

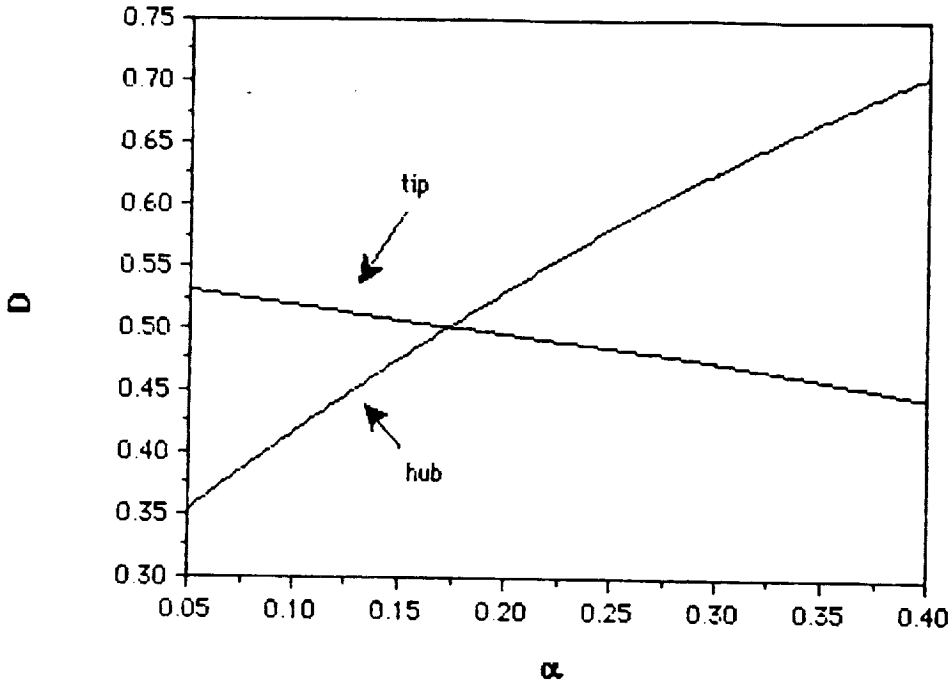

Figure F 11 Degree of Reaction variance with Blade Angle of Attack

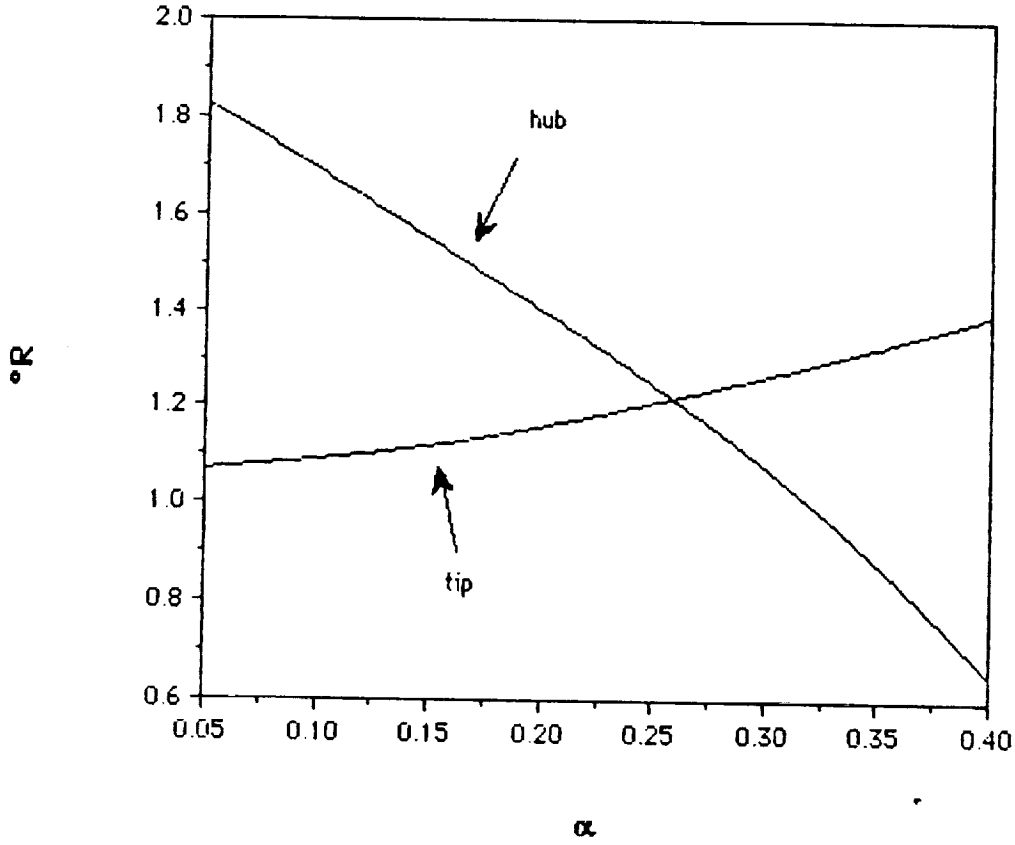

Figure F12

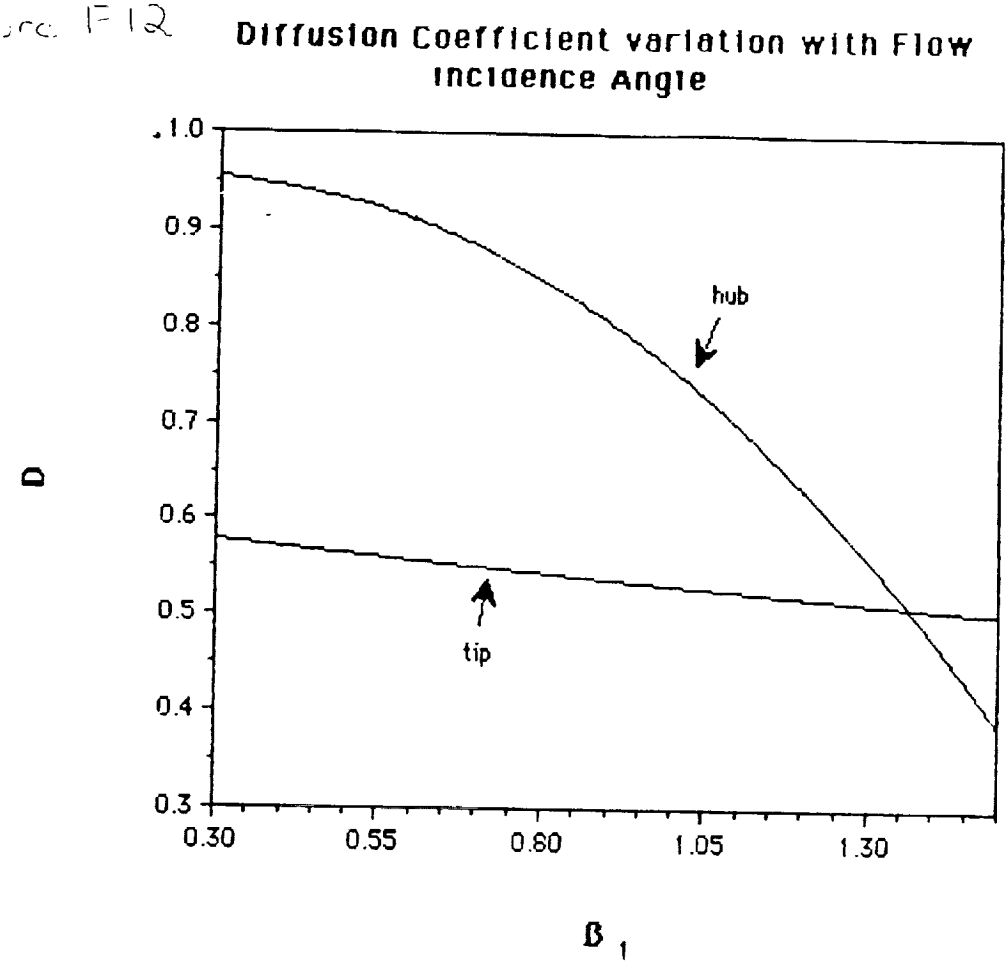

Figure F13

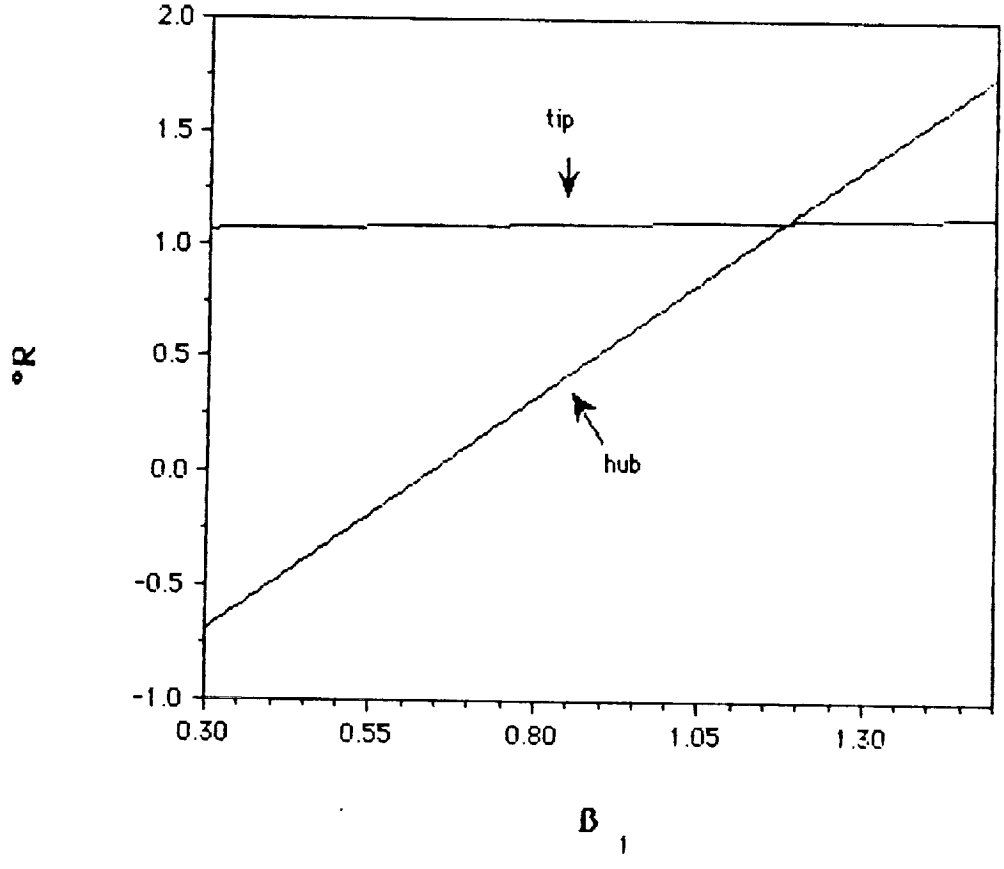

Figure F14 Diffusion Coefficient variation with Blade Enthalpy Change

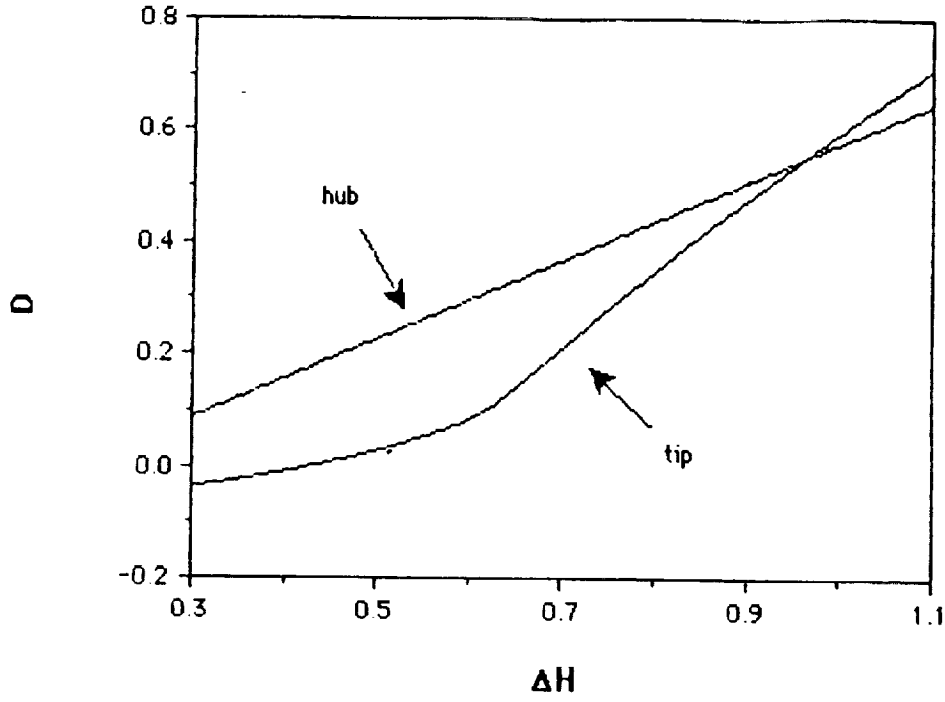

Figure F15 Degree of Reaction variation with Blade Enthalpy Change

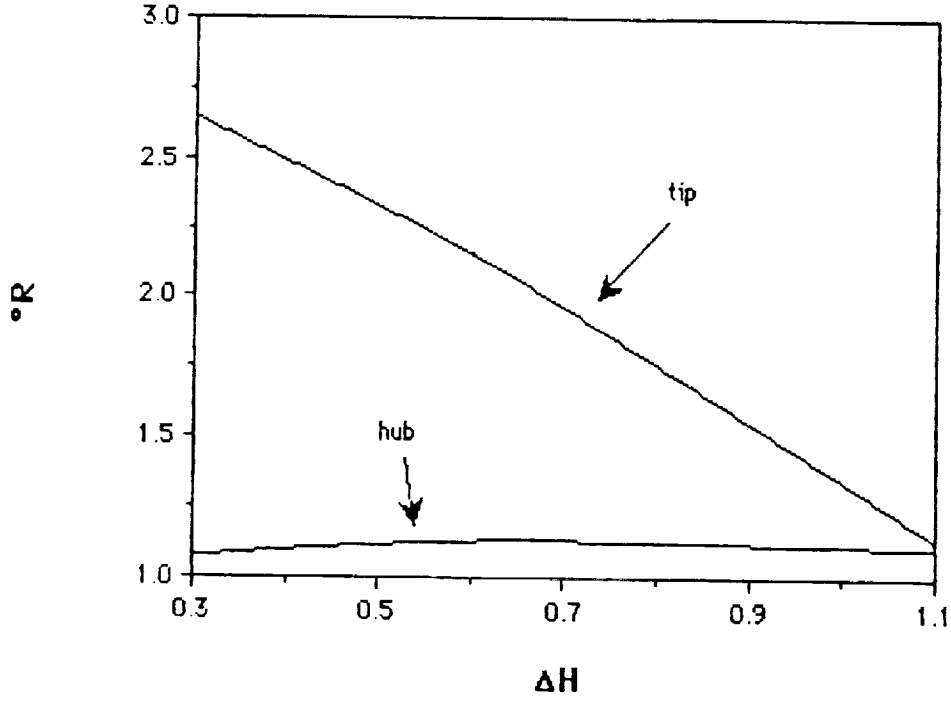

G: STABILITY

THE SKY SHARK

The first step in a proper stability analysis is the optimization of the horizontal and vertical tail sizes. This is most easily accomplished using the tail volume ratios, V_H and V_V, as gages of the actual tail sizes. The volume ratio is defined as the product of the tail moment arm length to the center of gravity and area of the tail divided by the product of the wing area and mean wing chord, or:

$$V=(l_t S_t)/(S_W c).$$

Using the rules of thumb given in the Design class, it can be seen that a horizontal volume ratio of from 0.7 to 1.0 is acceptable, while a straight ratio of horizontal tail area to wing area of from 0.17 to 0.3 is required. In the above equation the wing area, mean chord and tail moment arm are assumed to be fixed parameters, as they have been chosen by other members of the design team to meet specifications of their studies. S_W and c were set at 34 ft^2 and 2 ft respectively by the aerodynamics team, while l_t was chosen as 6.5 ft by the controls team. Using Program G-1 (in Appendix), both the horizontal volume ratio and the tail-to-wing area ratio were plotted for a range of horizontal tail areas from 0.1 to 15 ft^2, and the results appear on Figure G-1. It is apparent that, to stay within both constraints listed above, the horizontal tail area must be between 7.3 and 10.5 ft^2, yielding a volume ratio of from 0.698 to 1.00. To determine the optimum vertical tail volume ratio requires a bit more work. As given in the rules of thumb, the ratio of vertical tail area to horizontal tail area should be between 0.33 and 0.4. Likewise the ratio of vertical tail area to wing area is from 0.07 to 0.1. Again using Program G-1, keeping the wing area constant and varying the vertical tail area from 0.04 to 6 ft^2, and assuming a horizontal tail area of 10.2 ft^2, plots of the two area ratios were made in Figure G-2. It can be seen that a vertical tail area of from 3.43 to 4.02 ft^2 is desired, yielding a volume ratio of from 0.328 to 0.384. For the remainder of the stability calculations in this study, a horizontal tail volume ratio of 0.975 and area of 10.2 ft^2, and a vertical tail volume ratio of 0.382 with area of 4 ft^2 were assumed. It is important to note that both these volume ratios were chosen from the high end of their possible ranges. This is because it was felt that the added difficulties caused by the airborne test section would require greater stability on the part of the aircraft as a whole. It was believed that the slightly larger tail surfaces would be wise, even though the test

section is to be mounted above the aircraft center of gravity, theoretically contributing very little to the overall instability of the design.

Longitudinal stability is determined by examining the net moment coefficient about the aircraft center of gravity in the longitudinal direction. This is done by summing the moment contributions of the wing, horizontal tail, and the fuselage. The equation in this analysis is :

$$C_{Mcg}=C_{Mo}+C_{Malpha}*alpha.$$

C_{Mcg} is the net moment coefficient about the center of gravity, C_{Mo} is the net moment coefficient at zero angle of attack, C_{Malpha} is the moment curve slope and alpha is the flight angle of attack. C_{Mo} for the wing is:

$$C_{Mow}=C_{Mac}+C_{Lo}(X_{cg}/c - X_{ac}/c).$$

C_{Mac} is the moment coefficient about the aerodynamic center, C_{Lo} is the zero angle of attack lift coefficient, X_{cg} and X_{ac} are the locations of the center of gravity and aerodynamic center, and c is the mean wing chord. The aerodynamic data, that is C_{Mac}, C_{Lo}, X_{ac} and c, are supplied by the aerodynamics group and are from the NACA 1408 airfoil as seen in Appendix G-1. The resulting equation, then, is:

$$C_{Mow}=-0.05+0.05X_{cg}.$$

$C_{Malphaw}$ is given by:

$$C_{Malphaw}=C_{Lalpha}(X_{cg}/c - X_{ac}/c).$$

C_{Lalpha} is the lift curve slope of the wing, again given in the airfoil data. Therefore:

$$C_{Malphaw}=2.945X_{cg}-1.4725.$$

For the horizontal tail,C_{Mo} is given by:

$$C_{Mot}=yV_HC_{Lalphat}(e_O+i_W-i_t).$$

Here y is the tail efficiency, $C_{Lalphat}$ is the lift curve slope of the tail, e_o is the downwash angle, $2C_{Low}/(PI*AR)$, i_w is the wing incidence angle, and i_t is the tail incidence angle. Again the airfoil data for the tail is given by the aerodynamics group from the NACA 0009 airfoil and is in Appendix G-1. The volume ratio was selected above, and y is assumed to be unity. Thus:

$$C_{Mot}=-0.027+4.571(i_w-i_t).$$

The $C_{Malphat}$ component is given by:

$$C_{Malphat}=-yV_H\, C_{Lalphat}\, (1-de/dalpha),$$

where de/dalpha is the slope of the downwash angle, $2C_{Lalphaw}/(PI*AR)$. Since all quantities are known:

$$C_{Malphat}=-3.6397.$$

The moment coefficients of the fuselage are computed using the numerical integration method. In this method the fuselage is divided into several sections both forward and aft of the wing. The fuselage cross-section used can be seen in Figure G-1 (in Appendix) and is elliptical. Figure G-2 (in Appendix) shows the divisions of the fuselage, and the numerical data on each section is presented in Appendix G-2. Using Program G-2, this data was integrated to yield the following results:

$$C_{Mof}=-0.0074 \qquad C_{Malphaf}=0.0071.$$

This analysis was used for several wing areas, and each time it was apparent that the moment contribution of the fuselage was nearly negligible.

When summing all contributions above, the result is as follows:

$$C_{Mcg}=[-0.0844+0.05X_{cg}+4.571(i_w-i_t)]+[-5.119+2.945X_{cg}]*alpha$$

the key parameters being X_{cg} and (i_w-i_t). To optimize this equation, Program

G-3 (in Appendix) was used to vary (i_w-i_t) through a range of from 0 to 5 degrees, while varying X_{cg} from 12.5% to 35% of the wing chord. In selecting the ranges for X_{cg}, it is first necessary to examine the stick-fixed neutral point location. Any center of gravity location aft of the neutral point will be unstable. The equation for the neutral point is as follows:

$$X_{NP}/c=Xac/c+C_{Malphaf}/C_{Lalpha}+ \\ y^{V_H}C_{Lalphat}/C_{Lalpha}(1-de/dalpha).$$

Solving for X_{NP} yields a value of 1.733 ft, which is sufficiently aft of any of the center of gravity locations examined here. Figures G-3 and G-4 show the results for C_{Mo} and C_{Malpha} through eleven different values of X_{cg}. It is apparent that, while X_{cg} is the sole parameter for C_{Malpha}, it is relatively insignificant compared to (i_w-i_t) for C_{Mo}. It is assumed that an acceptable range for C_{Mo} is from 0.05 to 0.15. This indicates a value for (i_w-i_t) from 1.43 to 2.75 degrees. The aerodynamic group suggests an i_w of approximately 3 degrees, so i_t must range from -1.57 to -0.25 degrees. Because of the inaccurate nature of predicting tail downwash, and thus C_{Mot}, it is advised that the horizontal tail be built as a stabilator so that it can be varied as needed to yield optimum results. The plot for C_{Malpha} shows that the full range X_{cg}'s will adequately produce a negative curve slope. It is thus suggested that X_{cg} be placed at the aerodynamic center for the sake of simplicity in the design.

Lateral stability is determined by examining the yawing moment coefficient about the aircraft center of gravity. The two components of this coefficient are the wing-fuselage contribution and the vertical tail contribution. The wing-fuselage component, C_{nBwf}, is slightly destabilizing and is very small compared to the vertical tail contribution. It is an empirical value based on the fuselage geometry, wing area and span, and the length of the fuselage. For this design,

$$C_{nBwf}=-0.011\ rad^{-1}.$$

The equation for the vertical tail contribution to lateral stability is:

$$C_{nBv}=yV_VC_{Lalphat}(1+do/dB),$$

where do/dB is the variation of sidewash angle with sideslip angle. Assuming y is unity, the value of (1+do/dB) can be estimated as follows:

$$(1+do/dB)=0.724 + 3.06((S_V/S_W) / (1+\cos(gamma))) + 0.4(z/d) + 0.009AR,$$

where S_V is the vertical tail area, z is the vertical distance from the wing aerodynamic center to the fuselage centerline, d is the maximum fuselage depth, gamma is the wing sweep angle, and AR is the wing aspect ratio. Program G-4 (in Appendix) was then used to find the optimum value of this term, varying z from the fuselage centerline to the top of the fuselage, through a range of sweep angles from 0 to 10 degrees. Figure G-5 shows that gamma is relatively insignificant compared to z in the determination of this term. Also it can be seen that all values of z examined will produce a positive C_{nB}, as is desired. Therefore it is advantageous to place z exactly at the midpoint of the fuselage, the purpose to make construction simpler and to keep the wing as far from the test section as possible in order to decrease interference. At the same time it would be easy to make the sweep angle zero, again to ease construction. In so doing, the value of (1+do/dB) is 1.049. C_{nBv} is thus 1.878 rad^{-1}, and the total yawing moment coefficient is as follows:

$$C_{nB}=1.867\ rad^{-1}.$$

Finally, roll stability is determined by wing dihedral. Again, rules of thumb presented in class say that a minimum of 8 degrees dihedral is required for an RPV of this size. However, because of the test section, it was decided that slightly more dihedral was needed to compensate for the unusual flight conditions, and so 10 degrees was decided on as a better estimate for our design. It was then necessary to decide whether to use a straight-wing V-dihedral, or to use a more efficient polyhedral. It must be noted that the V-dihedral, while less efficient, keeps the center of gravity more centralized and is structurally more sound. for this type of dihedral, each degree increase increases the total wing area of the aircraft by (1-cosG)%, where G is the dihedral angle. Appendix G-3 shows the variation of wing area increase with increasing dihedral. It can be seen that at 10 degrees, an increase in wing area of only 1.5% is incurred. This increase is small enough

that any saving in wing area using a polyhedral design does not offset the structural advantages of the V-dihedral, and so the latter case is suggested for this design.

In conclusion, it is important to note that, from experience, a design which appeared excellent on paper never got off the ground because of improper stability analysis. Once proper sizing of the tail surfaces is accomplished, their location and incidence angle relative to the wing must be determined to ensure optimum longitudinal stability. The vertical location of the wing on the fuselage must be considered to ensure proper lateral stability. And finally the effect of wing dihedral must be analyzed to effect optimum roll stability. Also aerodynamic and structural considerations must be taken into account in order that all aspects of the design come together and mesh as a single system.

G: APPENDICES

THE SKY SHARK

```
DIMENSION SH(150),VH(150,2),SV(150),SV1(150,2)
```

```
 1)         DIMENSION SH(150),VH(150,2),SV(150),SV1(150,2)
 2)         S=0.
 3)         N=1
 4)         B=0.
 5)         SW=34.
 6)         DO 5 I=1,150
 7)         B=B+.04
 8)         SV(I)=B
 9)       5 CONTINUE
10)         DO 10 I=1,150
11)         S=S+.1
12)         SH(I)=S
13)         VH(I,1)=SH(I)/SW
14)         VH(I,2)=(6.5*SH(I))/(SW*2.)
15)      10 CONTINUE
16)         DO 15 I=1,150
17)         SV1(I,1)=SV(I)/10.2
18)         SV1(I,2)=SV(I)/SW
19)      15 CONTINUE
20)         CALL TPLOT(-011,SH,VH,150,150,2)
21)         CALL TITLE('HORIZONTAL TAIL AREA vs VOLUME RATIO AND AREA RATIO')
22)         READ(1,*)N
23)         CALL TPLOT(-011,SV,SV1,150,150,2)
24)         CALL TLABEL('VERTICAL TAIL AREA','TAIL AREA RATIO(SV/SH,SV/SW)')
25)         CALL TITLE('VERTICAL TAIL AREA  COMPARISON')
26)         STOP
27)         END
```

PROGRAM G-1: VOLUME RATIOS

```
DIMENSION WF(20),A(20),DX(20),DEDA(20),AL(20),CMC(20)
```

```
 1)         DIMENSION WF(20),A(20),DX(20),DEDA(20),AL(20),CMC(20)
 2)         REAL K
 3)         WRITE(1,*)'ENTER IWR,NUMBER OF SECTIONS'
 4)         READ(1,*)IWR,N
 5)         WRITE(1,*)'ENTER WING AREA,MEAN CHORD,ZERO-LIFT ANGLE OF ATTACK'
 6)         READ(1,*)S,C,AO
 7)         WRITE(1,*)'ENTER CORRECTION FACTOR'
 8)         READ(1,*)K
 9)         OPEN(UNIT=50,FILE='STAB.DATA',STATUS='OLD')
10)         DO 5 I=1,N
11)         READ(50,*)WF(I),A(I),DX(I),DEDA(I)
12)       5 CONTINUE
13)         CMO=0.
14)         CMA=0.
15)         DO 10 I=1,N
16)         X=K/(36.5*S*C)*WF(I)**2*(AO+A(I))*DX(I)
17)         CMO=CMO+X
18)      10 CONTINUE
19)         DO 20 I=1,N
20)         Y=1./(36.5*S*C)*WF(I)**2*DEDA(I)*DX(I)
21)         CMA=CMA+Y
22)      20 CONTINUE
23)C        WRITE(IWR,*)'CMO OF FUSELAGE=',CMO,'CMA=',CMA
24)         AL(1)=0.
25)         DO 30 I=1,15
26)         CMC(I)=CMO+CMA*AL(I)/57.3
27)         AL(I+1)=AL(I)+1.
28)      30 CONTINUE
29)         CALL TPLOT(-011,AL,CMC,15,20,1)
30)         CALL TLABEL('ALPHA(DEGREE)','CMcg')
31)         STOP
32)         END
```

PROGRAM G-2: FUSELAGE INTEGRATION

DIMENSION XCG(12), DI(875), CMO(875, 11), CMA(11)

```
      DIMENSION XCG(12), DI(875), CMO(875, 11), CMA(11)
      A=0. 25
      Z=0.
      DO 10 I=1, 11
      XCG(I)=A
      DO 15 J=1, 875
      DI(J)=Z
      Z=Z+1. E-4
      CMO(J, I)=-. 0844+. 05*XCG(I)+4. 571*DI(J)
   15 CONTINUE
      CMA(I)=-5. 119+2. 945*XCG(I)
      Z=0.
      A=A+. 0409
   10 CONTINUE
C     CALL TPLOT(-011, DI, CMO, 875, 875, 11)
C     CALL TLABEL('iw-it', 'Cmo')
C     CALL TITLE('Cmo VS (iw-it) FOR VARIOUS XcgS')
      CALL TPLOT(-011, CMA, XCG, 11, 12, 1)
      CALL TLABEL('Cma', 'Xcg')
      CALL TITLE('Cm ALPHA VS CENTER OF GRAVITY')
      STOP
      END
```

PROGRAM G-3: LONGITUDINAL STABILITY

DIMENSION GAM(10), ZW(100), CNB(100, 10)

```
      DIMENSION GAM(10), ZW(100), CNB(100, 10)
      A=0.
      DO 10 I=1, 10
      GAM(I)=A
      B=0.
      DO 15 J=1, 100
      ZW(J)=B
      ETA=. 8005+. 36/(1. +COS(GAM(I)))+. 421*ZW(J)
      CNB(J, I)=1. 793*ETA-. 011
      B=B+. 00475
   15 CONTINUE
      A=A+. 0175
   10 CONTINUE
      CALL TPLOT(-011, ZW, CNB, 100, 100, 10)
      CALL TLABEL('VERTICAL DISTANCE FROM WING CENTERLINE TO FUSELAGE CE
     &NTERLINE(FT)', 'CnB')
      CALL TITLE('VARIATION OF CnB WITH Zw AND SWEEP ANGLE')
      STOP
      END
```

PROGRAM G-4: LATERAL STABILITY

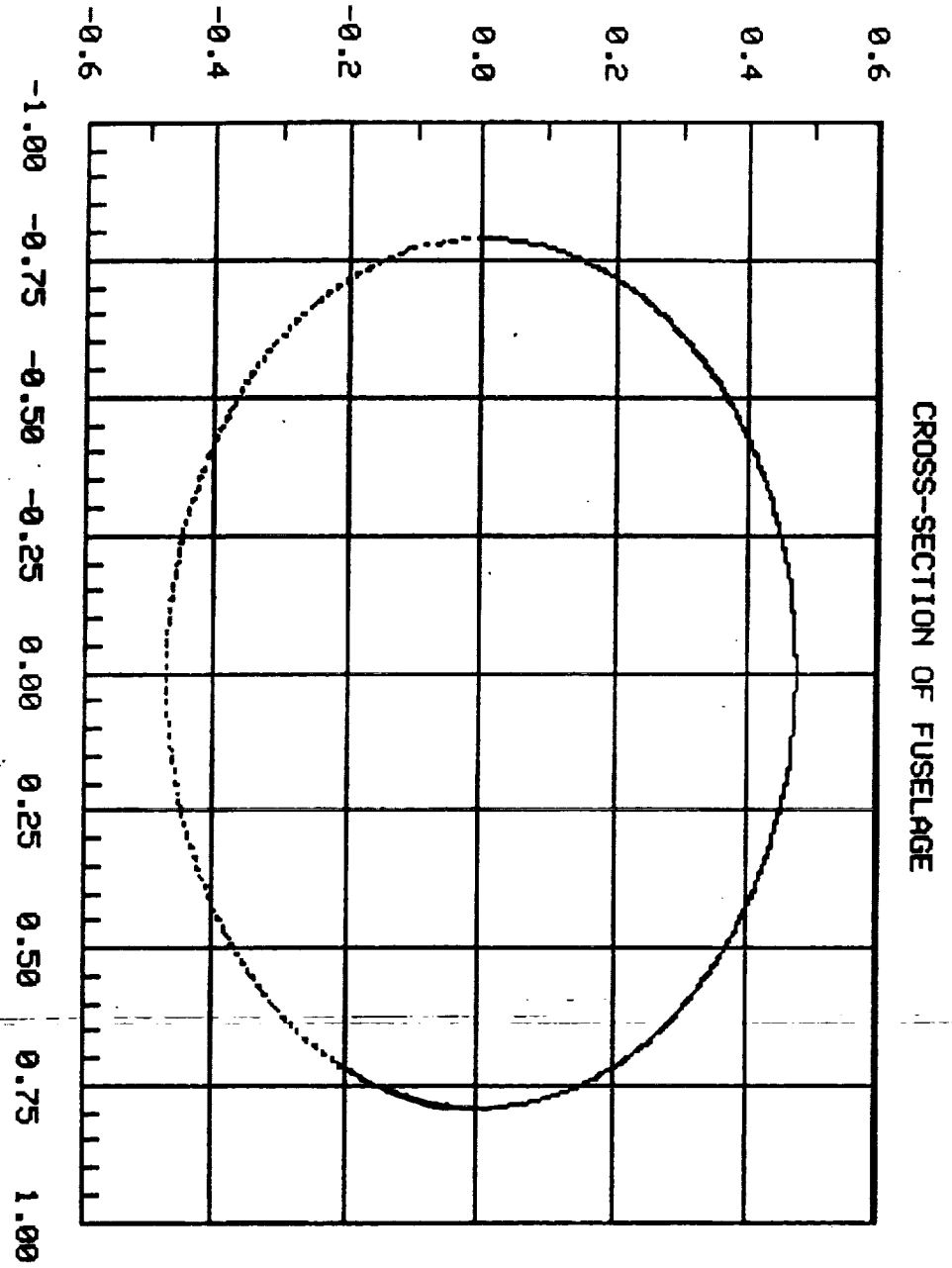

FIGURE G-1 FUSELAGE CROSS-SECTION

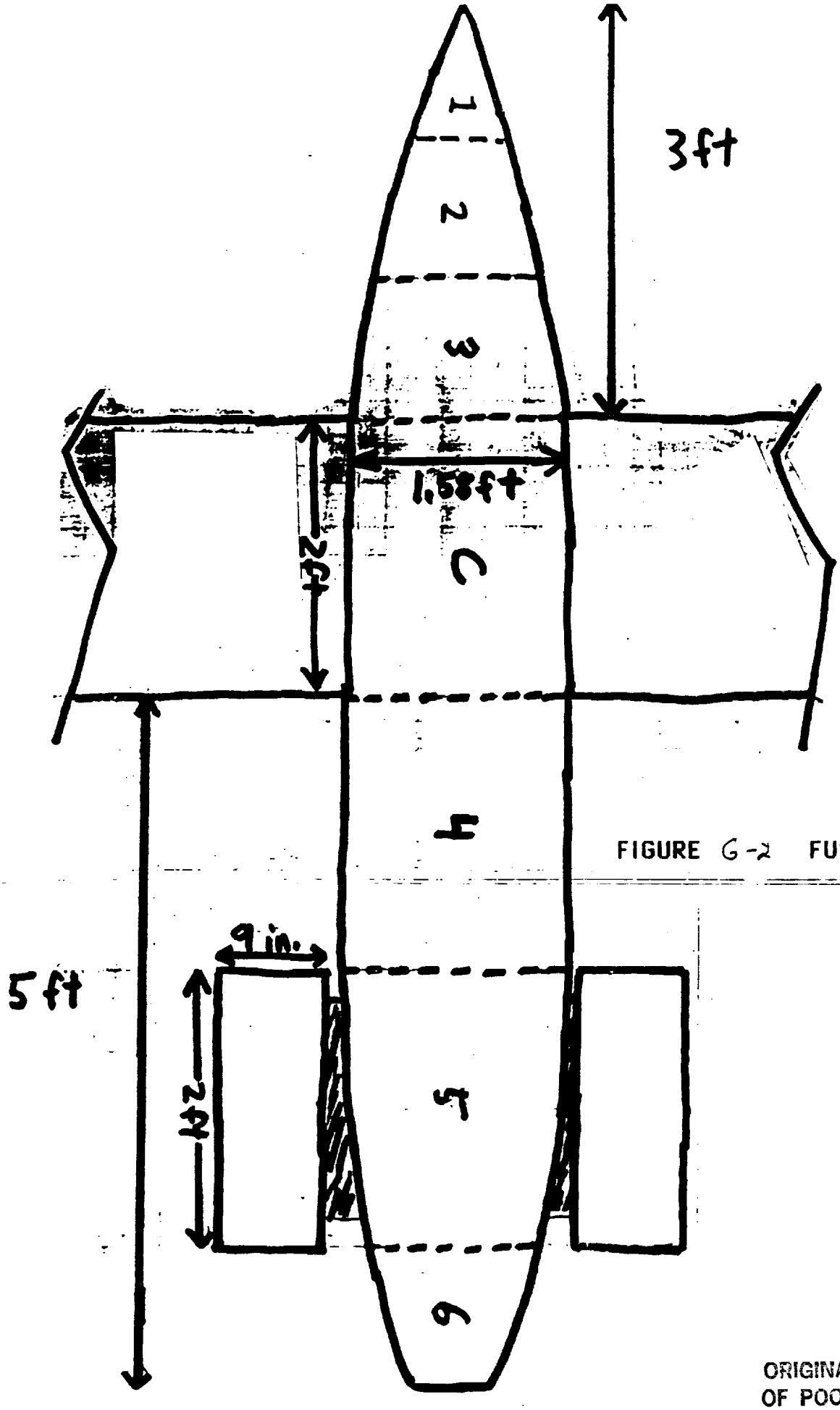

FIGURE 6-2 FUSELAGE DIVISIONS

APPENDIX G-1

AERODYNAMIC DATA

NACA 1408	C_{MAC}=	-0.025
	C_{LOo}=	0.10
	C_{Lalpha}=	5.89 rad^{-1}
	X_{ac}=	0.125 ft
	c=	2.0 ft
NACA 0009	C_{Lalpha}=	4.688 rad^{-1}
	e_o=	-0.006
	de/dalpha=	0.2037 rad^{-1}

APPENDIX G-2

FUSELAGE DATA FOR LONGITUDINAL STABILITY

SECTION	Wf(ft)	ALPHAf(degrees)	DELTA	X(ft)de/dalpha
1	0.56	0.0	1.0	1.2
2	1.0	0.0	1.0	1.25
3	1.36	0.0	1.0	2.5
4	1.58	0.0	2.0	0.094
5	3.4	0.0	2.0	0.439
6	1.0	11.0	1.0	0.659

APPENDIX G-3

WING AREA INCREASE WITH INCREASE IN DIHEDRAL ANGLE

DIHEDRAL(DEGREES)	AREA INCREASE(%)
8	0.9
9	1.2
10	1.5
11	1.8
12	2.2
13	2.6
14	3.0
15	3.4
16	3.8
17	4.4
18	4.9

G: FIGURES

THE SKY SHARK

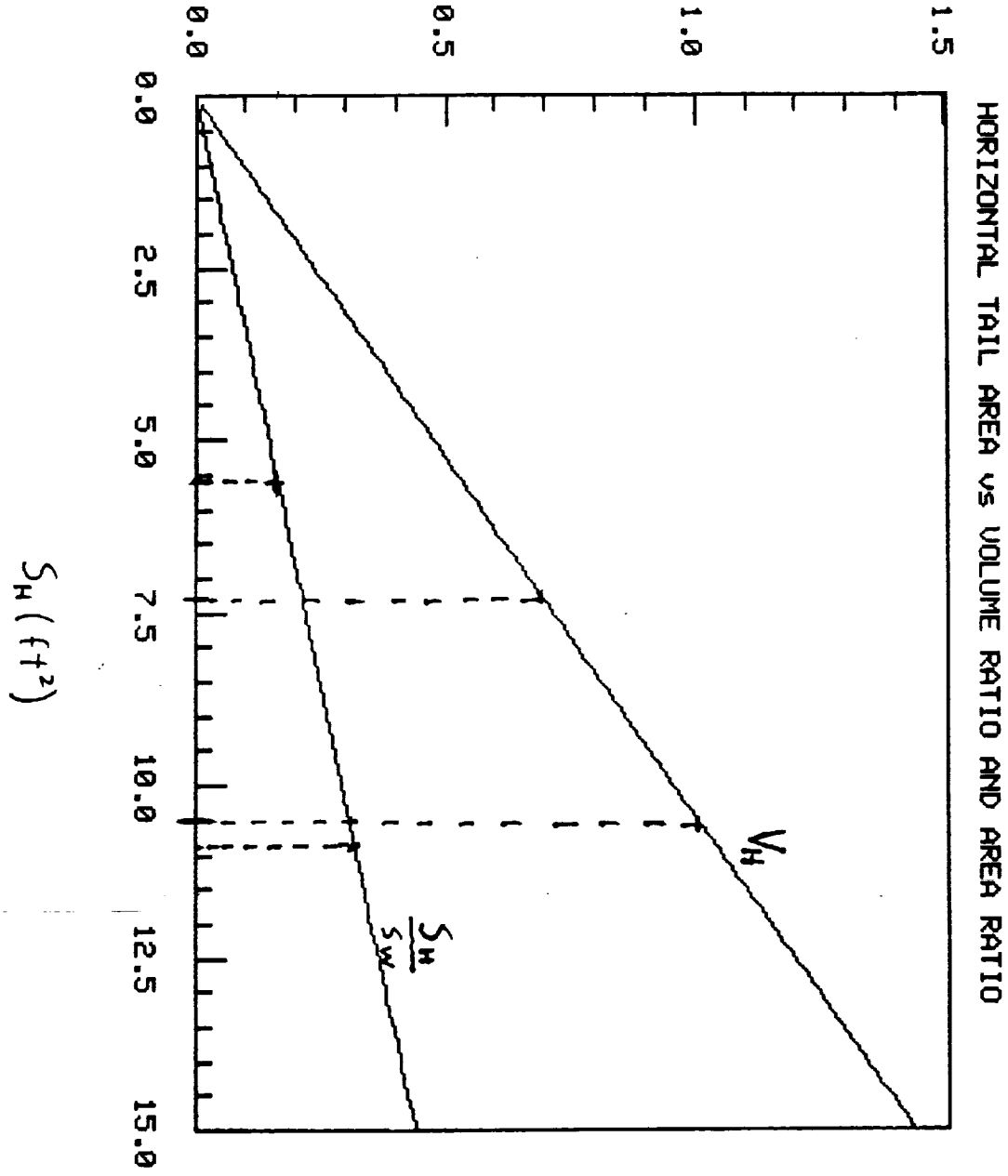

FIGURE G-1: HORIZONTAL TAIL VOLUME RATIO

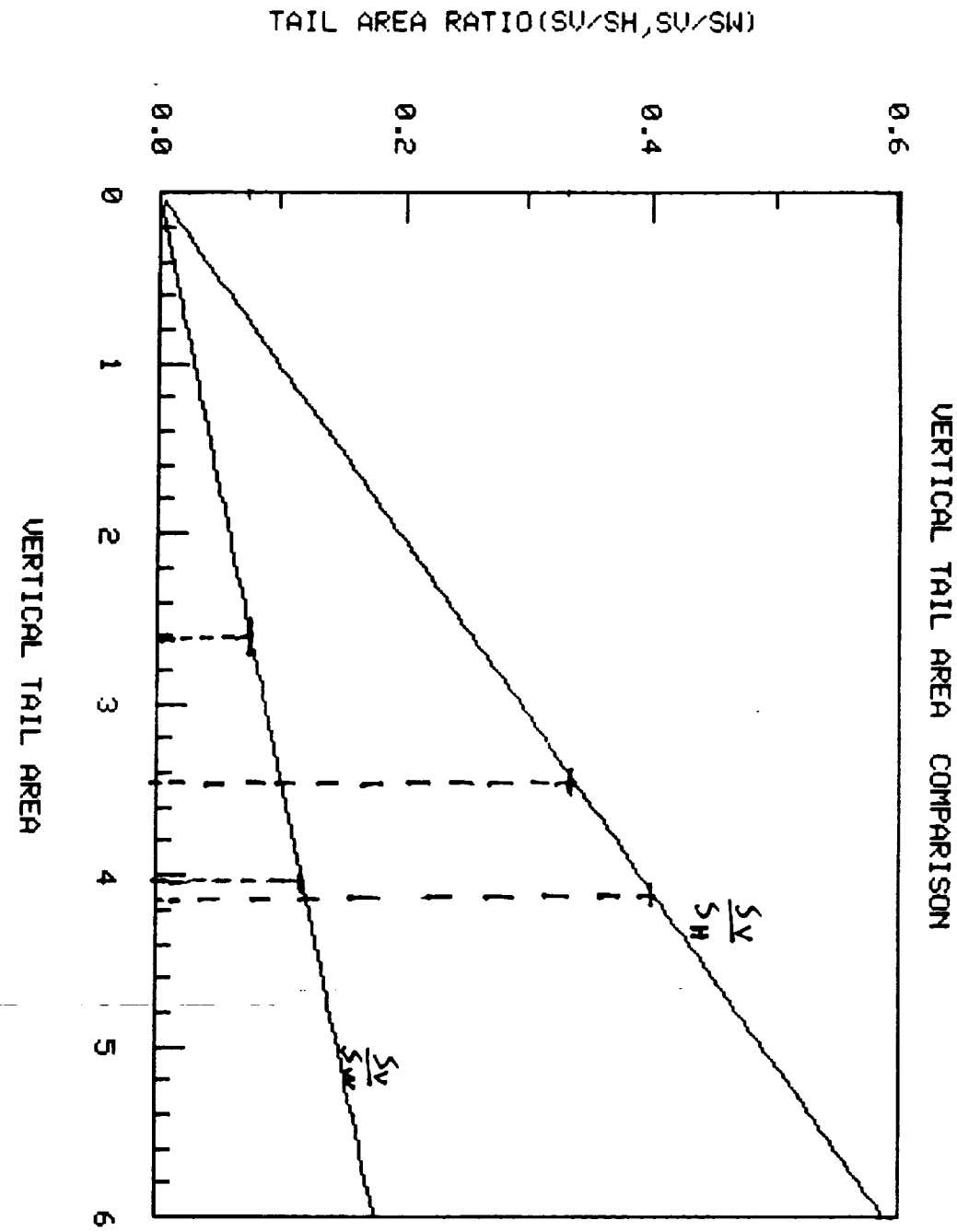

FIGURE 6-2: VERTICAL TAIL VOLUME RATIO

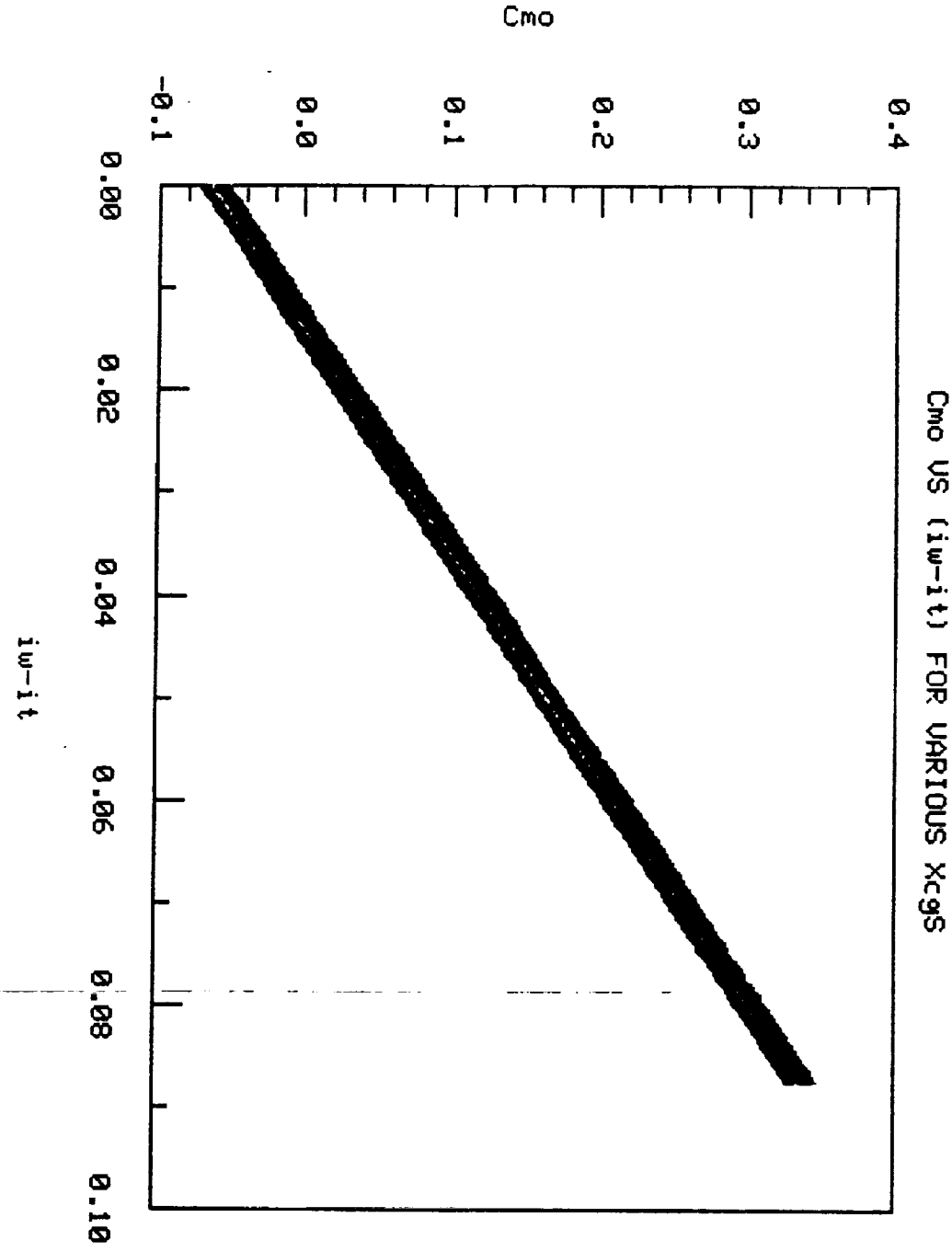

FIGURE G-3: LONGITUDINAL STABILITY(Cmo)

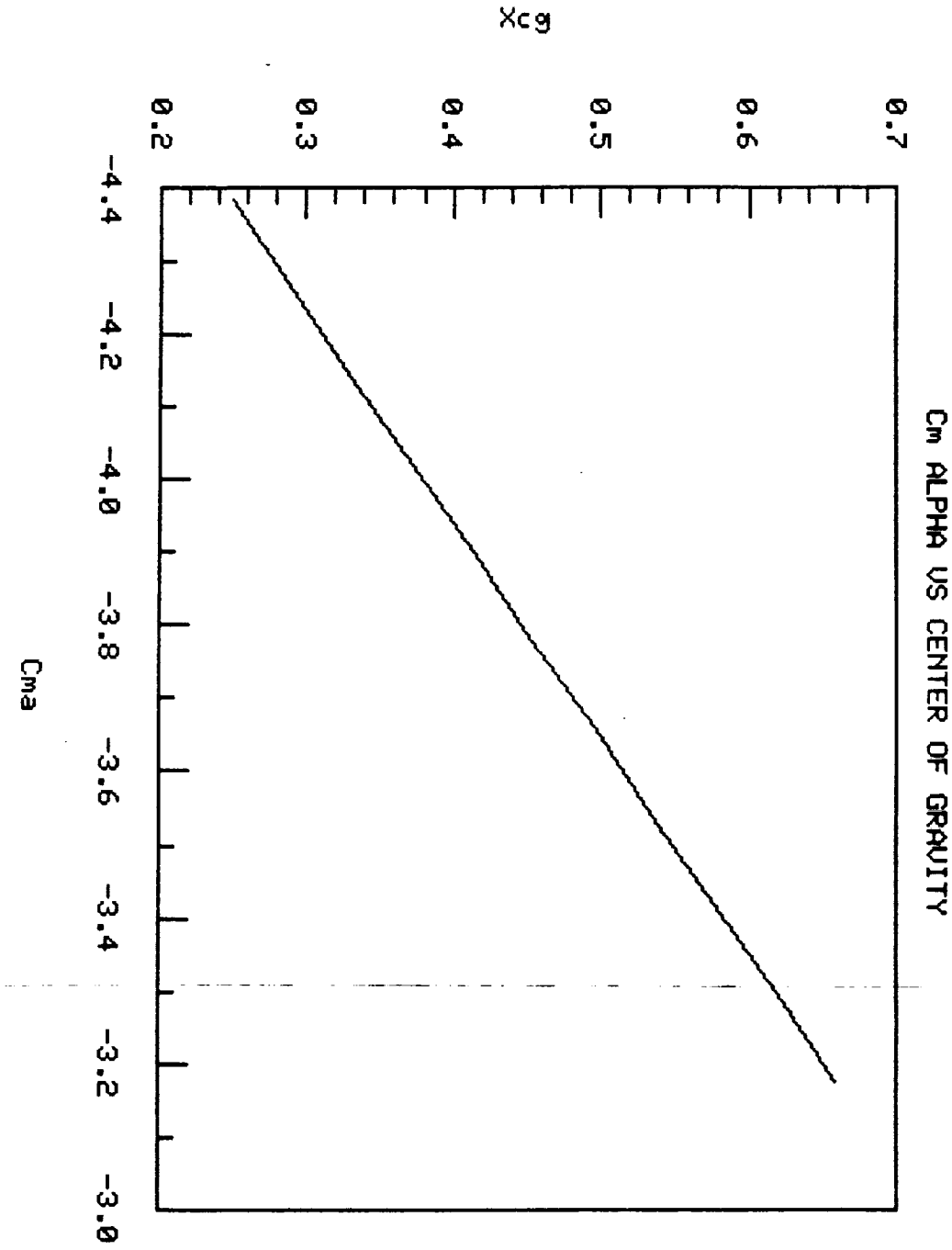

FIGURE 6-4: LONGITUDINAL STABILITY(Cm alpha)

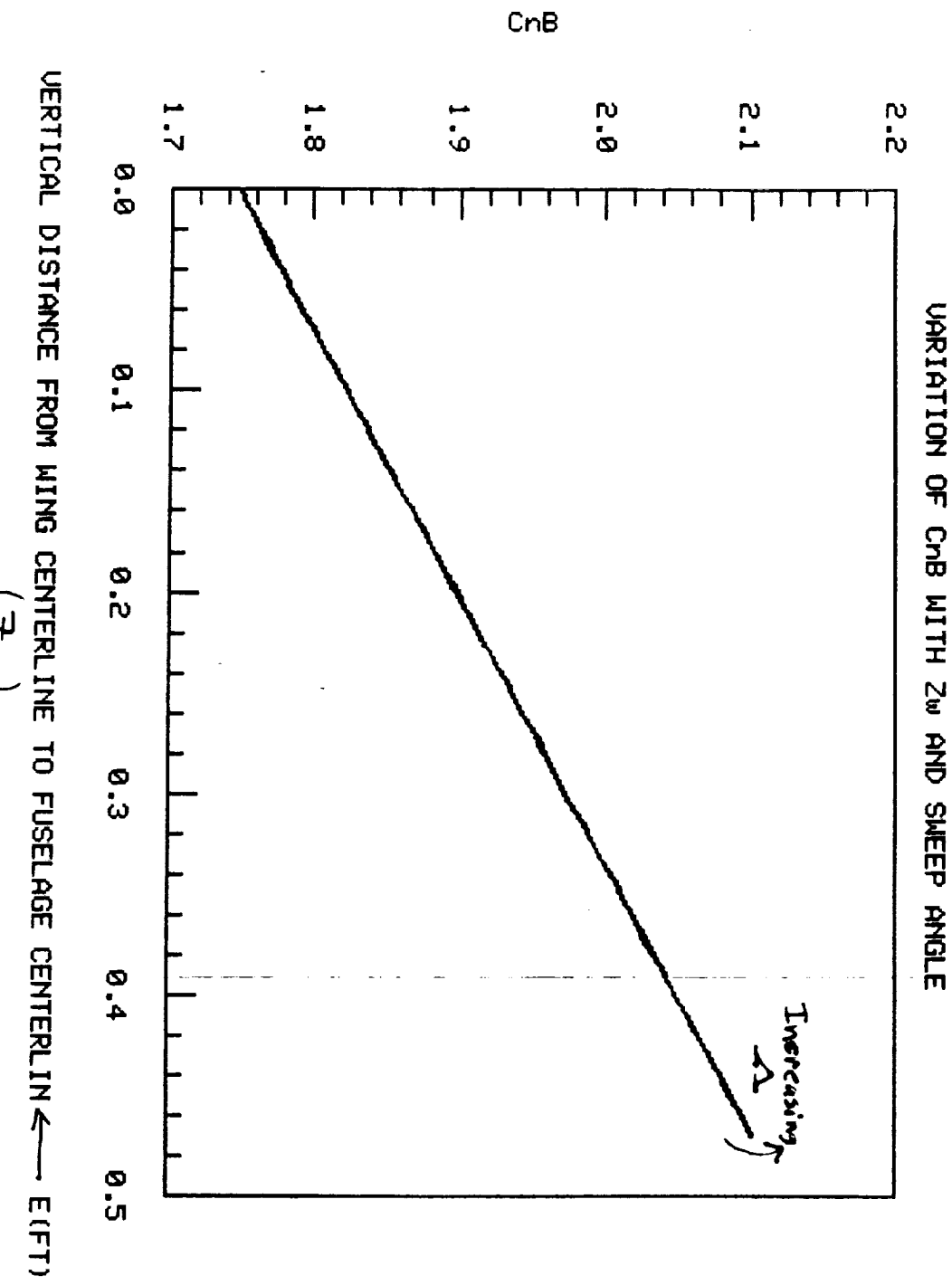

FIGURE 6-5: LATERAL STABILITY

H: CONTROL SYSTEM

THE SKY SHARK

The dynamic control of the Sky Shark will depend on the ability to overcome forces generated by the wing specimen and any control surfaces needed to keep the aircraft in steady level flight. First, the wing specimen will be examined. The principle forces are lift and drag;

$$Drag = .5*rho*St*v2*Cd \quad and \quad Lift = .5*rho*St*v2*Cl$$

Since controls will have to overcome the maximum disturbances, that case will be examined. The angle of attack will be set at 13°, Cl=.92, Cd=.015. This yields the following equations;

$$D = (5.942\ e\ -5)*v2 \qquad and \quad L = (3.645\ e\ -3)*v2$$

The drag force will be overcome by the thrust from the engines, while the design of winglets was needed to overcome the rather large side forces generated by the vertically mounted wing specimen. Although rudder deflection would more than adequately eliminate any side forces, there would be a large yaw moment generated from the rudder. Since this yaw moment could not be controlled, an alternate solution was needed to handle the side forces.

The side force dilemma could only be resolved by use of winglets. The winglets could generate a sufficient side force without producing any significant yaw moments (see Figure H-1). Once the winglet design was confirmed, the size, location, and optimal angle of deflection had to be determined. Since drag was a major consideration for the Sky Shark's design, all three parameters would be optimized to minimize the total drag from the winglets.

There are a few "figures of merit" which will be key indications as to the overall performance of the winglet design. Ideally, the winglet will overcome the side forces of the test specimen without placing the aircraft into dynamic instability about the other two principle axes, namely longitudinal dynamic control and roll control. Since the implementation of the winglets practically nullified the roll instability caused by the wing sample, conventional ailerons were sufficient to handle any roll deviation (see Figure Hc2). Therefore, the primary concern dealt with longitudinal control, or more precisely, minimizing the product of the drag forces and the

distance from the aircraft center of gravity to the aerodynamic center of the winglets (see Figure H-3). Another consideration is that the winglet's drag must not be too large a burden for the powerplant. Since both of these measures hinged around minimizing drag, that was the foremost "figure of merit" .

There were many parameters involved in this design study. The atmospheric density depended on the altitude of the aircraft. Since the aircraft needed to overcome the maximum side force generated by the wing sample, the density was fixed to that at sea level conditions. Although flight velocity affected the side force generated by the sample, it equally affected those forces generated by the winglets. A maximum velocity of 190 feet per second was used when considering the largest possible drag forces from the winglets.

The wing sample's area and airfoil type was also a potential variable parameter. The NACA 0006 airfoil was chosen for this study, and the Sky Shark aerodynamic team set the specimen's area at 3.33 square feet with a chord of 1.33 feet. One important wing sample variable was the angle of attack. Varying the angle of attack consequentially varies the coefficients of lift and drag for the airfoil.

There are four primary parameters dealing with the winglets. The first is the winglet chord. The winglet could be placed at various chord positions on the wing. Winglet area would also play a key role in both the overall performance of the design as well as the structural considerations of the design. The necessary angle of deflection of the winglets would dictate the coefficients of lift and drag, and thereby the forces produced by the control surfaces. The last parameter is the selection of the winglet airfoil type. This parameter was also left open to vary.

There are certain constraints contained implicitly within this design. The wing sample as well as the winglets are restricted to angles which do not exceed the positive or negative stall angles for that air section. For the air sections used in this analysis, these values were typically -12 degrees to +13 degrees. There was a constraint on the atmospheric density due to the limitation on the altitude of the aircraft during its mission profile. The Sky Shark was constrained to a maximum of 3000 feet in altitude. There were structural limitations which had to be considered when sizing the winglets. An upper limit of five square feet was chosen by the Sky Shark structural team.

Probably the most important constraint came from the Sky Shark propulsion team. There was a concern that the twin ducted fan powerplants could possibly fall short of the thrust needed to maintain mission requirements. Therefore, an upper boundary was set by the propulsion team for the maximum amount of drag produced from the wing specimen and control surfaces under extreme deflections. This value was set at five pounds as a maximum total drag.

The major relationships between the design parameters and measures of an acceptable design are based on a few basic principles. The first principle relates the side lift force generated by the wing sample to the lift forces generated by the winglets, that is;

$$\{1/2*\rho*v**2\}*St*Cl(\alpha) = 2*\{1/2*\rho*v**2\}*Sw*Cl(\beta) \qquad (1)$$

Note that the term $\{1/2*\rho*v**2\}$ is common to both sides of the equation, and therefore has no bearing on that relationship. Another relationship important to the design is;

$$D = \{1/2*\rho*v**2\} * [St*Cd(\alpha) + 2*Sw*Cd(\beta) \qquad (2)$$

Note that this equation does depend on the atmospheric density as well as the flight velocity. It is important to note that both of these equations include the coefficients of drag and lift for the winglets and the wing sample. Although these values are functions of angle of attack, they are also functions of the chord;

$$CL = Cl / (1 + Cl / (\pi* (S / C**2))) \qquad (3)$$

The last parameter that has a considerable impact on the above equation is the type of airfoil. Each different airfoil section has different lift coefficients for different angles of attack, therefore the trim angle for the winglets depends on the airfoil section of the winglets.

The actual procedure of the trade study consisted of three simple steps. The first step consisted of a computer program written on the Prime. This program set the wing sample at the critical angle of attack. Three parameters, winglet size, chord, and angle of attack was then swept to primarily see any

effects caused by different chord sizes. The chord length was run from 1.6 feet, the value of the wing's chord at the tip, to larger values as the winglet was moved closer to the root. General trends in overall drag and winglet sizes were examined, and an optimal chord size was chosen.

Once an optimal chord size was set, the same program was used, this time only varying winglet area and deflection. The winglet's angle of attack was swept from 0 to + 14 degrees, and corresponding winglet areas were computed. At the same time the overall drag of the winglets was computed and the optimal size and angle of deflection needed to overcome maximum wing sample disturbance could be found.

With the optimal winglet configuration set, another smaller program was used to find the lift coefficient needed from the winglets at every angle of attack for the wing sample. The results of this program would dictate what angle of deflection the winglets would have to be at in order to trim the aircraft, depending on which winglet airfoil was being examined.

There were some very interesting results determined from this trade study. One can quickly see that the optimal chord length was the minimum chord length of 1.6 feet. This set the value of the winglet chord and placed the winglet at the tip of the wing. Winglet areas were then calculated for a sweep of deflections and the results are found in Figure H-4. The general trend of the graph indicates a dramatic decrease in area as the winglet's deflection was increased. In order to pick an ideal size and deflection combination, drag from the winglets had to be examined. Figures H-5 & H-6 illustrate the effect of winglet area on the overall drag. An optimal design point was found to be at an angle of deflection of seven degrees and with a winglet area of 2.56475 square feet. This area was later increased by making the winglet into a rudder-control surface configuration (see Figure H-7).

With the winglet sized, there were still a couple of items to be examined. The total drag for the wing sample and winglets was examined throughout the flight velocity range to check on any limitations on flight speed (see Figure H-8). At maximum velocity the configuration was still within the constrained drag range, with a maximum drag of approximately 4.25 pounds.

The last step in the trade study examined the relationship between the angle of attack of the wing sample and the necessary angle of attack of the winglets. Since different airfoil sections could be used for the winglets,

necessary lift coefficients was plotted in place of angle of attack (see figure H-9). Consulting various lift curves would determine the necessary angle of deflection needed by the winglet. For a given airfoil section, this would yield information which could be implemented into a state feedback stability augmentation system.

Since the primary surfaces (specimen, winglets) are all in line with the center of gravity, lateral control is not greatly disturbed. The given data base provided in lab suggested the rudder area to be one half the area of the vertical tail, or two square feet. Using this area and the governing equation;

$$\partial N = 1/2\ \rho\ *v2*Sw*bw*Cl\alpha*\tau*(Sv*lt/(S*c))*\Delta\partial r$$

This yielded $\Delta N = 1.13\ V2\ \Delta\partial r$, and at a maximum deflection of 30°, $\Delta N = .59\ V2$. This is ample lateral control for any unforeseen yaw instability.

Longitudinal control required the sizing of elevators. Using the basic longitudinal analysis;

$$\Delta M = 1/2\rho*V2*Sb*Vh*\eta*Cl\alpha*\tau*\delta e$$

and

$$\Delta M = 1/2\rho*V2*[St*Ltest*Cdt + 2*Lwl*Sw*Cdw]$$

can be set equal, and using the extreme disturbance of 13°, the necessary area for the elevator can be found. An elevator was selected at .25 the area of the horizontal tail. This was more than sufficient to control the aircraft, even with a very small elevator deflection (1-3°). With these new sizes, the elevator angle needed to trim the aircraft could be computed. This was determined to be;

$$-0.034 = -1.42\ \alpha + 1.61\ \delta e$$

The roll control of the aircraft was simplified by the use of the winglets as mentioned above. Conventional sized ailerons were placed on the Sky Shark to test their ability to control the aircraft at maximum disturbance. The ailerons were sized at 1.7 feet by 1.0 feet, and were placed one foot from the tip of the wing, or 5.8 feet from the aircraft centerline. The necessary angle of deflection was then computed and found to be 23.22°. This was well within

the range of the elevators (Δ max was set at 30°) even for a taper ratio of .8, which was the maximum taper proposed by the aerodynamics team.

Figure HC-1

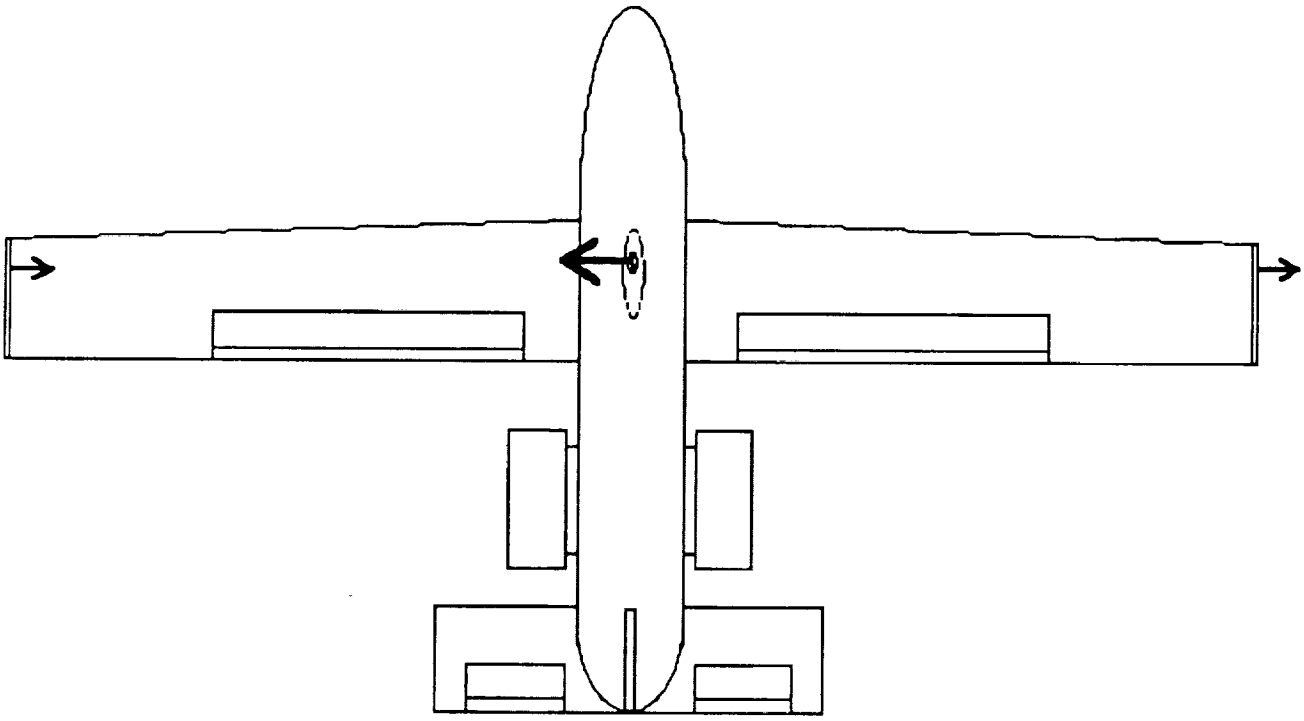

The Sky Shark's design includes the implementation of winglets. These control surfaces allow the aircraft to maintain straight and level flight without placing an unacceptable burden on the powerplant. The winglets balance the side force produced by the test specimen without creating significant dynamic yaw instability.

Figure HC-2

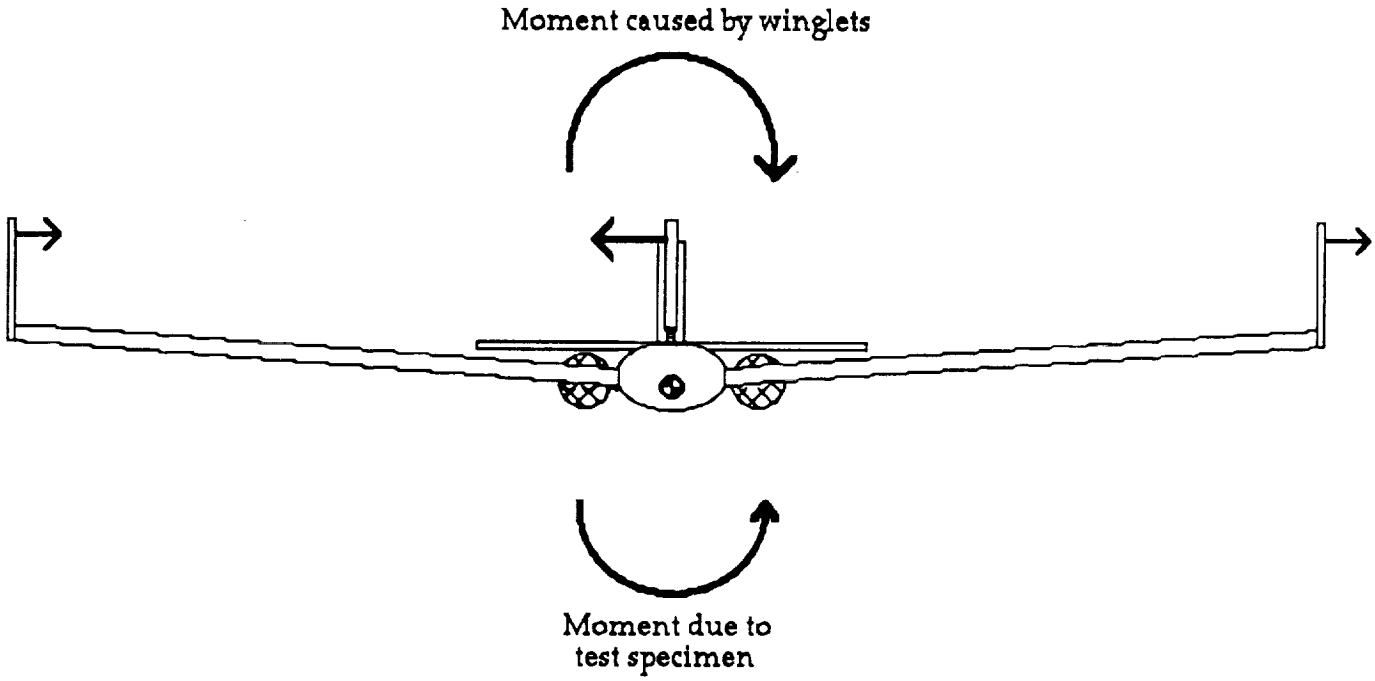

Figure HC-3

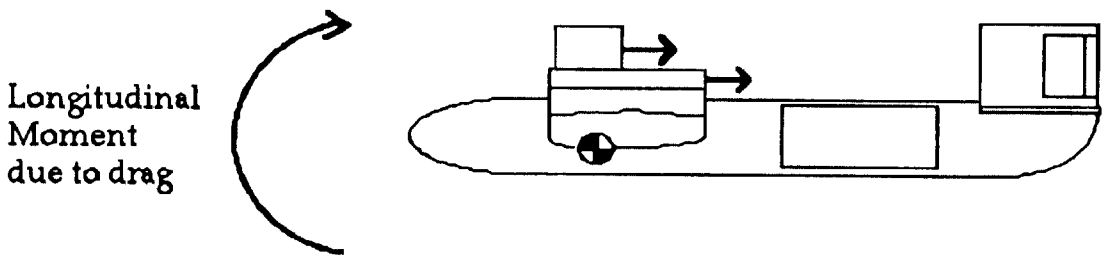

Figure HC-4 Deflections & Sw

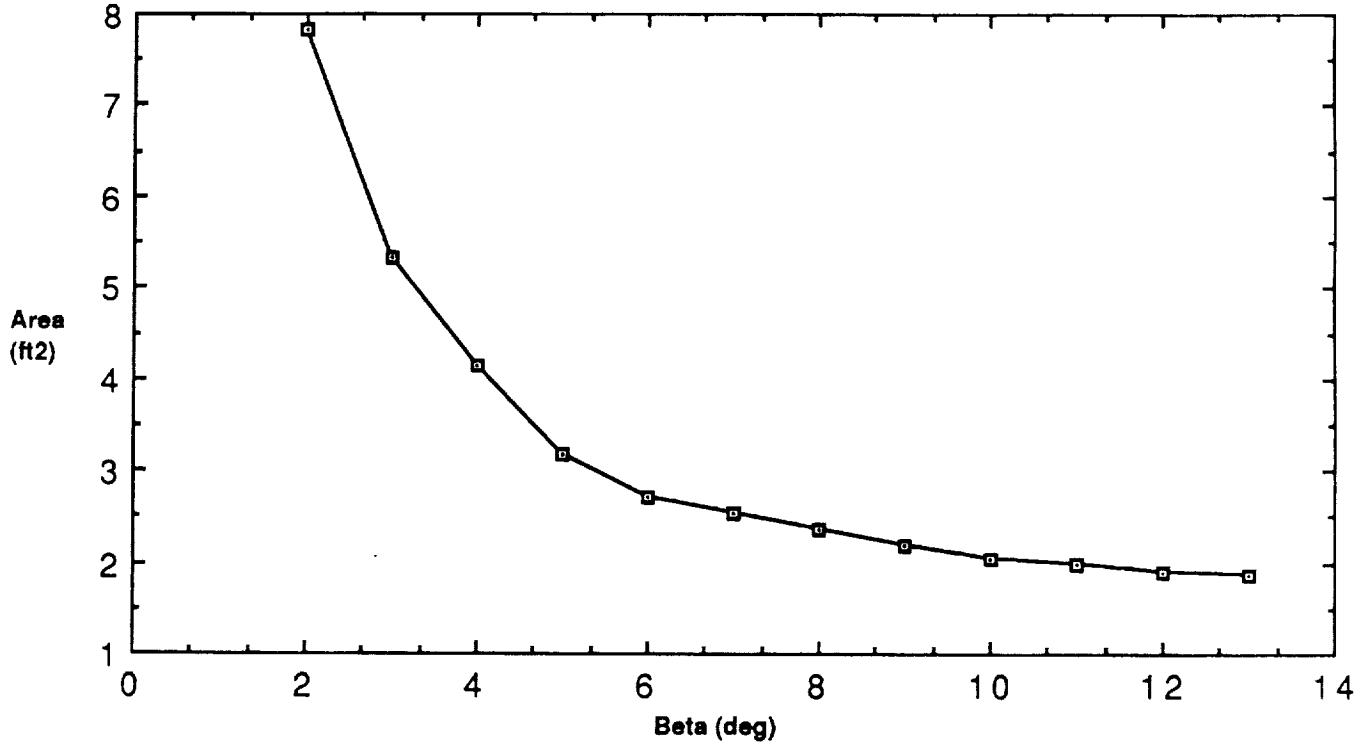

Figure HC-5 Drag Coefficients

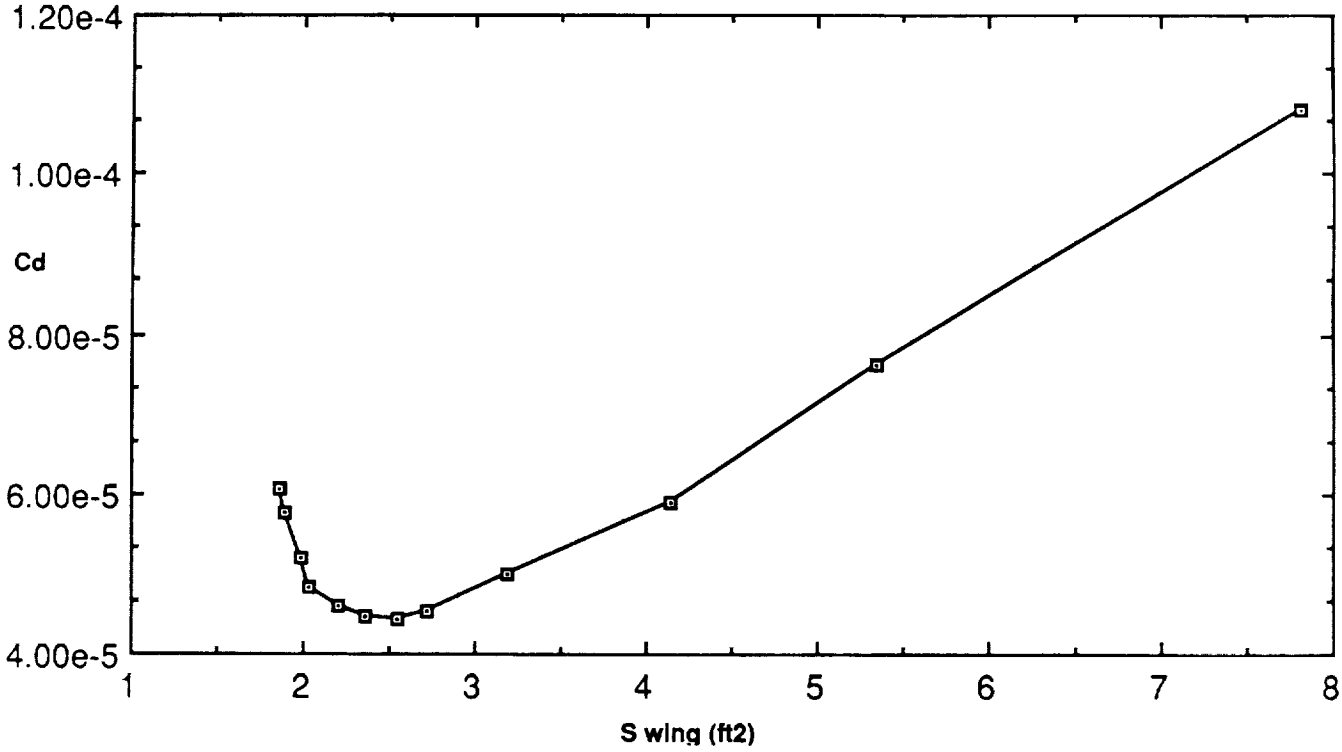

Figure HC-6 Drag Coefficients

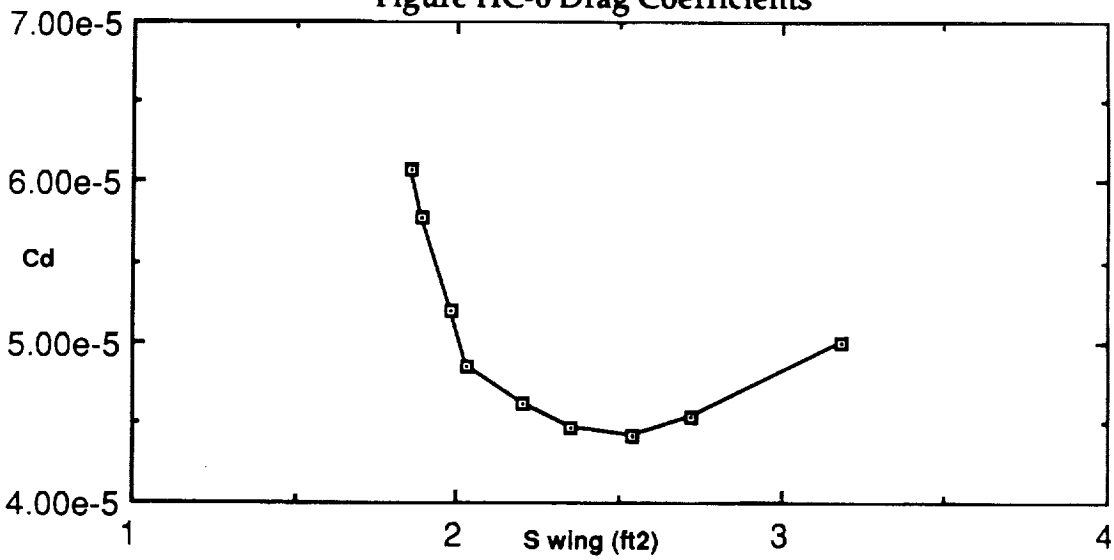

Figure HC-7

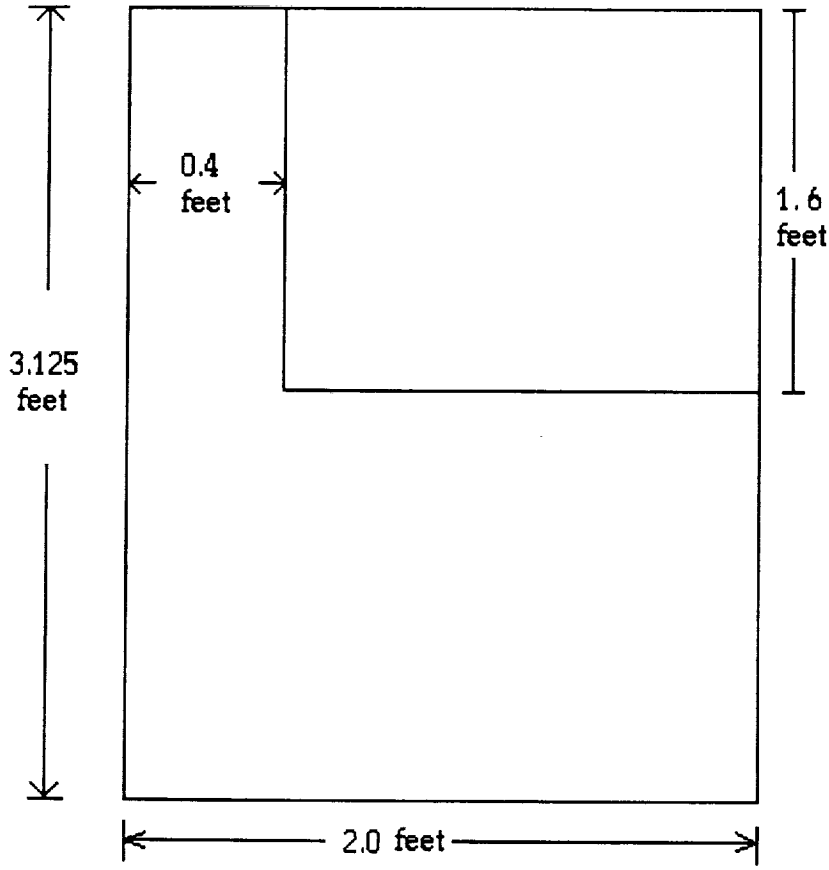

Winglet configuration

Figure HC-8 Aircraft Drag

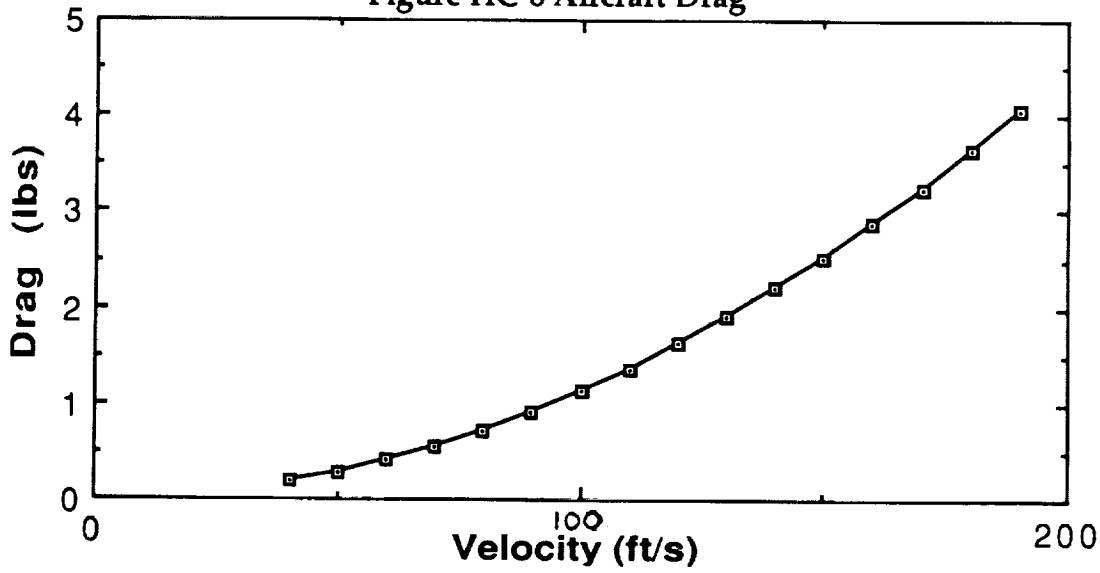

Figure HC-9 Necessary Cl at Alpha

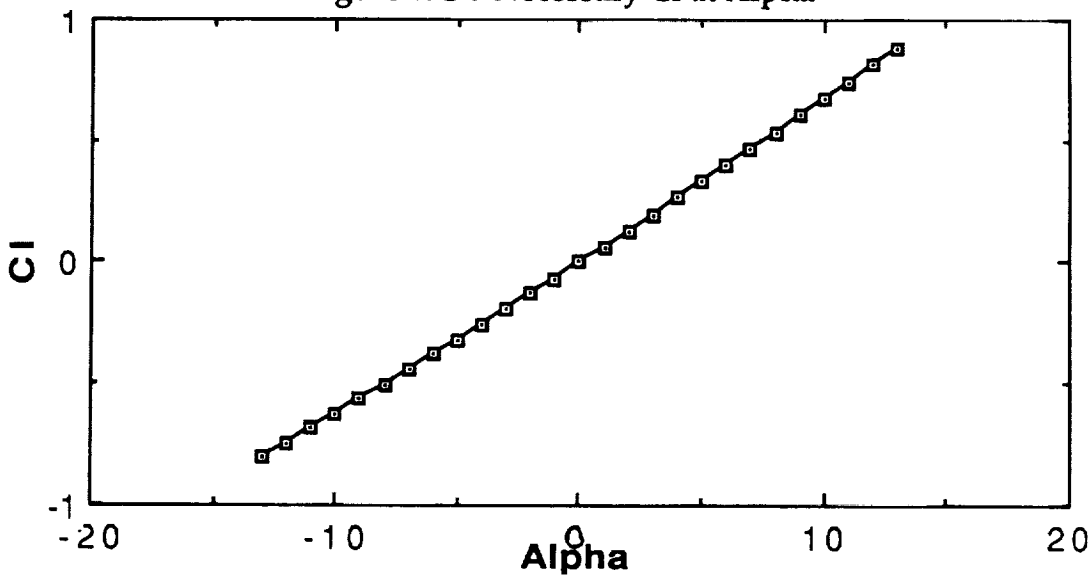

H: FIGURES

THE SKY SHARK

I: PERFORMANCE ESTIMATION

THE SKY SHARK

The Sky Shark's performance analysis was based on the values used for the prescribed mission. These values occur under optimal conditions, and do not include other factors, such as line-of-sight operation, dynamic disturbances, and operator limitations. There were a number of parameters examined, and these including maximum rate of climb, absolute and service ceilings, range, endurance, minimum glide angle, take-off and landing velocities, turning and maneuver radii, and landing distances.

The first parameter was maximum rate of climb. This was obtained using the following relation;

$$R/C\ max = (Pavailable - Prequired)/weight$$

This rate is a maximum at sea level and at one optimum flight velocity. For the Sky Shark this maximum rate of climb was found to be 35.8 ft/s.

The next parameters to be examined were absolute and service ceilings. The absolute ceiling can be found by plotting the maximum rates of climb against altitude. When the aircraft reaches a maximum rate of climb of zero, the aircraft is at the absolute ceiling. This can be expressed in the following manner;

$$Y = mX + b$$

where "Y" denotes the altitude, and "X" denotes the maximum rate of climb. The value "b" in this case represents the absolute ceiling. In order to evaluate this equation two point are needed. The values of 35.8 ft/s at sea level, and 31.6 ft/s at 2000 feet were the respective rates of climb and altitudes used in this analysis. The absolute ceiling was found to be 17,047 feet. The service ceiling could then be found using the same equation. By definition, the service ceiling is the altitude at which the aircraft has a rate of climb of 100 ft/min or 1.67 ft/s. Replacing this value for "X" gives a service ceiling of 16,253 feet.

The next value determined was the minimum glide angle for maximum decent length. This value is given as;

$$\gamma\ min = \tan^{-1}(1/(L/D\ max))$$

Maximum lift over drag can be found by examining the thrust required curve vs. velocity. The point of minimum thrust required is the point of maximum L/D. This value of L/D was found to be 13.33. This yielded a minimum glide angle of 4.3°.

The next factors to be found were take-off and landing velocities. These values are given as;

$$V_{takeoff} = 1.2\ V_{stall}$$

$$V_{landing} = 1.3\ V_{stall}$$

The stall velocity of the aircraft was given by the aerodynamic team as approximately 32 feet per second. The resulting performance velocities are Vtakeoff = 37.8 ft/s, and Vlanding = 40.96 ft/s.

Endurance was the parameter of primary concern for the Sky Shark. Since the Sky Shark's mission entails the sampling of pressures at various Reynolds numbers, there would be a maximum operating time, chosen to minimize fatigue on the pilot. This value was set at 40 minutes. Although this value of endurance would restrict total range, this value was found in case the aircraft had to be flown for an unforeseen extended period. The equation governing the range is;

$$R = (\eta/Cp)*(Cl/Cd)*\ln\ (Wi/Wf)$$

where η is the propulsive efficiency, Cp is the specific fuel consumption, Wi is the total weight of the aircraft, and Wf is the empty weight of the aircraft. Using the values for the Sky Shark, a maximum range was calculated as 46.9 miles. This range was found assuming that the aircraft would be flying at an average flight velocity of 100 ft/s throughout the mission.

Three turning radii were then examined. These turning radii included normal turn radius, pull-up radius, and pull-down radius. Pull-up radius is minimum radius at which an aircraft could pull its nose up. This is also the case for pull-down radius except the aircraft is turning down from inverted flight. These radii can be found from the following equations;

$$R_{turn} = V2/(g*(n2-1)**1/2)$$

$$Rpu = V2/(g*(n-1));$$

$$Rpd = V2/(g*(n+1))$$

where g =32.2 ft/s2 , V=Vmax= 190 ft/s, and n is the structural load factor. The structures team set the maximum load factor at approximately six, and for this analysis a maximum load factor of four was chosen for aircraft safety. This yielded the following radii: Rturn = 289.5 ft, Rpu = 373.7 ft, and Rpd = 224.0 ft.

The last parameter to be examined was landing distance. This distance can be broken up into two parts, air landing distance (Xair), and ground roll and brake distance (Xgb). The total landing distance is then X=Xair + Xgb. The ground and braking distance is fixed by the following equation;

$$Xgb = 1.69\ W2/(g*\rho*S*Clmax*[D+\mu*(W-L)])$$

Certain parameters were set in the above equation. The aircraft was assumed to be landing empty at sea level. The aircraft would employ flaps to obtain a maximum Cl of 1.5 and spoilers to eliminate all lift at touchdown. The coefficient of friction was assumed to be .4 (rough surface), and the drag was calculated at landing speed. This yielded a roll-brake distance of 44 feet. The second part of the equation, Xair is a function of obstacle height;

$$Xair = H\ obstacle/\ Min.\ glide\ angle$$

For the prescribed obstacle height of 50 feet Xair would equal 666 feet for a total 710 feet. This is above the landing distance constraint, therefore two options are possible. The first option is to loosen the obstacle height constraint to fit the landing distance limitation. This new obstacle height would be 19 feet. The other option would be to land the aircraft in a downward spiral. This would place the aircraft at risk of stall and the aircraft would be very difficult to control at slower, landing speeds, therefore either the obstacle distance must be reduced to 19 feet, or the landing distance increased to 710 feet.

J: LAUNCH AND RETRIEVAL

THE SKY SHARK

Launch:

The method of launch for the Sky Shark incorporates a catapult capable of imparting a velocity of 80 ft/s to the aircraft. The catapult would be constructed using a compressed spring or elastic bands to provide the necessary force to the aircraft. Using a simple potential and kinetic energy analysis, approximate quantities for the length the catapult must operate through and the spring constant may be determined. This method does not take into account drag from the aircraft, so the resultant values should be increased by 10% to insure their suitability. The equation relating these quantities is:

$$x=V\,(m/k)^{.5}$$

where x is the distance through which the catapult must act, V is the flight velocity, m is the mass of the aircraft, and k is the spring constant. For a spring coefficient of 100 lb/ft, for example, a length of 12 feet would need to be considered. After the aircraft leaves the catapult, it is a simple matter for it to climb out of the 300 ft diameter circle available for launch. The catapult is an aspect of the proposal which needs considerably more investigation before accurate design proposals for it can be presented. These results, however, do show the feasibility of such a system.

Retrieval:

Section I offered some suggestions for retreival of the aircraft, and this section will now expound on these results. Reference J.1 gives the equation for landing distance as:

$$X_{LD}=h_{obst}/g+R(g/2)+V_{TD}t_{FD}+W/g(1/2B)\ln[1+B/A(V_{TD})^2] \qquad (*),$$

where h_{obst} is the obstacle height, given as 50 feet in the design specifications, g is the landing incidence angle, R is the radius of flare, V_{TD} is the touch down velocity, t_{FD} is the time of free roll, and A and B are given as follows:

$$A=mW+R \qquad\qquad B=1/2rC_DS.$$

The m term is the runway friction coefficient, assumed to be 0.8 for a rough

surface. First it was assumed that the free roll time of the installed landing gear would be zero, and so $V_{TD}t_{FD}$ would be eliminated. This is acceptable based on currently available, simple, spring-loaded landing systems for small RPV's. It was also assumed that the approach speed of the aircraft would approximate the touch-down speed, which, as seen in section I, is 40.96 ft/s. Therefore, the value for R can be computed as follows:

$$R=V_{TD}^2/(g(C_{LF}/C_{LA}-1)).$$

Reference J1 says that for most ducted-drive aircraft, such as jets and fans, C_{LF}/C_{LA} can be approximated as 1.2. Carrying out the calculation gives an R of 260.52 feet. Similarly, for a drag polar as follows:

$$C_D=0.023+0.044C_L^2,$$

Approximate calculations for drag coefficient values capable of stopping the aircraft in the required area yeild a C_D of 9.983. Achieving this high drag coefficient will be accomplished through the use of tension brakes in the landing gear. It is now possible to calculate values for A and B:

$$A=308.52 \qquad B=0.4034.$$

It is known from the design specifications that a maximum allowable landing distance of 300 feet is permitted. Putting all the known values in (*) and solving for g yields:

$$130.26g^2-297.32g+50=0,$$

or:

$$g=0.1828 \text{ rads}=10.45 \text{ degrees.}$$

This value is based on a small angle approximation. Changing the g term in (*) to tan(g) , and using 10.45 degrees for g, X_{LD} approximates 297.60 feet, which is adequate for the design specifications. From this point refueling and changing of the test specimen may be accomplished, a process which,

optimally, should take only several minutes.

Turnaround:

Turnaround involves several processes but should be able to be handled by two individuals in a reasonably short period of time (15 minutes). First, the aircraft must be brought back to an area where fuel, fresh batteries and other replenishables are present. This should take little more than 3 or 4 minutes. Next, the data stored in the aircraft's memory chips must be dumped to the on-sight computer before power is cut to the chips. This should take approximately 2 to 3 minutes. While the data transfer is going on, the other technician can begin refueling the two ducted fan engines, taking 4 to 5 minutes. If necessary, fresh batteries can be placed in the aircraft, taking 2-3 minutes. The aircraft must then be mounted on the catapult, have the gear reset and a control check carried out, taking 3-5 minutes. The aircraft can then be launched and another series of data points recorded.

K: DATA ACQUISITION

THE SKY SHARK

The wind tunnel has served as a primary source of aerodynamic data for flight vehicles. Yet within the wind tunnel, certain flow conditions cannot be achieved. Therefore, the Sky Shark has been designed to be used as an airborne aerodynamic data acquisition system that will collect surface pressure distributions on two and three dimensional lifting surfaces at low Reynolds numbers.

The following two studies will explore the overall data acquisition system selection and the pressure transducer system selection as it pertains to the flight mission.

DATA ACQUISITION SYSTEM PROPOSAL:

The objective of this study is to design an airborne aerodynamic data acquisition system capable of measuring and recording pertinent surface pressure distribution data. The system that will measure actual pressure data from the test specimen will be studied in depth. The system that will measure and record the necessary associated data such as airspeed, angle of attack,etc. will only be briefly discussed. This study will result in an overall data acquisition system that falls within the prescribed constraints and meets the desired design goals.

The final design should meet various design goals which are described by the figures of merit. It is hoped that the weight of the overall system will be kept well below 10 lbs., with an ideal weight being 4 lbs.. The volume is hoped to be below 50 in^3. The accuracy of the system is extremely important considering the basic mission is to collect pertinent test data. It is desirable to choose a pressure transducer/scanning device with an error below +/- 0.1 psid and an output of 11 or 12 bits to the digital word. The telemetry systems also should transmit an 11 or 12 bit digital word. The storage device must be able to store twenty minutes of data which translates into 5.5 million pieces of data. The speed of the transducer/ scanning device is hoped to be at least 4500 channels per second with a range of 0 to 50 psid. The cost of the overall system should be kept as low as possible, yet the integrity of the test data will not be compromised for low cost.

The following parameters will be varied: accuracy, cost, weight, volume, speed, range, amount of storage available.

The final design must take into account various fixed parameters. It is expected that the system will consist of 90 pressure ports located on the test

specimen. Twenty minutes of data will be taken with each port being scanned at least 50 times per second (to insure accuracy).

The only constraints on the design are that of volume and range. The volume must be less than 0.8 x 1.4 x 4 ft. due to aircraft fuselage size, and the range must be at least from 0 to 50 psid.

The study will be divided into two parts (Table 1 in Appendix). The first part will look at the pressure transducers along with accompanying signal conditioner and encoder. From previous research, it was found that the signal from the transducer must be conditioned, to remove bias, filtered and sometimes amplified. The signal is then multiplexed and encoded from analog to digital. Four such systems will be studied. The second part of this study will look at the choice of storing the data or transmitting it to the ground through a telemetry system. Five such systems will be studied.

In the following two parts, each system's specifications will be briefly described and then those specifications will be compared with the mission's figures of merit and design constraints. Finally, an overall system design will be chosen and the secondary aircraft sensor system will be described. The information included in this study is based on publicly available company literature.

PRESSURE TRANSDUCER/SCANNING DEVICES:

ESP 48 from Pressure Systems:

The ESP 48 consists of 48 silicon integrated pressure transducers, internal multiplexing, amplification, and an integral calibration valve which permits simultaneous on line calibration of all transducers. The system scans at rates in excess of 20,000 measurements per second. The range is from 0 to 100 psid with an error of 0.1 % FS.The unit weighs 7 oz., has specifications of 1.15" x 2.7" x 1.2", and costs $8000 a piece. The output is 5 VDC through one channel. Its power requirements are as follows: +5VDC @ 75mA, +12 VDC @ 120 mA, and -12 VDC @ 600 mA.

To meet the design constraints, 2 ESP 48 systems, giving 96 pressure channels, must be used. Even with the 2 systems, the ESP 48 has an extremely small volume and the lowest weight of the five systems studied(Fig K-1 and K-2). Tubing from the pressure ports connect directly to each of the 96 pressure transducers. The system then calibrates, multiplexes, and amplifies all within the small volume. The output is through one channel which can easily be stored or sent to the ground through a telemetry system. The scan rate is very high and the range well covers what was desired. The main drawback of the system is the relatively high cost. Also, although the system is fairly accurate, a greater accuracy is desired for this mission (Fig K-3).

S8256 Flight Pressure Measurement System from Pressure Systems:

The S8256 consists of a microcomputer based Flight Data Acquisition and Control Unit and electronically scanned pressure scanners designed specifically for aircraft pressure monitoring. The system is capable of handling up to 384 pressure ports scanned at rates up to 1000 channels per second. Calibration data can be stored in the DACU that corrects for thermal zero and sensitivity shifts. It also has on-line auto rezeroing which corrects for any zero shift of the transducers, internal multiplexing, and amplification. The overall configuration of the system consists of a main flight DACU that is connected to multiple pressure scanners which in turn are connected to the pressure ports in the test specimen. The system can store the data in a data system or send it to the ground through a telemetry system.

The transducers have a range of 2.5 to 100 psid with an error of 0.25% FS. The overall unit has a weight of 9 lbs., dimensions of 3.25" x 4.9' x

12.1225", and a cost of $17,600. The output is 5 VDC through one channel. The power requirements are as follows: +15 VDC @ 1.5 a, -15 VDC @ 1 a, +5 VDC @ 3 a, and +28 VDC at 1 a.

The S8256 is very capable of meeting the design constraints of 90 pressure ports. Its specifications quote its scanning speed at 1000 channels per second, yet with the system scaled down to our needs (100 channels, 42 oz., $14,600), the speed should improve to meet our goals. The overall weight and volume are extremely high compared to the other systems studied. The cost is relatively high; the range is acceptable. The accuracy of the system is lower than would be desired. Overall, the system seems to be designed for a larger scale aircraft and mission.

20C-25 from Scanivalve:

The 20C-25 is an electronic pressure scanning module that consists of 4 remote pressure sensor modules each with 8 discreet silicon pressure sensors. The 4 modules connect into the amplifier-multiplexer unit. In this system each remote pressure has its own reference pressure, calibration tubulations, and calibration valving. The 20C-25 was designed for use inside of flaps and control surfaces of flight test vehicles where it would be important to measure high frequency flow. The data from this system is multiplexed into one channel and can be either stored or sent to the ground. The transducers have a range of 0 to 50 psid with an error of 0.08% FS. The overall weight is 6 oz. with dimensions of 3.89" x 1.27" x 0.68" (4 remotes- 1.26" x 0.14" x 0.25"). The output is 5 VDC with a power requirement of 15 VDC @ 45 mA. The cost of the system is $7350.

Three 20C-25 systems would be needed to achieve the 90 channel design constraint. Even with three systems, the weight is very low and the volume is very small. The scan rate well meets our goals as does its range of 0 to 50 psid(Fig K-4 and K-5). With three systems, the telemetry or storage system would have to handle three channels of data, yet this should not be a problem. The cost, $22,050, is very high compared to the other systems studied(Fig K-6). The clearest attribute of the system is its excellent accuracy resulting in errors of only +/- 0.04 psid(Fig K3). It amplifies, multiplexes, and calibrates without any bulky hardware.

LQ-080 Kulite Miniature IS Pressure Transducers:

The Kulite Miniature IS are flight qualified individual transducers that can be constructed directly on the surface of the test specimen. The method maintains the integrity of the surface contours so that no turbulence is generated. It is possible to place 100 transducers per inch. The Kulite IS has a small pressure sensitive area, extreme resistance to vibration and shock, small physical size, and low power dissipation. Each transducer weighs 0.2 g, has dimensions of 0.125"' x 0.04" x 0.38", and costs $350 a piece. Their range is 25 to 100 psid with an error of 0.5 % FS. The power requirement is 5 VDC.

The individual transducers have minimal weight and volume, yet with each transducer, electrical excitation is needed as well as a conditioner, multiplexer, and encoder (if data is to be stored; raw voltages can be sent directly to the ground through a telemetry system). The transducers also take continuous readings, so that some type of control unit would also be needed to monitor data taking. The cost of adding the transducers on to each of the various test specimens would also increase the cost of the system. Beyond these considerations, the accuracy is poor(Fig K-3), and the range does not cover the lower pressures that might exist on the test specimen. The cost is much too high for the purpose of this mission(Fig K-6).

DATA STORAGE/ TELEMETRY DEVICES:

Tattletale Model VI:

The Tattletale has been designed for applications where large data storage capacity is needed at minimum cost. The RAM based data storage system can handle 224 K byte of data with an attached, power switched 20 Megabyte hard disk. A TTBASIC operating system allows the 224 K RAM to be written as a block to the disk during storage and allows for operation and program development from any terminal or computer(before and after the mission). It also comes with the ability to connect with an RS-232 interface to quickly download data into a computer memory. The system has an 11 channel input, with a 11 bit analog to digital converter (in case the pressure transducer system does not already do this). The system weighs only 1.5 lbs. with dimensions of 2.9" x 5.0" x 8". The power required is minimal, 6-10 VDC @ 20 mA; it can operate from a single 9 volt alkaline transistor radio battery.

The Tattletale is extremely light with low volume as is desired for this

mission. The 20 Megabyte hard disk is a perfect way to extend memory capability to meet the design constraints of 10 Meg while keeping the weight low. The power requirements are low, and the TTBASIC system will increase the ease in which the data is stored, retrieved, and analyzed. The accuracy of 11 bits is a definite advantage; it will help insure accurate and pertinent data. The cost of $1600 seems reasonable.

Englewood Telemetry System Model 100:

The Englewood system consists of one data channel with a range of just over one mile. Its weight is 6.5 lbs., with dimensions of 8" x 5" x 4". The cost is approximately $1500, and the power requirement is 12 VDC @ 1 amp.

The Englewood is a complete wireless radio data link. The weight is very high as is the volume. The cost is reasonable compared with the other systems, yet expensive for only one data channel. It might be possible to use the system with a pressure transducer device outputting only one data channel, yet an accuracy of only 8 bits will not insure data integrity.

Remtron RTS-1 Telemetry System:

This system consists of a telemetry encoder and FM transmitter on board the aircraft, and a telemetry decoder, FM receiver, and computer interface on the ground. The RTS-1 is capable of transmitting 8 channels of data with 8 bits to a digital word. Through this system, raw voltages can be sent directly to the ground where voltage conversions will take place. The weight is 4 oz. with dimensions of 3" x 3.6" x 1". The cost is $3000 each with a power requirement of 12 VDC @ 50 mA.

The RTS-1 is a relatively expensive system, yet its weight and volume are extremely low(Fig K-7 and K-8). Eight channels of data would work well for this mission, but an accuracy of only eight bits would lessen the accuracy of the test data. This system would be a possible choice to transmit the aircraft sensor data where high levels of accuracy are not as important.

KDC Video Cassette Data Recorder RTP-65:

The RTP-65 stores signals on a special type of video tape. It is programmable for calibration and encoding functions. Its weight is 40 lbs. with dimensions of 17.5" x 12.2" x 12.7". At a tape speed of 9.52 cm/sec, twenty-six minutes of data can be recorded. The cost is $ 1400, with a power

requirement of 11 to 30 volts.

The video cassette recorder is much to heavy and too large for this mission (Fig K-7 and K-8). Its power requirements are large which would result in extra weight in batteries. It is also doubtful whether the system could handle a minimum of 4500 channels of data per second.

System 10KUD:

The System 10 was designed for high speed data storage. The unit has a built-in front panel keyboard with LCD readout. With this feature, channels and bits can be set to desired values for use in calibration. It can also zero and scale data instruments rapidly and easily. Four "A" cards can be inserted into the unit which will provide precision timing, conditioning, multiplexing, and a memory of 172 K. Data storage can be increased by additional buffer memory cards. The system is equipped with a computer interface through which it can be attached to download data and an interface through which the data can be sent to the ground through a telemetry system. The system can also be used to scan individual pressure transducers at a rate of 2500 channels per second. With dimensions of 4" x 5.32" x 14.3" and a weight of 11 lbs., the System 10 costs approximately $4095. The unit can handle up to 160 channels and requires power of 23-29 VDC @ 0.5 amps.

The System 10 is very heavy for the purpose of this mission and has a very large volume. The cost is also quite high(Fig K-9). It does have a high accuracy of 11 bit digital words, yet to increase the memory to the design constraints would take at least ten extra memory cards. The system does have many advantages such as a built-in keyboard through which changes can be made easily without an interface with a computer and on-line calibration of data instruments. Overall, the system seems too small for this mission terms of memory and too big in terms of technology and cost.

THE FINAL SYSTEM:

The final system(see Table 2) will consist of the following: 90 pressure ports located along the test specimen, tubing that connects to an eletronic pressure scanning module(with transducers), an accompanying signal conditioner and encoder, an interface with a RAM type storage device, and a secondary system that will involve aircraft sensors, a signal conditioner and

encoder, an interface with both the RAM storage device and a FM transmitter, and a ground system. A microprocessing unit (MPU) will control the functions of the scanning module and the RAM storage device.

The pressure transducer/scanning device chosen was the Scanivalve 20C-25 electronic pressure scanning module. The 3 Scanivalve modules needed incorporate the transducers, signal conditioner, encoder and multiplexer into one unit. The weight of the system is a mere 1.5 lbs. with a volume of 14.14 in^3(Fig K-1 and K-2). Although the ESP 48 weighs less and has a smaller volume, the accurate of the systems was the deciding factor. For this mission, accurate test data is the primary concern, and the Scanivalve has an incredibly low error of +/- 0.04 psid(Fig K-3). The scanning rate is high at 4500 channels per second, and the range of 0 to 50 psid also meets the design goals(Fig K-4 and K-5). The cost of $22,050 is high(Fig K-6), yet at the beginning of this study it was stated that accuracy would not be compromised for cost.

The storage/ telemetry device chosen was the Tattletale VI. A telemetry system was ruled out because the accuracy of the digital word transmitted, 8 bits, was not great enough to insure the integrity of the test data. With 90 pressure ports scanned at 50 times per second, 4500 channels will be scanned per second. Over a twenty minute test taking span, this would result in 5.4 million pieces of test data. The memory of 20 Megabytes will more than cover the amount of data to be taken with an accuracy of 11 bits to the digital word(Fig K-10). The TTBASIC system will increase the ease in which the data is retrieved and analyzed. The Tattletale system is extremely small, 11.6 in^3, with a weight of 18 oz.(Fig 7 and 8). The cost is quite reasonable at $1600 (Fig K-9).

In order to design a system that would better meet the mission's design goals, a system would have to be custom made. The cost of these types of systems were not available, yet it may be a viable alternative.

Secondary Subsystem:

The secondary subsystem provides the necessary associated data to actually fly the aircraft and to later analyze the pressure data. Seven channels of data will be used in this system to measure angle of attack, angle of attack of the test specimen, angle of yaw, angle of roll, altitude, airspeed and rate of climb.

The angle of attack and yaw will be determined by a five tap sensor placed on the aircraft and on the test specimen with integral pitot static taps and a separate side mounted pitot static tube. The angle of attack is measured through a pressure difference varying with altitude and airspeed. The airspeed can be determined by a pressure difference determined by an altimeter which itself is a sensitive pressure transducer. The aircraft sensors, especially the angle of attack devices must exhibit an extremely high accuracy because the integrity of the pressure data depends on it.

The data from the seven channels will be conditioned and multiplexed very much like the pressure data(see Table 2 in Appendix). The data will then be both stored with the pressure data and transmitted to the ground through a telemetry system most likely the Remtron RTS-1 system. The Remtron system weighs a mere 4 oz. with a volume of only 10.8 in^3(Fig K-7 and K-8). It has eight channels with an eight bit digital word. On the ground, the data will be decoded and displayed for the pilot use. Control commands from the pilot will be transmitted back to the aircraft through a different frequency.

Number of Transducers and Chordwise Placement

The number of transducers and chordwise placement of the pressure ports was determined by studying the graph of the pressure coefficient along the chord. As stated earlier the maximum number of pressure ports is 90. It is desirable to have the best representation of the pressure distribution as possible. Based on typical pressure distributions it was decided to concentrate a greater number of pressure ports at the leading ten percent of the test specimen due to the abrupt pressure changes in this region. Away from the leading edge the pressure changes are more uniform and less pressure ports are necessary. Therefore, the pressure ports can be located farther apart on the trailing 90 percent of the test specimen. Based on this logic, the location of pressure ports on the upper and lower surfaces, in X percent of the chord, is as follows:

.5, .75, 1.25, 2.5, 5, 7.5, 10, 15, 20, ..., 90, 95, 100

These locations should provide an adequate representation of the pressure distribution on the test specimen. Given these locations, there would be a total of 25 ports on the upper surface and 25 ports on the lower surface for a total of 50 ports. The remaining 40 ports could be used at another spanwise position in order to study tip effects or two and three dimensional effects including separation along the span.

K: APPENDICES

THE SKY SHARK

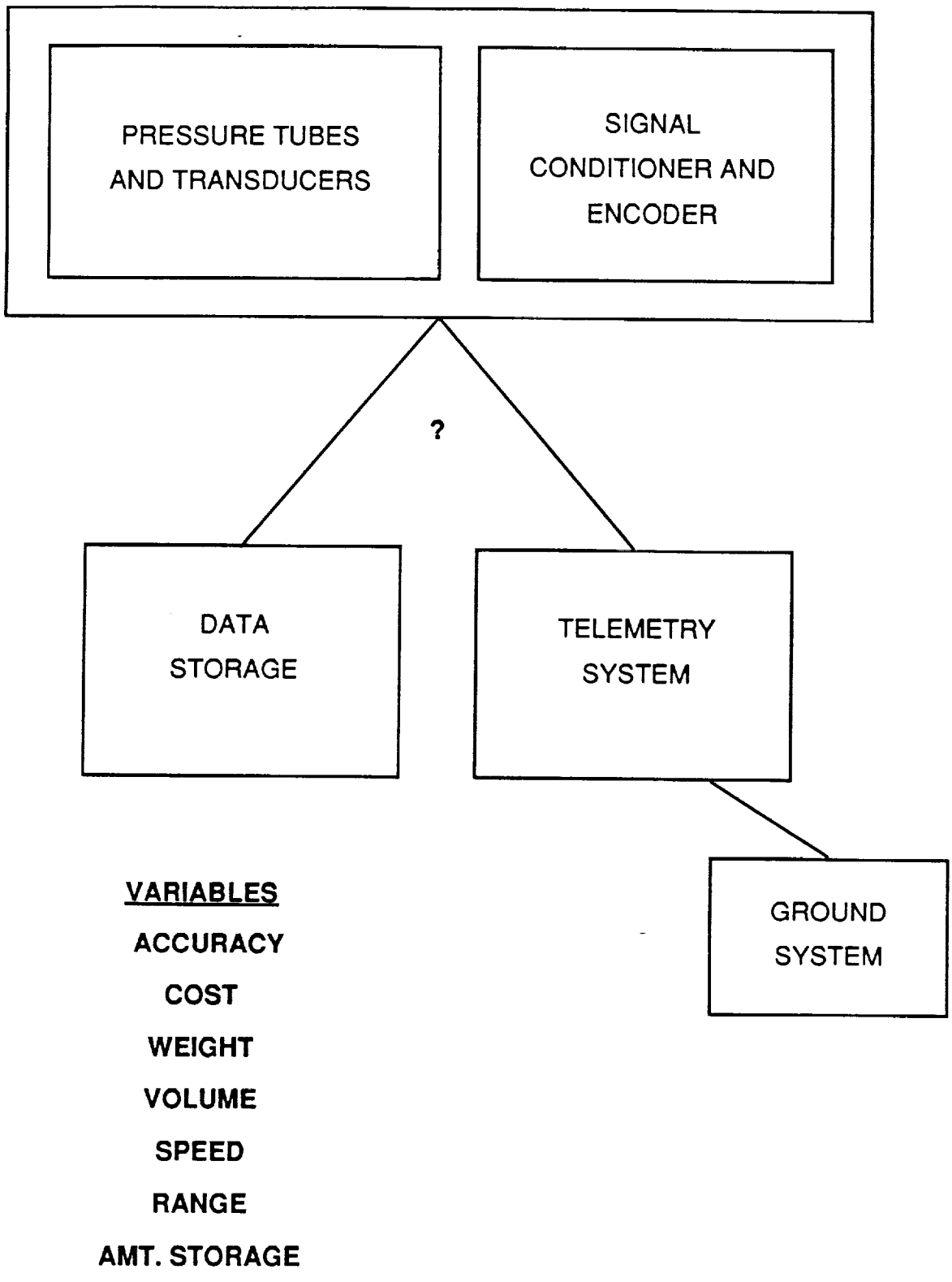

TABLE 1: INITIAL PRESSURE DATA ACQUISITION SYSTEM DESIGN

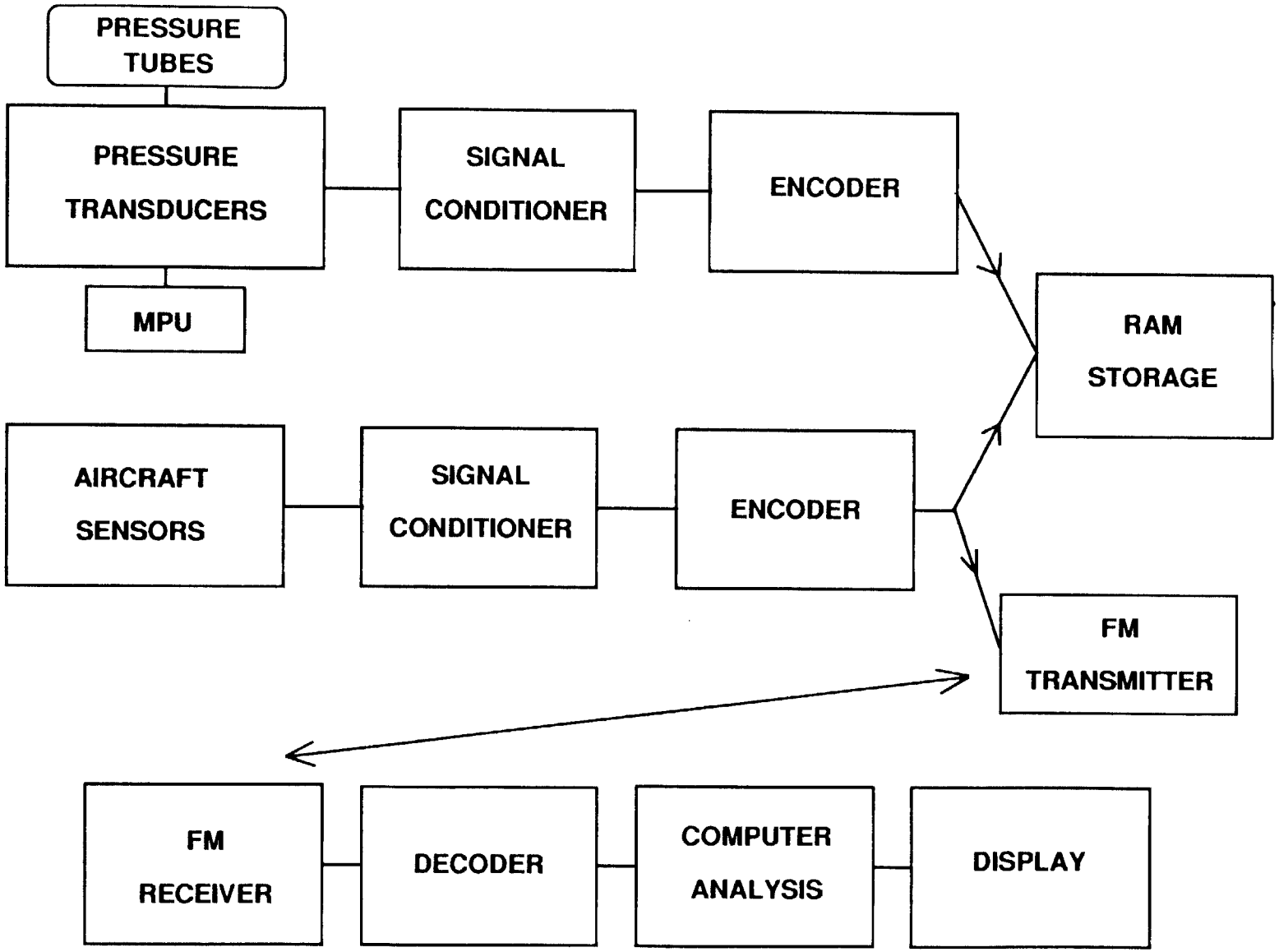

TABLE 2 : FINAL DATA ACQUISITION SYSTEM DESIGN

K: FIGURES

THE SKY SHARK

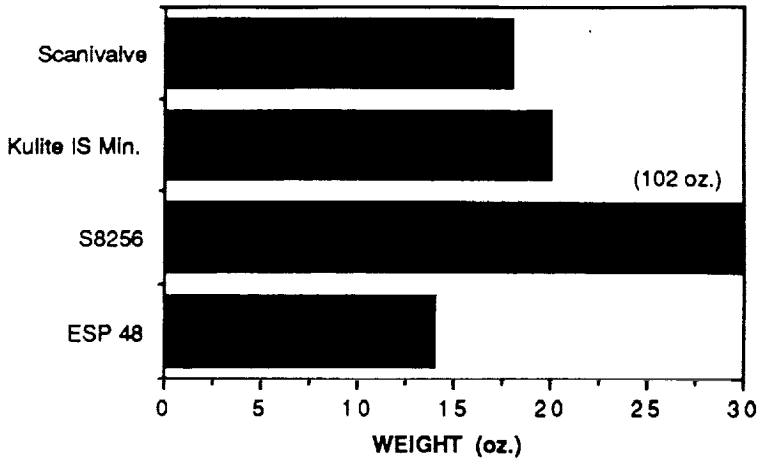

FIG 1: Comparision of Transducer/ Scanning Device Weights

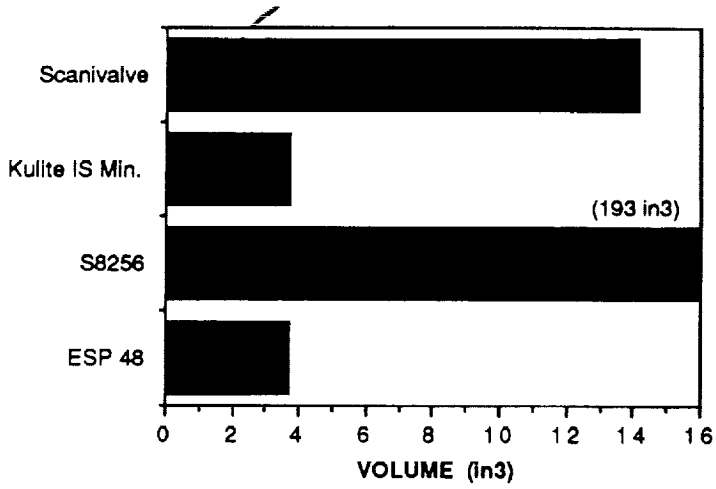

FIG 2: Comparision of Transducer/Scanning Device Volume

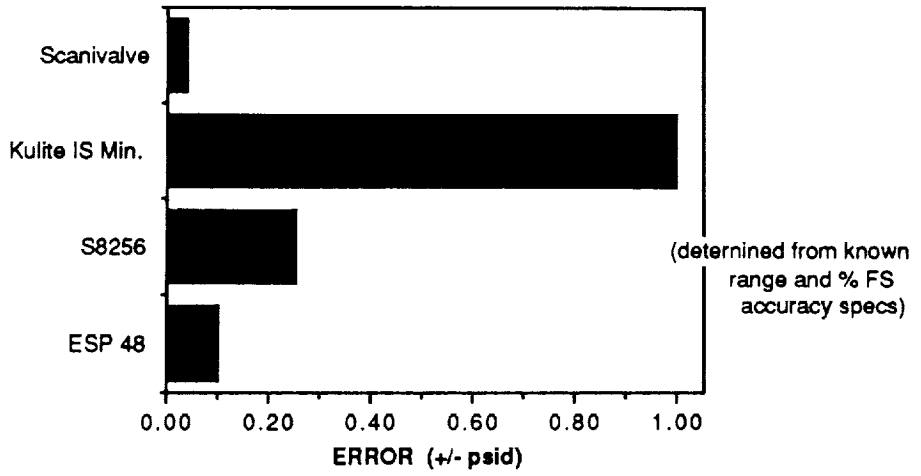

FIG 3: Comparision of Transducer/ Scanning Device Accuracy

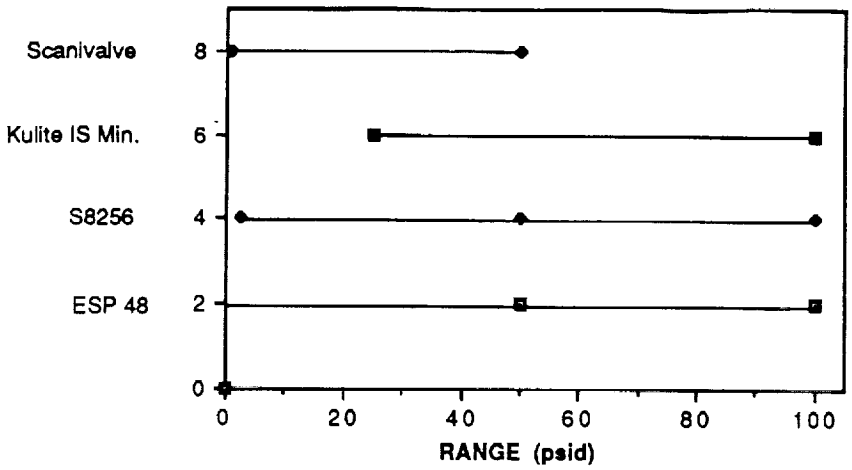

FIG 4: Comparision of Transducer/ Scanning Device Range

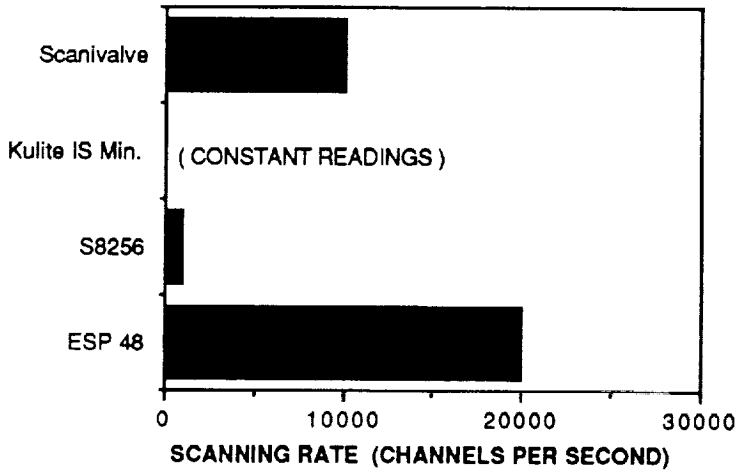

FIG 5: Comparision of Transducer/ Scanning Device Speed

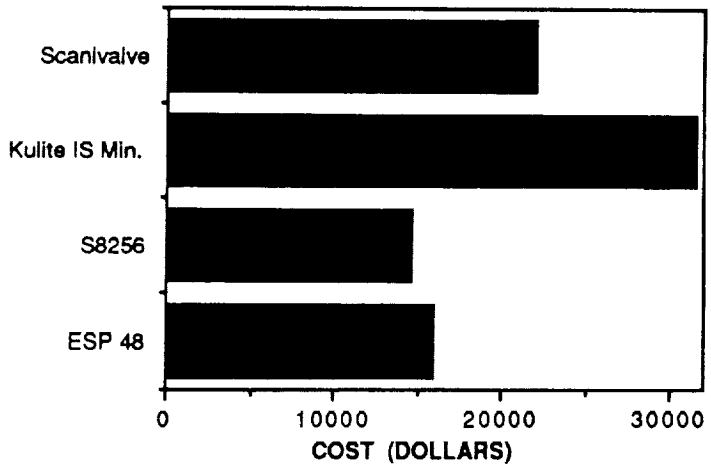

FIG 6: Comparison of Transducer/Scanning Device Cost

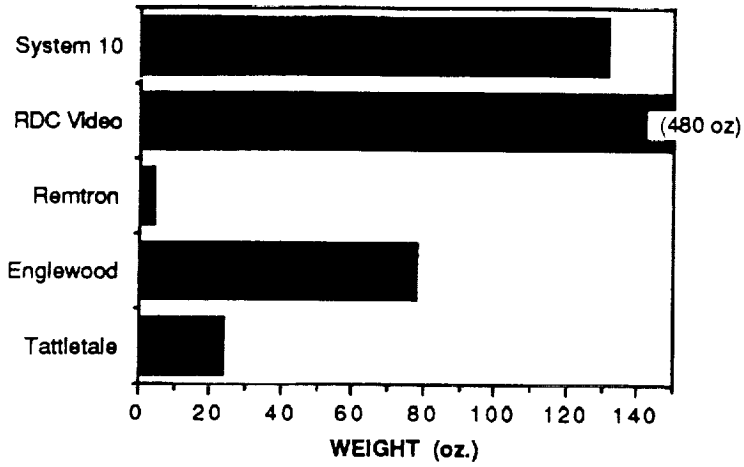

FIG 7: Comparision of Storage/Telemetry Device Weight

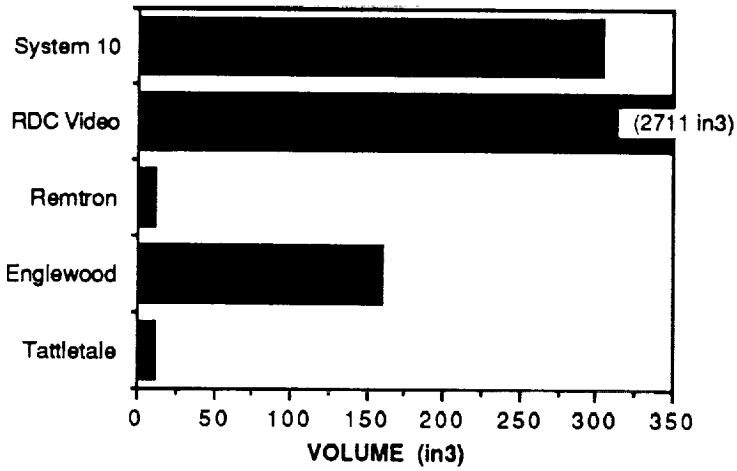

FIG 8: Comparision of Storage/ Telemetry Device Volume

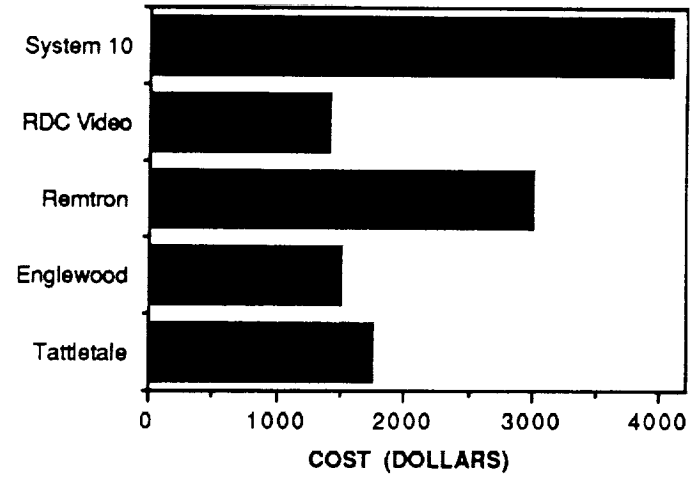

FIG 9: Comparision of Storage/Telemetry Device Cost

	bytes of storage	accuracy of digital word
System 10	172 K+	11 bits
KDC Video Cassette	26 min.	----
Remtron	----	8 bits
Englewood	----	8 bits
Tattletale	20 M	11 bits

FIG 10: Comparision of Storage/Telemetry Device Storage and Accuracy

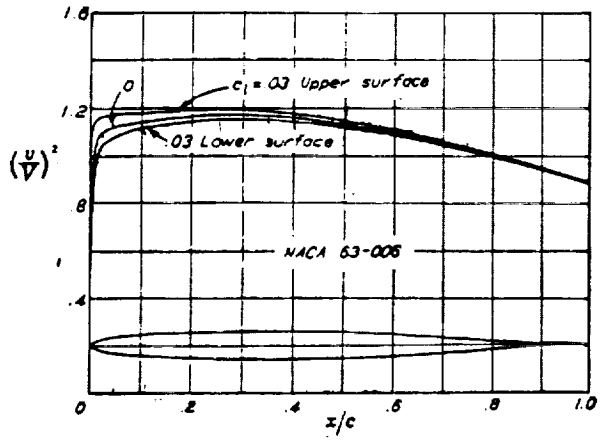

Figure 11

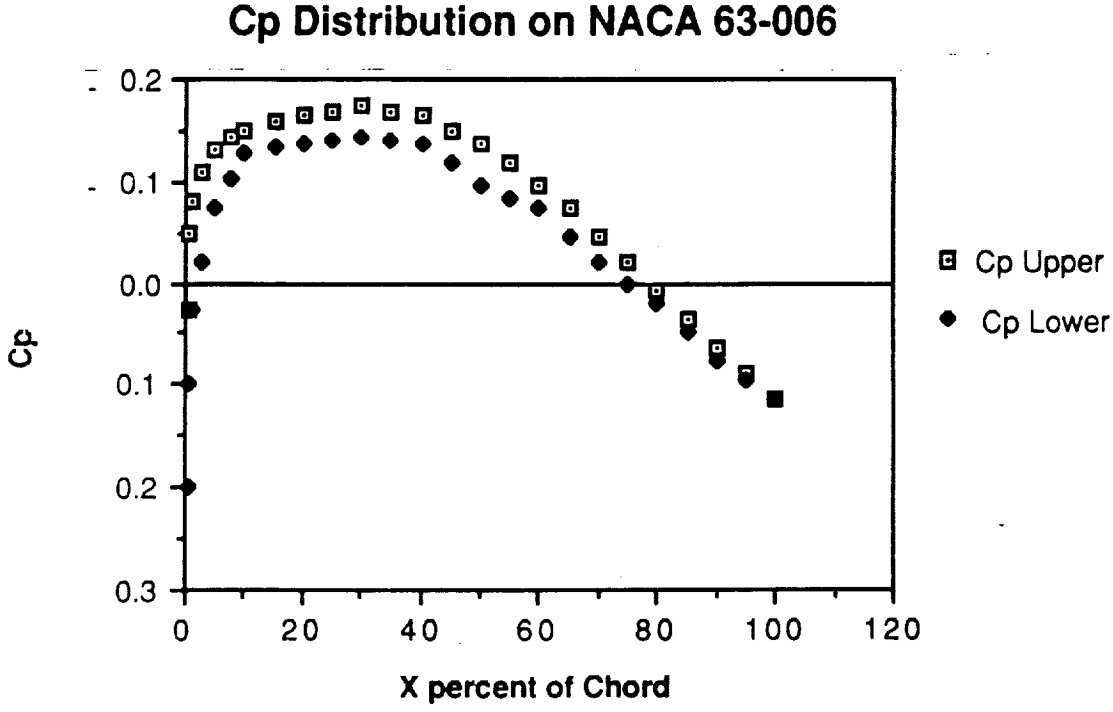

Figure 11A

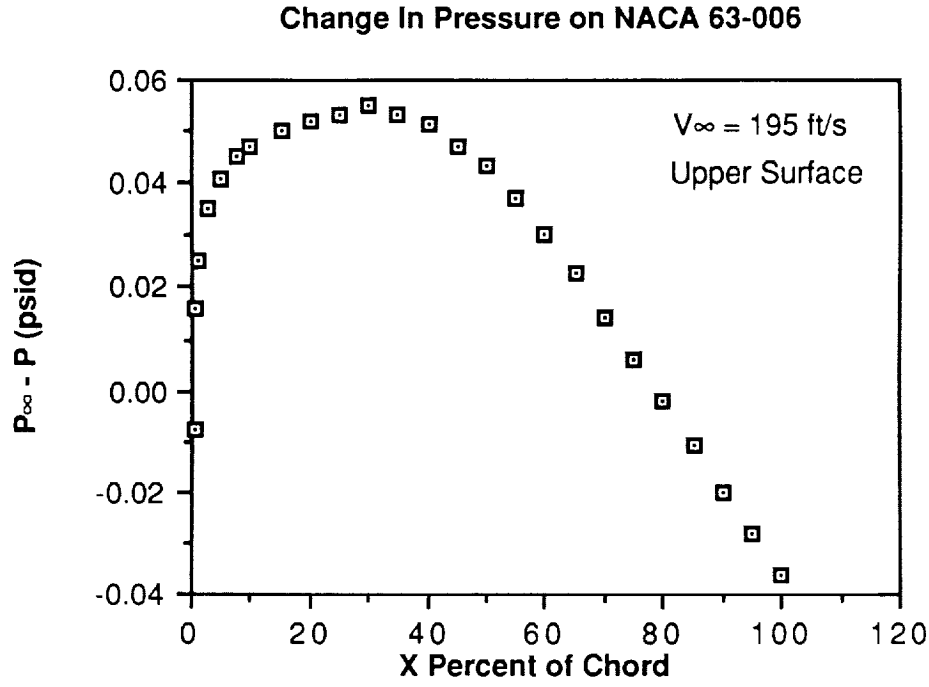

Figure 12

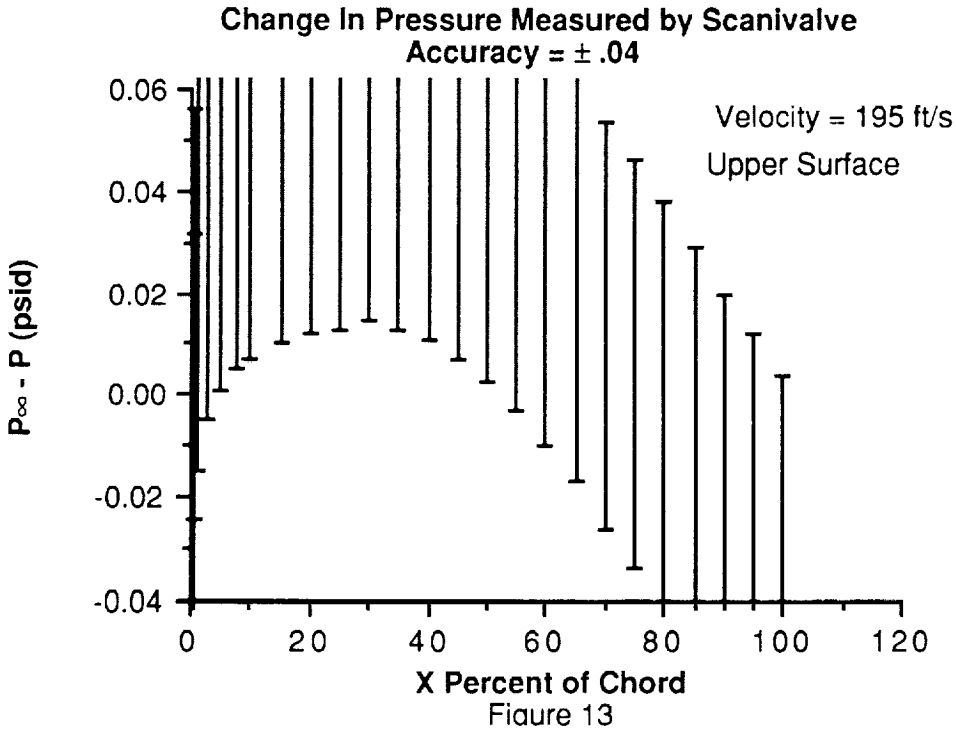

Figure 13

L: STRUCTURAL DESIGN

THE SKY SHARK

The dicussion portion of this section will be divided into three parts, namely;

1. DESIGN OVERVIEW
2. LOAD ANALYSIS
3. SPAR GEOMETRY

Design Overview:

The objective of this trade study was to find the best possible wing spar geometry/material combination to be integrated into our technology demonstrator, the Sky Shark. The figures of merit were quite straightforward for this study; make certain that the wings can sustain the loads placed upon them during normal flight conditions. If the wing either breaks or critically deforms, the design is therefore unacceptable.

From here, one is forced to study the parameters and constraints placed upon the system. The parameters of the system deal primarily with those variables affecting those loads to which the wing will be subjected. These include the the aircraft weight, the maximum flight velocity, the wing and winglet geometry (span, aspect ratio, taper, area, and dihedral angle), and wing weight. Also included in the list of parameters are the cost, the ease of manufacture, and the maintainence required. The constraints on the actual design are few but critical; the wing thickness (4.7 inches) and the weight of the spar. The ultimate design of the spar is no good if the dimensions of the design are larger than the thickness of the wing itself. Likewise, the wing weight must be as light as possible, lest the overall weight of the aircraft is to increase.

The design was a step-by-step process. First, certain parameters such as the total weight of the aircraft and the wings external geometry were set constant in order that the plane be able to aerodynamically fulfill its mission requirements. Next, individual trade studies were performed to determine the wings target weight and limit load factor. Then, the loads in which the plane is to be subjected were calculated via Lin Air® and computer codes (see Appendix L-1 which determined the deflection and stresses in spars with regard to different geometries (see Figures L-1 and L-2) and materials (see Figures L-3). From these calculations, and optimizing the parameters, a final design was settled upon.

Load Analysis:

The loading of the wing and the spanwise moment and force distribution along the wing was the major focus of this study. The moments and forces related to the lift were the only to be considered due to the order of magnitude separating them from the forces due to drag.

The first step in calculating the loads associated with the wing was deciding upon the load factors the plane would experience. This required constructing a velocity versus load factor (V-n) diagram (refer to Figure L1). The limit load factor of the plane was chosen after comparing the limit load factors of various single prop aircraft, and whose average limit load was 3.42. Therefore, a value of n_{lim}=3.5 was chosen. The dive velocity was calculated by using the Sky Shark's drag profile and then equating it to the plane's weight, and from this derive the resulting velocity, whose value is 252 ft/s. From this, and the techniques described in " Airplane Strength and Rigidity Flight Loads", the diagram was constructed.

Next, a factor of safety had to be determined. As with any design, increasing the factor of safety of the vehicle usually translates into a subsequent increase in overall weight; a luxury not afforded the aerospace engineer. Therefore, a value for the factor of safety of 1.2 was selected. This was based on the judgement that this would be adequate due to the minimal risk to life owing to the non-human cargo of the RPV.

Before the loads on the wings could be modelled, however, it was imperative that the wing weight first be estimated. A trade study was performed on small aircraft, and a weight fraction value for the total wing weight of .1 compared to the plane's overall weight was arrived at, culminating into a total wing weight of .1*(60 lbs)=6 lbs, or three pounds per wing. But because of the the high aspect ratio, low overall structural weight of the fuselage and instrument package, and the additional moments created by the winglets, a total wing weight of 10-12 lbs was thought to be acceptable. Therefore, an individual wing weight of five pounds was used in the calculations.

At this point, we were now ready to examine the spanwise lift distribution over the wing. To develop this model, the program Lin Air® was utilized. It should be noted here that a deficiency in the program is that it does not take into account the effects of the winglets, thus introducing a source of error. The lift distribution of the plane flying at $V_{max\ cruise}$=190 ft/s

was examined, and the values then recorded. From here, the lift distribution was plotted, and a third-degree polynomial was used to curve fit the data points (see Figure L-4). It is this approximation for the lift, or;

$$c_l=.3791-.0207*X+.00906*X^2-.00114*X^3 \quad (1)$$

that is used in the programs created (see Appendix L-2) to determine the stresses and deformations due to bending. The accuracy of this method is illustrated by summing the incremental lifts through thirty steps, which results in a value of 29.74 lbs., or an error of .09%.

The first step in creating both programs was defining a coordinate system (see Figure 2). As can be seen, the lift along the wing relative the X-Y axis is:

$$Lift=Lift*\cos(\text{ø}) \quad (2)$$

where ø is the angle of inclination of the wing. Both programs utilize a differential length approach. The programs begin at the wingtip and travels a distance ∂x, which is the wing length divided by the number of iterations, each time through the loop. At each individual station, the program calculates local values for the cord length, spar section weight, lift, moment (both cruise and maximum, see Figure L-5) , and then stores the results in seperate files. The value for maximum force in the Y-direction then becomes:

$$\Sigma Yforces=FS*LLF*\partial l-\partial W_w \quad (3)$$

where FS is the factor of safety, LLF is the limit load factor, ∂l is the incremental lift, and ∂W_w is the section spar weight. For the determination of the maximum stress, the formula for stress due to bending is used:

$$Stress=Moment*c/I \quad (4)$$

where c is the distance measured from the neutral axis and I is the moment of inertia. The moment used in the above equation is the moment caused by the maximum forces in the Y-direction plus 98.7lbs*ft, which is the moment induced by the winglet at full surface deflection. The moments of inertia

used are for a circle, box, and S-beam of equal height and cross-sectional area, thus weight (see Appendix L-3). For determining the maximum deflection, the formula:

$$y_{def}=P*(X/2)^3/(3*E*I) \quad (5)$$

is used, which is the equation of deformation of a point load at a distance X/2 from the origin. This equation is found on p.399 of "Mechanics of Materials", and is applied to the differential elements, and then simply totalled.

Spar Geometry and Material:

The geometry of the wing's internal geometry was chosen to be a single spar. This design was chosen over a variety of internal layouts, including multiple spar, monocoque, semi-monocoque, and foam supports. The single spar design was chosen for a number of reasons, including it's ease of manufacturability and repair, low cost, and the way it lends itself to structural analysis.

Once the single spar design has been established, then one must then decide upon a spar configuration. As can be seen in Figures L-1 & L-2, the performance evidenced by the S-beam is superior to the circle in both stress and deformation analysis, and far superior to that of the box. Thus, the S-beam is logical choice in this instance.

MATERIALS SELECTION:

The purpose of this trade study is to strategically identify the class of materials best suited for the wings of remotely piloted vehicle (RPV) named the Sky Shark. The Sky Shark is an experimental aircraft designed to take surface pressure measurements on a vertical tested specimen mounted on top of the aircraft near the nose. The total weight of the vehicle (including payload) is approximately sixty pounds. This trade study models the wings as a pair of flat plates in order to easily approximate the wing loading. Wings fabricated out of five classes of materials are then over a number of primary design consideration to see which class of material is best for the design. These materials tested are an aluminum alloy, cast iron, a magnesium alloy, steel and wood. The materials are first limited by a design weight requirement that restricts the total weight of the wings to less than a total of twenty-five pounds. Calculations are then made on the newly sized wings to determine the maximum allowable normal and shear forces within this weight range. The material that best meets these design limitations is the class of materials best suited for the wings of the Sky Shark .

The purpose of this trade study is to determine the best class of materials for the wings of the Sky Shark, not the exact material. It is first assumed that the exact material will be determined in a later, more thorough trade study. Therefore, several more generalizing assumptions can be made. First of all, for the purpose of this trade study, it is assumed necessary to simplify the wing loading analysis. This simplification will allow for easier manipulation of the relevant material parameters and help to gain insight into the best class of materials. Therefore, the wings will be modeled as a pair of flat plates of finite thickness. This assumption allows for an easier calculation of the weight and cross-sectional area of the wings, because the restrictions of moment of inertia calculations has been eased. The calculation of the maximum allowable shear and normal forces is equally as simple. Secondly, it is assumed that the maximum allowable stresses on the wing corresponds to the yield strength of the material in tension and in shear rather than the ultimate strength. This is an aerodynamic assumption based on the fact that if the the wing material yields and the overall wing shape is altered, the wing effectiveness could be greatly reduced resulting in extreme danger to the aircraft.

A detailed study into materials selection requires that the classes of materials be evaluated against the oftentimes competing claims of primary and secondary considerations. In addition, there are two additional considerations that have been determined to be the of the upmost importance in the selection of a material for the wings of the Sky Shark: the density of the material and its cost effectiveness. Initially, the thought was to examine a candidate material from seven different classes of materials. However, because the cost of advanced metallics, ceramics and plastics is generally known to be extremely high, these three classes were cut from the list of possible classes even before their relevant parameters were tested versus the primary and secondary considerations. The Sky Shark is designed to take the best possible experimental measurements. Therefore, in order to outfit the Sky Shark with the latest (and most expensive) in pressure measurement technology, the cost of the plane's materials must be limited as much as possible. As a result, a candidate material was chosen only from the material classes of woods, steels, aluminum alloys, magnesium alloys and irons.

It was also initially hoped to select the materials based on primary and secondary considerations in addition to density and cost effectiveness. The primary considerations were tensile strength, shear strength and fabricability. The secondary considerations were corrosion, fatigue, fracture toughness, stiffness and repairability. All of these considerations would then to be examined versus the design weight and the resultant cost. However, because of the generalizing assumptions made earlier, it was deemed that the secondary considerations would not play a role in this initial materials selection trade study. Because this trade study selects only the class of materials, the trade study will examine the materials against the primary design considerations only. The secondary considerations will, however, be utilized in more thorough trade studies in the next phase of design.

The candidate materials and their relevant parameters are listed in Appendix L-4.

As stated previously, there are several wing parameters that are set. First, the wing has a chord length of 2 ft (24 in) and a span of 17 ft (204 in). The cross-sectional area of the wing, then, varies only with changes in the thickness of the wing. Secondly, the wings will be designed to a Factor of Safety of 1.5. All calculations for this trade study were made using the Excel spreadsheet software developed by the Microsoft Corporation.

The first step in the trade study is examine the effect that changes in the thickness of the wing has on the weight of the wing. All of the materials were examined in 0.005 in increments of wing thickness starting from zero. The weight of the wing was then calculated from known parameters.

$$Weight_{wing} = Density \ / \ Volume$$

where, Weight (lbs)
Density (lbs/in^3)
Volume = 12 in * 204 in * thickness (in)

The design weight limit for the wings is twenty-five pounds. Wood has the lowest density (0.018 lbs/in^3) of the candidate materials. Therefore, the wing thickness was incremented until the weight of the the wood wings reached the maximum allowable for the design. A copy of the Excel spreadsheet containing these and all of the rest of the necessary calculations is attached. Figure L-6 shows how the the weight of the wings vary for the incremental increase in the wing thickness for the candidate materials.

Wood is the lightest material and therefore the first choice for the wing material at this point in the trade study. The next step is to examine how the candidate materials vary within the twenty-five pound wing weight limit. This should yield greater insight into how wood stacks up against the other materials.

Figure L-7 shows dramatically that wood is the best material in this weight range. The wood wing can have a large number of finite thicknesses and still fit into the design weight range. The aluminum and magnesium alloys also a good number of finite thickness available for design within the weight range, but not nearly as many as wood. Steel and iron, however, have a limited thickness range within the weight limit and are immediately eliminated from further competition with the other materials. These materials will, however, be used in comparison with the remaining candidate materials for their strength to resist normal and shearing forces. Figure L-8 shows the exact advantage wood has in data within the weight range. There are twenty-four thickness values that wood can have and still meet the wing weight requirements. In comparison, aluminum has only five while steel has only two. The later two materials are used often on wings of commercial

jets. However, this aircraft in this family are extremely heavy in comparison to the Sky Shark . Therefore, the trend is once again to choose wood and the class of materials for the wings because of the size of the data base within the weight limit. Having such a large data base allows the designer to work over a range of values in the initial design stages. This circumvents the tendency toward point designing which nearly always spells doom to the designer.

Wood has then been clearly established as the favorite for the class of materials for the wings of the Sky Shark . The next step is to examine how wood stands up against the other materials to normal and shear forces. If wood can hold its own against these stronger materials and meet the design wing loading requirements, then wood will be chosen as the class of materials on which to base the next phase of the materials selection trade studies.

The maximum normal force in the wing can be calculated for the various thicknesses of the candidate materials within the total weight requirement for the wing. Once again, these calculations are attached in the Excel spreadsheet. Because of the simplifying assumptions made previously, the maximum normal force in the wing is a function of the tensile yield strength of the candidate material, the factor of safety and the cross-sectional area of the wing.

$$P = (\text{Tensile Yield Strength} / \text{Factor of Safety}) * A$$

where, P = Maximum normal force (lbs)
A= Cross-sectional area (in^2)

Figure L-9 shows how the maximum normal force varies for the candidate materials within the weight limit. Wood stacks up very well against the other materials in this range. This nearly solidifies wood as the choice for the class of materials for the wing design.

The final step is to look at how wood fares against the other materials in shear. Shear is the most important direction of the wing loading as this is the direction of lift. Lift is the largest force on the wing, much larger than drag. Therefore, if wood cannot meet the design requirements for shear loading, it can still be ruled out as the class of materials for further wing design for the Sky Shark .

Maximum shear in the wing is calculated in exactly the same manner

as the maximum normal force with the exception that the Shear Yield Strength is substituted for Tensile Yield Strength.

$$V = (\text{Shear Yield Strength} * \text{Factor of Safety}) * A$$

where, V = Maximum shear load (lbs)

Figure L-10 displays the results. Wood is the weakest of the materials in shear, but yet strong enough to meet the design requirements. Therefore, wood is the choice for the next phase of design.

It was stated previously that fabricability was another primary design consideration. There is no way to mathematically examine the effect of fabricability on the material selection. Of the candidate materials, however, wood is by far the most fabricable. This is witnessed in the fact that wood is the material most often chosen by RPV enthusiasts. All of the RPV's that are flown every day across the country are a testimonial to the results arrived at through this trade study. Therefore, wood is chosen as the class of materials for further wing design for the Sky Shark

L: APPENDICES

THE SKY SHARK

APPENDIX-PROGRAM#1

```
1 REM PROGRAM-STRESS ANALYSIS
2 REM WRITTEN BY GREG BRANCH
3 OPEN"WING DATA" FOR OUTPUT AS #1
4 OPEN"WING DATA2" FOR OUTPUT AS #2
5 OPEN"WING DATA3" FOR OUTPUT AS #3
6 OPEN"WING DATA4" FOR OUTPUT AS #4
7 OPEN"WING DATA5" FOR OUTPUT AS #5
8 OPEN"WING DATA6" FOR OUTPUT AS #6
9 OPEN"WING DATA7" FOR OUTPUT AS #7
10 HY=1.5
15 ALP=12
17 FOS=1.2
18 LLF=3.5
20 S=34
23 E=10.1*1E+07
24 I=3.2/(12^4)
30 CO=2
40 TR=.8
50 L=8.689
60 N=30
70 DX=L/N
80 WW=5
90 V=75
100 DEN=.00237
110 CT=CO*TR
120 COUNT=0
130 VT=(S/2)*CO*(1-.5*(1-TR))
140 Q=.5*DEN*V^2
150 FWX=-65.8*COS(ALP)
160 MZW=-FWX*HY
170 MZ=MZW
175 HF=DX/2
180 FOR X=(L-HF) TO HF STEP -DX
190 COUNT=COUNT+1
200 C=CO*(1-X*(1-TR)/L)
210 DS=C*DX
220 CL=.3791-.0207*X+.00906*X^2-.00114*X^3
230 DL=Q*CL*DS*COS(ALP)
240 LT=LT+DL
250 DWW=WW*DS*C/VT
260 DMZ=DL*X-DWW
270 DMZW=DL*X*LLF*FOS-DWW
280 MZ=MZ+DMZ
290 MZW=MZW+DMZW
295 YDEF=((DL*(DX/2)^3)/(3*E*I))*12
298 PRINT COUNT,LT,DL,C
300 PRINT #1,COUNT
302 PRINT #2,MZ
303 PRINT #3,MZW
304 PRINT #4,DMZ
305 PRINT #5,DMZW
```

```
306 PRINT #6,DL
307 PRINT #7,X
310 NEXT X
315 PRINT"TOTAL LIFT=";LT
320 END
```

```
300 STCR=2*MZW/ICIR
303 STBX=2*MZW/IBOX
305 STBE=2*MZW/IBEA
310  PRINT #1,YSCR
312  PRINT #2,YSBX
313  PRINT #3,YSBE
314  PRINT #4,STCR
315  PRINT #5,STBX
316  PRINT #6,STBE
317  PRINT #7,X
320 NEXT X
350 END
```

APPENDIX- PROGRAM #2

```
1 REM PROGRAM- DEFLECTIONS
2 REM WRITTEN BY GREGORY BRANCH
3 OPEN"CIRCLEA" FOR OUTPUT AS #1
4 OPEN"BOXA" FOR OUTPUT AS #2
5 OPEN"IBEAMA" FOR OUTPUT AS #3
6 OPEN"STCIRCLEA" FOR OUTPUT AS #4
7 OPEN"STBOXA" FOR OUTPUT AS #5
8 OPEN"STIBEAMA" FOR OUTPUT AS #6
8 OPEN"COUNT" FOR OUTPUT AS #7
10 HY=1.5
15 ALP=12
17 FOS=1.2
18 LLF=3.5
20 S=34
23 E=10.1*10^6
25 ICIR=4.11
26 IBOX=1.088
27 IBEA=6.08
30 CO=2
40 TR=.8
50 L=8.689
60 N=30
70 DX=L/N
80 WW=5
90 V=75
100 DEN=.00237
110 CT=CO*TR
120 COUNT=0
130 VT=(S/2)*CO*(1-.5*(1-TR))
140 Q=.5*DEN*V^2
150 FWX=-65.8*COS(ALP)
160 MZW=-FWX*HY
170 MZ=MZW
175 HF=DX/2
180 FOR X=(L-HF) TO HF STEP -DX
190 COUNT=COUNT+1
200 C=CO*(1-X*(1-TR)/L)
210 DS=C*DX
220 CL=.3791-.0207*X+.00906*X^2-.00114*X^3
230 DL=Q*CL*DS*COS(ALP)
240 LT=LT+DL
250 DWW=WW*DS*C/VT
260 DMZ=12*(DL*X-DWW)
270 DMZW=12*(DL*X*LLF*FOS-DWW)
280 MZ=MZ+DMZ
290 MZW=MZW+DMZW
291 YDCR=((LT*LLF*FOS*((L-X)/2*12)^3)/(3*E*ICIR))
292 YDBX=((LT*LLF*FOS*((L-X)/2*12)^3)/(3*E*IBOX))
293 YDBE=((LT*LLF*FOS*((L-X)/2*12)^3)/(3*E*IBEA))
294 YSCR=YSCR+YDCR
295 YSBX=YSBX+YDBX
296 YSBE=YSBE+YDBE
```

APPENDIX L-4

CANDIDATE MATERIAL PARAMETERS

MATERIAL	UNIT WEIGHT (LB/IN^3)	YIELD STRENGTH (KSI)	
		TENSILE	SHEAR
Aluminum Alloy 2024-T4	0.100	44	25
Cast Iron Malleable	0.276	36	24
Magnesium Alloy AM 100A	0.065	22	21
Steel 0.6% Carbon	0.283	60	36
Wood Douglas Fir	0.018	7.4	1.1

L: FIGURES

THE SKY SHARK.

Graph L1: Velocity vs Load Factor

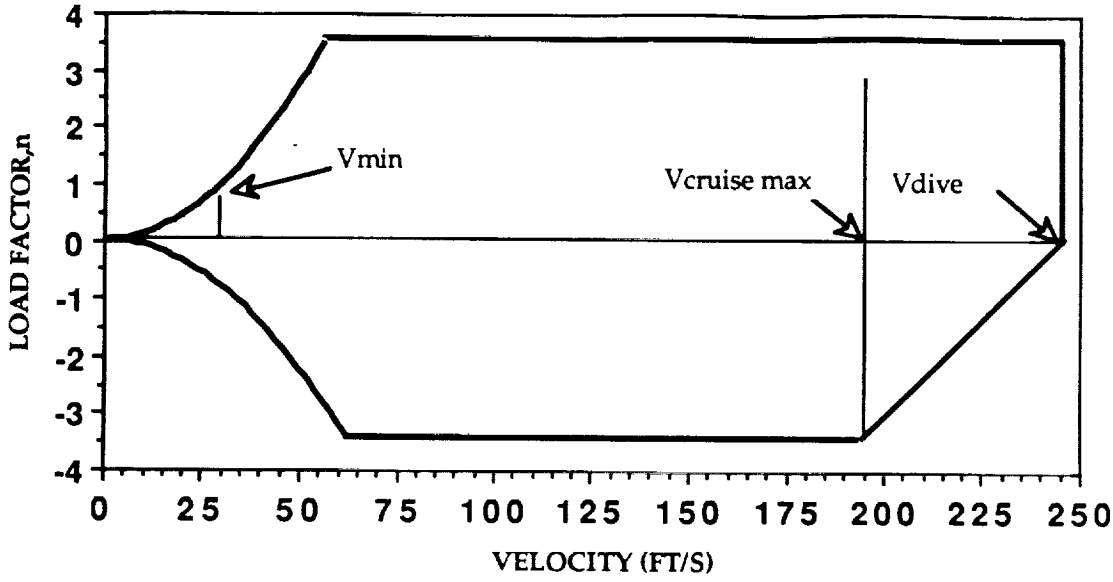

Graph L2: Coordinate System

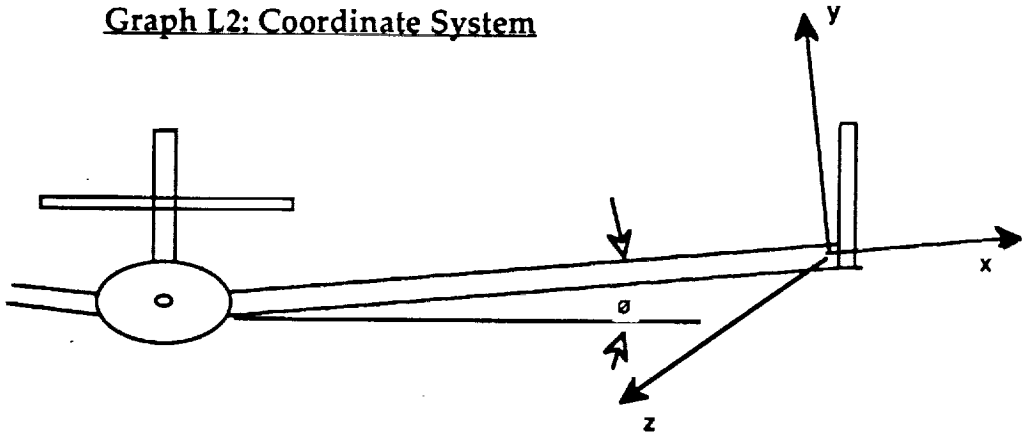

Graph L3: Spar Geometries

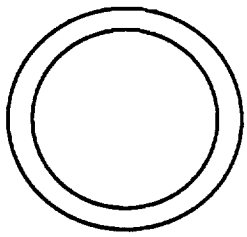

Circle

Area=2.26 in*in
Height=4 in
I=4.11 in^4

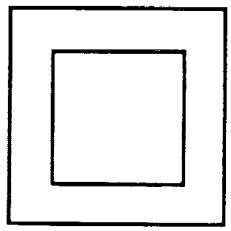

Box

Area=2.26 in*in
Height=4 in
I=1.088 in^4

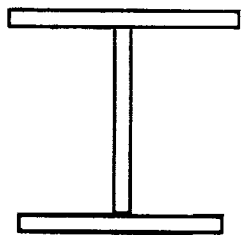

S-Beam

Area=2.26 in*in
Height=4 in
I=6.08 in^4

Appendix: Spanwise Deflections in Aluminum Spars

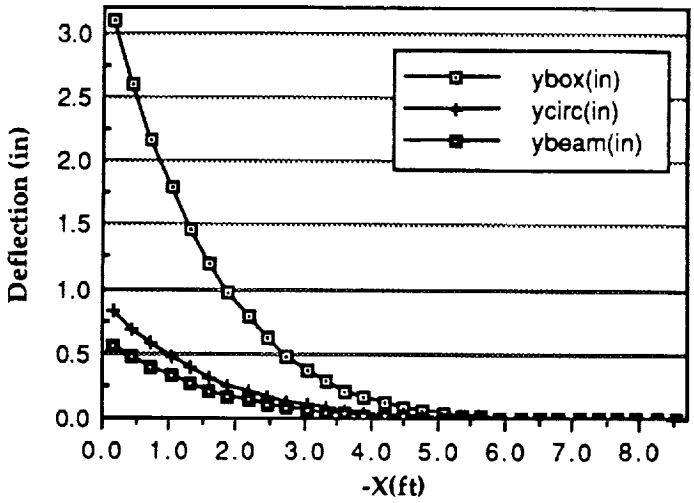

Appendix: Spanwise Maximum Stress

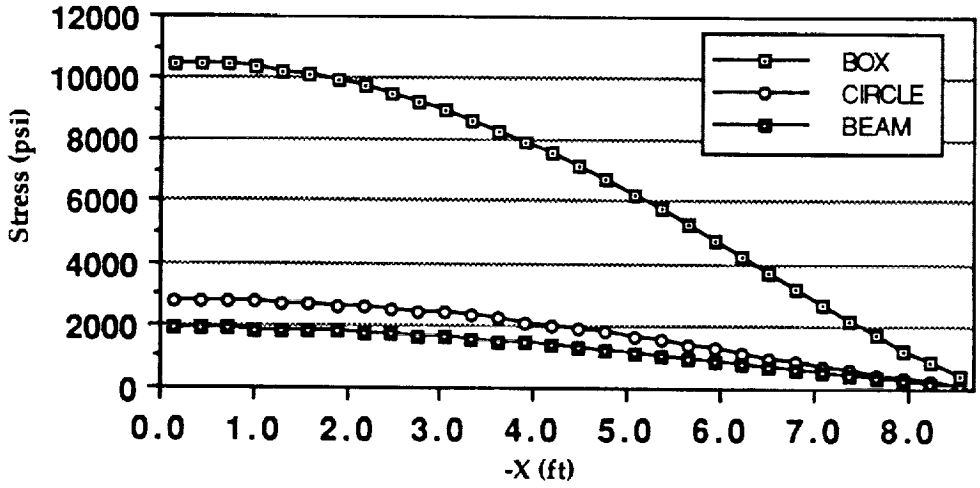

Appendix: Spanwise Moment Distribution

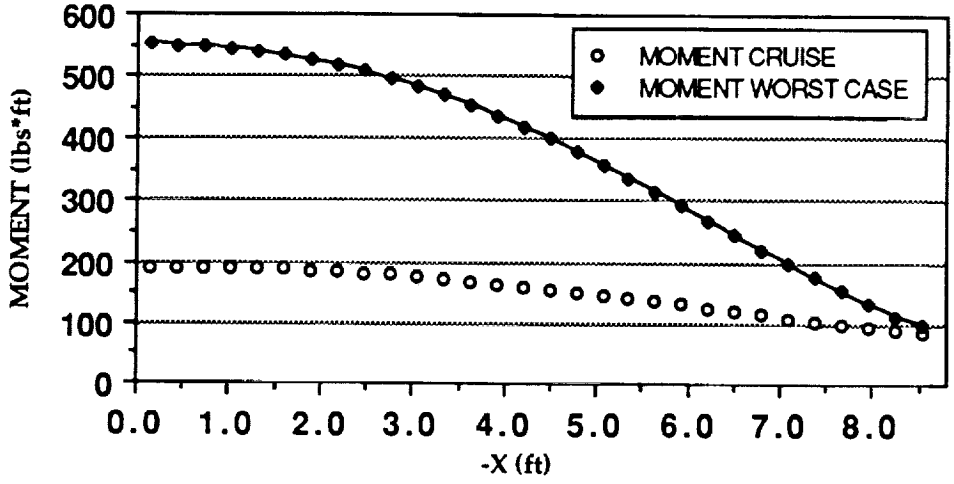

Appendix: Spanwise Lift Distribution

y = 0.37911 - 2.0718e-2x + 9.0584e-3x^2 - 1.1355e-3x^3 R^2 = 0.983

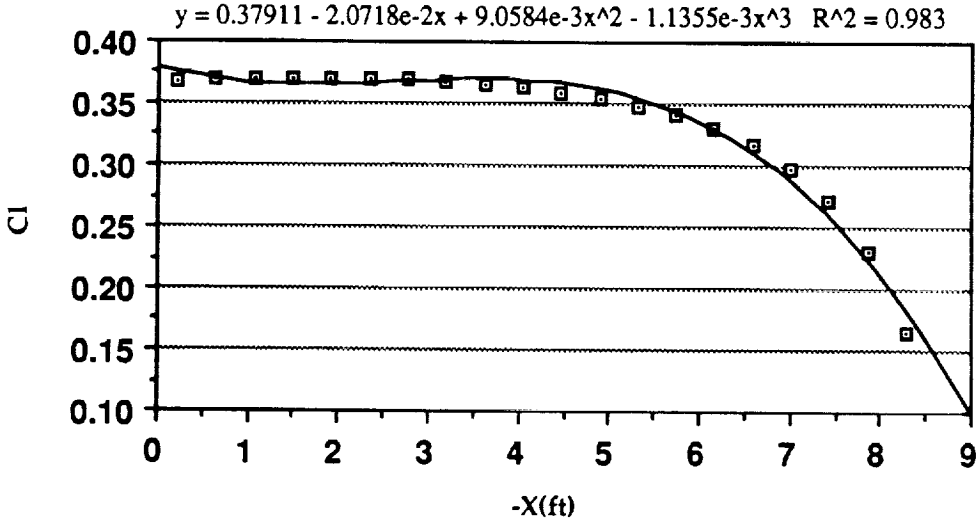

FIGURE L-6: WING WEIGHT FOR VARIOUS PLATE THICKNESSES

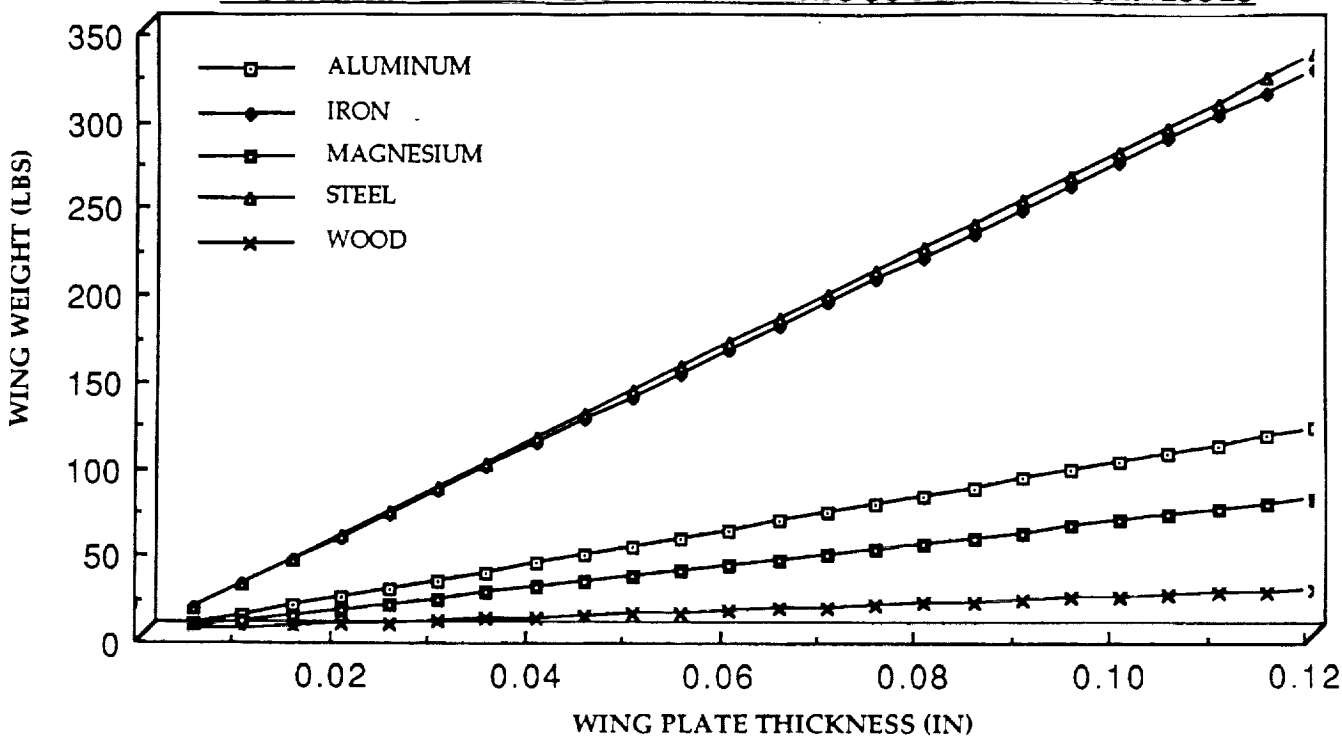

FIGURE L-7: WING WEIGHT WITHIN WEIGHT LIMIT

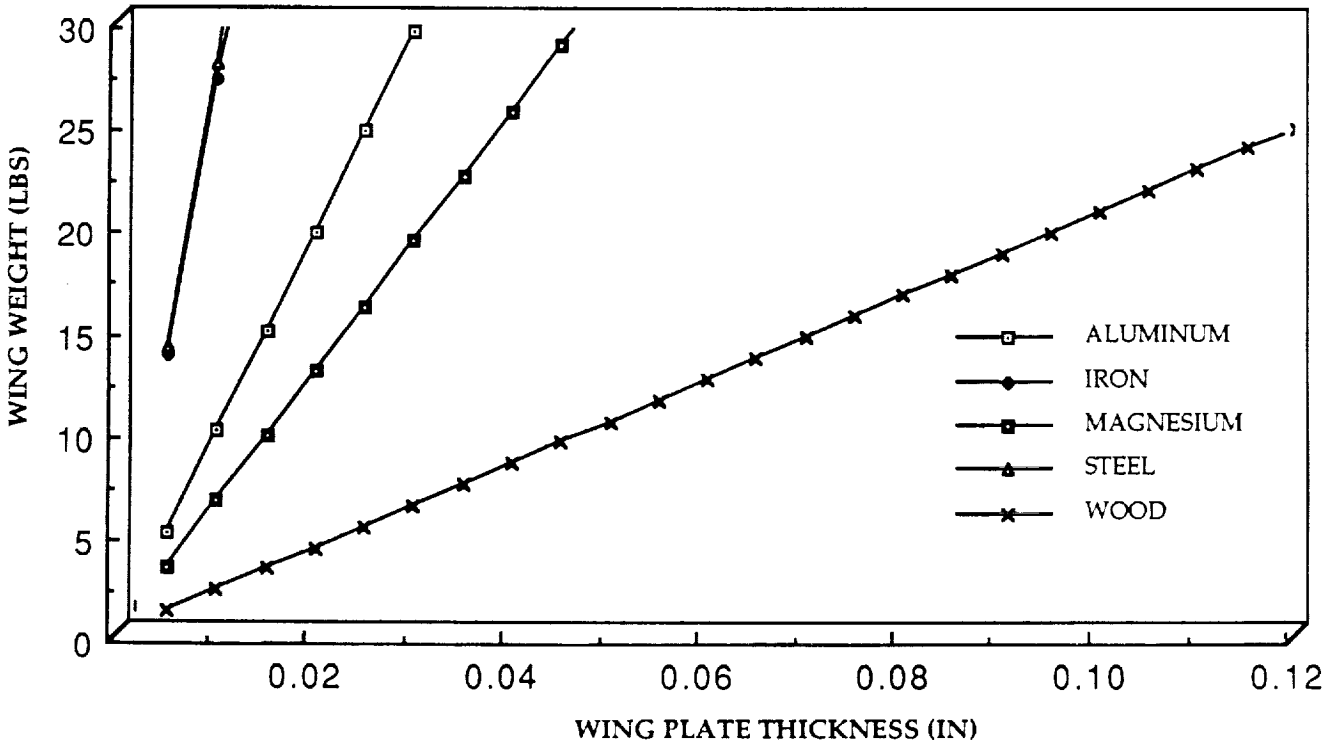

FIGURE L-8: INCREMENTAL THICKNESSES WITHIN WEIGHT DESIGN LIMIT

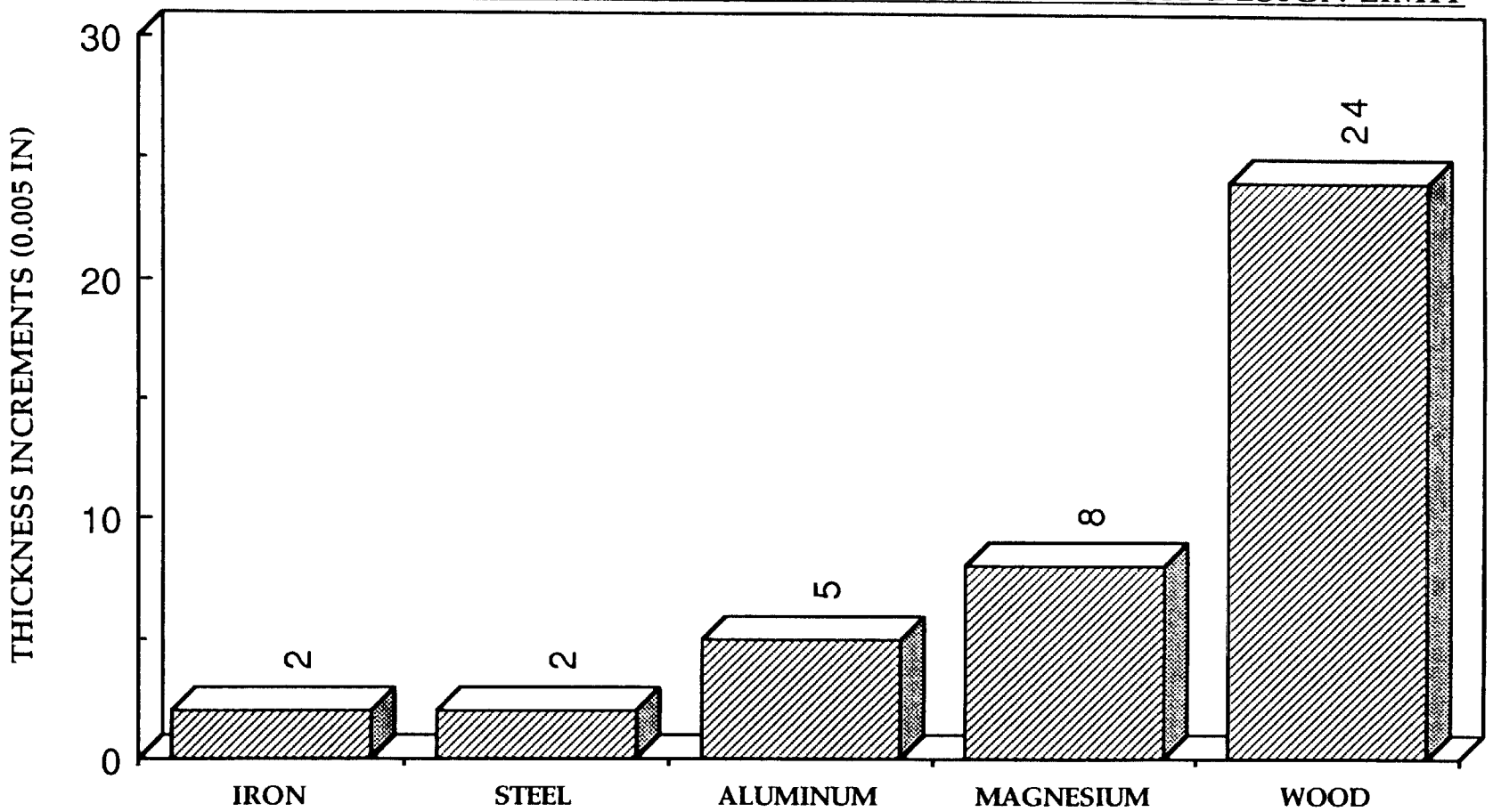

FIGURE L-9: MAXIMUM NORMAL FORCE WITHIN DESIGN WEIGHT LIMIT

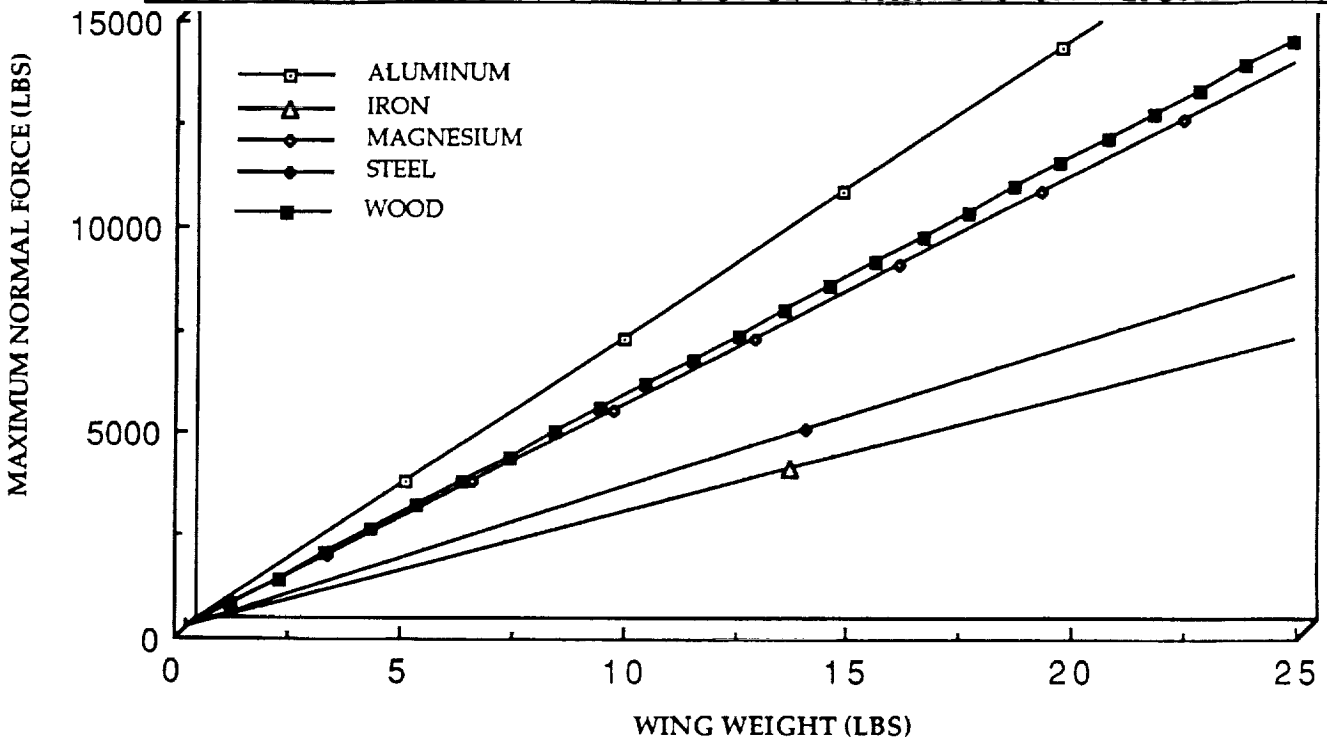

FIGURE L-10: MAXIMUM SHEAR FORCE WITHIN DESIGN WEIGHT LIMIT

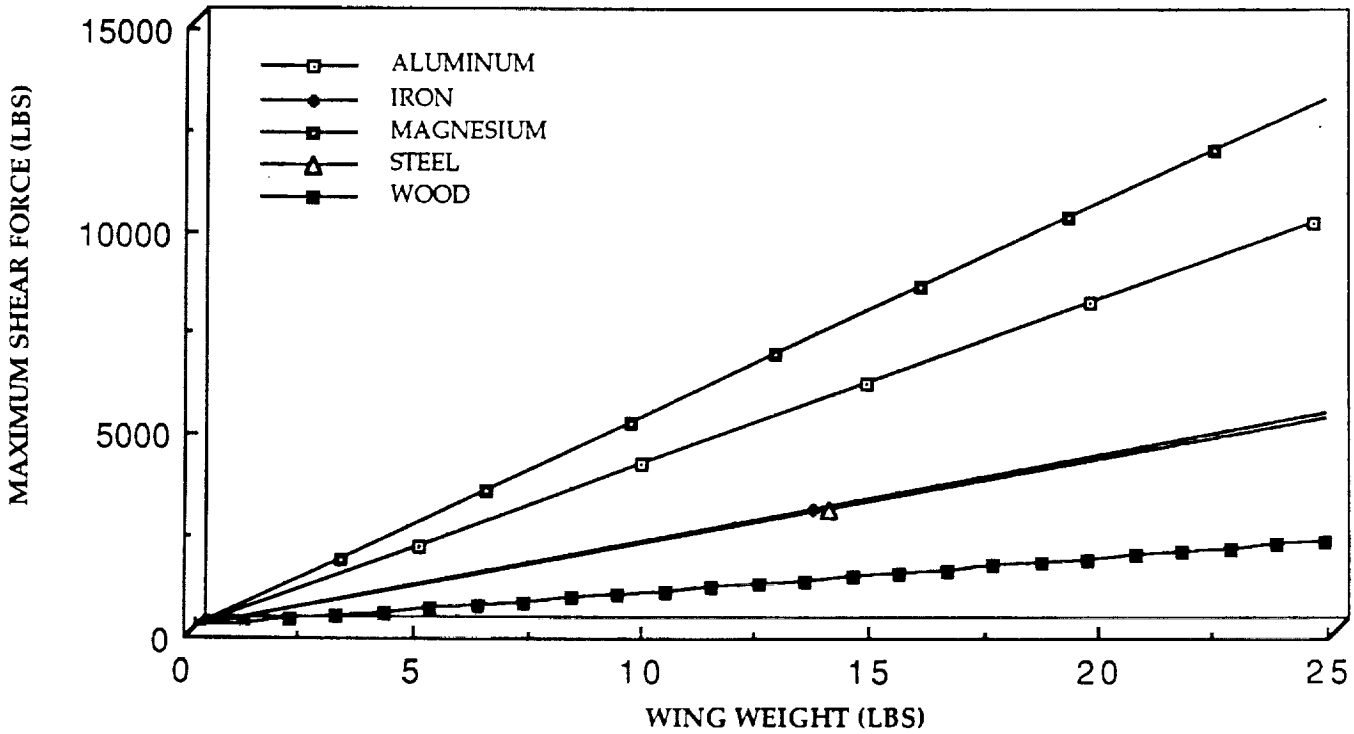

M: MANUFACTURING

THE SKY SHARK

With respect to manufacturing, the Sky Shark is a very simple plane to build. This is because from the very first stages of conceptualization, both cost effectiveness and simplicity of form were stressed. The final design of our prototype, then, reflects our attention devoted to the maxim "less is more".

Starting with the structure of the wings, manufacture is simplified by use of a single-spar geometry and a linear taper. The ribs used shall be of conventional design, spaced about one foot apart, and the covering, as with the rest of the plane, will be of heavy-duty plastic polymer, Monocote®. The structural connections will be made via a combination of rivets and welding.

The fuselage design is also extremely straightforward, and can be divided into two parts; the nose cone and the main fuselage. The nose cone will be composed of fiberglass and will be mounted onto the fuselage via hinge connections for ease of removal. The nose cone will house the instrument package and will therefore be filled with foam rubber insulation in order to guard the costly equipment from damage due to shock. The main fuselage is a metal truss structure with bolt connections for ease of repair and replacement. The undercarriage of the main fuselage section will be composed of removable fiberglass panels instead of the Monocote® covering. These panels serve two purposes: 1.) To supply the underside of the plane with an added degree of strength needed for the underside. 2.) An easy way of entry into the plane's interior, aiding in manufacture and serviceability. The test section connection will be a universal joint motor fastened to the topmost portion of the fuselage. The engines will also be connected to the plane via pin connected metal rods.

Finally, the tail and rudder section will be a simple metal rod-truss structure with a Monocote® covering. All control surfaces will be manipulated via flexible pull-push rod connections.

N: SAFETY CONSIDERATIONS

THE SKY SHARK

The risks associated with the Sky Shark, a 60 lb. vehicle capable of flight velocities in excess of 130 mph., are obvious. As with any product, safety should always take first priority in the mind of the manufacturer. A product which is unreasonably dangerous, or which poses risks to society greater than the benefits derived from its existence should be either redesigned or removed from the marketplace. This responsibility falls upon the the manufacturer both in an implicit moral fashion as well as an explicit statement found in this country's policies of strict tort, stating "responsibility be fixed wherever it will most effectively reduce the hazards to life... that reach the market. It is evident that the manufacturer can anticipate against some hazards... as the public cannot."(Justice Traynor, Escola v. Coca-Cola Bottling Co. of Fresco). Therefore, responsibility rests upon the shoulders of the manufacturer to produce items which are as safe as possible. With this in mind, we, the designers of the Sky Shark , propose the following measures to be enacted:

1. A quality control committee be initiated, whose responsibilities include:
   a. Tests be routinely conducted on the Sky Shark in order that all dangers, both obvious and concealed, can be determined.
   b. Affect measures to remove or lessen those dangers uncovered by the aforementioned tests whenever possible.
   c. Make certain that the Sky Shark complies with all safety requirements found in all industry and governmental codes.

2. Warnings labels be designed and affixed to the vehicle regarding those dangers to the general public as well as the operator uncovered by the tests conducted by those in quality control.

3. A section devoted to safety be included in the operators manual. This section should include:
   a. Obvious dangers (crash, explosion, etc.)
   b. Concealed dangers which could not feasibly be designed out of the aircraft.
   c. A copy of the disclaimer found in the sales agreement.

4. A disclaimer of responsibility be included in the sales contract. This disclaimer should enumerate the responsibilities to which the purchaser is consenting, which includes the requirement that all those associated with the plane's operation MUST both first read and understand the section regarding safety found in the operators manual. Furthermore, it is the salesperson's responsibility to review this disclaimer with the client, and to alert them to those liabilities to which they are consenting.

O: COST ANALYSIS

THE SKY SHARK

COST BREAKDOWN

THE SKY SHARK

MATERIALS:

		COST ($)
A. WOOD		
1. Wing		60
2. Fuselage		20
3. Empennage		25
	TOTAL:	105
B. SUPPLIES		
1, Bonding Material		20
2. Monokote		20
3. Tools		40
	TOTAL	80
C. HARDWARE		
1. 2 Ducted Fan Engines		350
2. Data Acquisition System		23650
3. Control System (Radio and Servos)		225
	TOTAL	24,225
LABOR: ($10/hour)		
1. Wing Construction		600
2. Fuselage Construction		200
3. Empennage Construction		250
4. Servo Installation		100
5. Data Acquisition Installation		100
	TOTAL	1250

TOTAL COST:	Materials	105
	Supplies	80
	Hardware	24225
	Labor	1250
		25660

P: TECHNOLOGY DEMONSTRATOR

THE SKY SHARK

The primary objective of the technology demonstrator was to demonstrate the capabilities of specific areas of the actual airplane design. Namely, the stability characteristics of the basic aerodynamic configuration. The aircraft was scaled down to approximately forty percent full scale. Due to an inability to match flight Reynold's numbers, it was necessary to change airfoils. A Selig 3021 airfoil was selected for the demonstrator in order to avoid low Reynold's number performance degradation and provide adequate lift with low drag. The demonstrator was constructed using a forward mounted propellor instead of ducted fans, due to the availability of the electric power plant. It was felt that this would not change the stability characteristics significantly as long as the center of gravity was accounted for in the movement of the engine. The winglets were also left off of the design since they would serve no purpose when the test section was not mounted on the aircraft.

CONSTRUCTION:

Wing:

The wing of the demonstrator had a taper ratio of .8 from the root to the tip. Balsa ribs were placed at intervals of three inches connected by balsa spars. The two balsa spars ran the length of the wing. The spars were placed along the top and bottom of the wing at approximately thirty one percent of the chord. 1/16 inch balsa caps connected the upper and lower spars to form a rigid wing box. The two halves of the wing were joined at the center using 1/16th inch plywood epoxied to the main spars. The two halves were joined with a seven degree dihedral angle to help compensate for the lack of ailerons in the demonstrator design. The leading edge was carved from a 3/4 inch square balsa rod and rib caps of 1/16 inch balsa were placed on the top of the ribs between the leading edge and the spars. Rubber bands were used to attach the wing to the fuselage. The central portion of the wing was reinforced using balsa and plywood sheeting in order to withstand the force of the rubber bands stretched over the surface. The entire wing was covered using Black Baron plastic film attached using an iron.

Fuselage:

The demonstrator fuselage was constructed using 1/8 inch plywood

formers that were covered with a laminated outer skin fabricated by attaching 1/16 inch balsa sheets to 1/64 inch plywood. The lower front of the fuselage was covered with fiberglass fabric in order to help the fuselage withstand a belly landing. The engine was held in place by an aluminum engine mount attached with screws to a 1/4 inch firewall at the front of the fuselage. A removable balsa shroud was constructed to enclose the engine. The empennage was epoxied to the rear of the fuselage and 1/4 inch dowel rods were inserted through the fuselage to allow for the rubber bands, holding the wing in place, to be easily attached. The entire fuselage was coated with Black Baron plastic film.

CONTROL:

To simplify construction and flight control, the only control surfaces on the demonstrator were the elevator and rudder. Ailerons on the demonstrator were considered unnecessary due to the primary objective being to test the stability of the aircraft. The elevator was attached to the horizontal stabilizer using a monokote hinge while the rudder was attached to the vertical stabilizer using plastic hinges. Control of these surfaces was achieved through the use of Nyrods that were attached to the surfaces with control horns. The Nyrods ran through the fuselage to individual servos. The servos were connected to a radio receiver controlled by signals sent from a Futaba transmitter.

Longitudinal stability for the demonstrator was determined in the same way as in the actual design, changing only the aerodynamic data for the airfoil. A list of the stability characteristics and calculations can be found in Appendix P-1.

PROPULSION SYSTEM:

The propulsion system for the demonstrator was an Astro 15 electric motor. The motor was mounted on the front of the demonstrator and had an electronic speed controller connected to the radio receiver. A flexible plastic propeller ten inches in diameter and having a pitch of 6 was attached to the Astro 15. The flexible propeller was used to prevent potential damage to the engine when belly landing the aircraft since adequate clearance was not

available. This propeller was determined to provide adequate thrust to propel the technology demonstrator. A larger propeller with greater pitch was desired (an 11-10, for example) but was unavailable in a flexible form. The battery pack for the electric propulsion system was estimated to have an endurance of three minutes at maximum drain.

FINAL PRODUCT:

The final demonstrator design deviates from the original plans in only a few areas. Originally it was planned to taper only the leading edge of the wing, but it was later decided to taper both the leading and trailing edge which allowed the spars to remain at the same percentage behind the leading edge of the wing and allowed them to run straight from wing tip to wing tip. This helped to avoid awkward angles at the center of the wing which would complicate the mating of the left and right wing halves. The other deviation from actual design deals with the location of the center of gravity. The center of gravity of the demonstrator turned out to be too far back and it was necessary to move the wing back one inch to change the location of the center of gravity. This modification improved the center of gravity location, but it was necessary to add some ballast to the front of the demonstrator to get the CG in it's proper location.

Another problem encountered with the final construction of the demonstrator was that the rudder was poorly trimmed. In spite of this, the plane was considered flyable.

FLIGHT TESTING:

The technology demonstrator was scheduled for take off at approximately 7:20 AM on Thursday April 27th. There was a light wind from the southeast. The plane was hand launched and made an initial dip most likely due to the poor trim conditions at launch. It then began to climb and bank into a left turn. The aircraft climbed to an altitude of approximately 150 ft and circled. The plane flew for several minutes and at times appeared to bump around which was due to thermal activity disrupting the flight of the aircraft. The aircraft was brought slowly down in a power-off condition and glided in for a belly landing and landed without incident.

RESULTS:

Results of the flight test proved the general capability of the design to maintain flight stability throughout the take off, cruise, turning, and landing flight regimes. We were not able to demonstrate stability with the test specimen in place as the control surfaces designed to counteract the instabilities induced in the static system, winglets and ailerons, were not included.

P: APPENDIX

THE SKY SHARK

APPENDIX P-1

Calculation of Tail Incidence Angle:

C_{lo}	.277
C_{la}	4.97 rad^{-1}
C_{mac}	-.026
de / da	.372
e_o	.021
V_H	.975
X_{cg} / c.	25
iw	3°

Equations and Calculations:

$$C_{mcg} = [\ 7E\text{-}4 + .343\ X_{cg} + 4.517\ (\ iw - i_t\ )] + [\ -4.1125 + 6.15X_{cg}\ ]$$

Substituting and simplifing,

$$(\ iw - it\ ) = .0175$$

Assuming iw was mounted at 3 degrees, it was determined that the incidence angle of the tail was approximately -2 degrees.